Volume 58
Number 24
25 March 2022
Pages 3837–3982

ChemComm

Chemical Communications

rsc.li/chemcomm

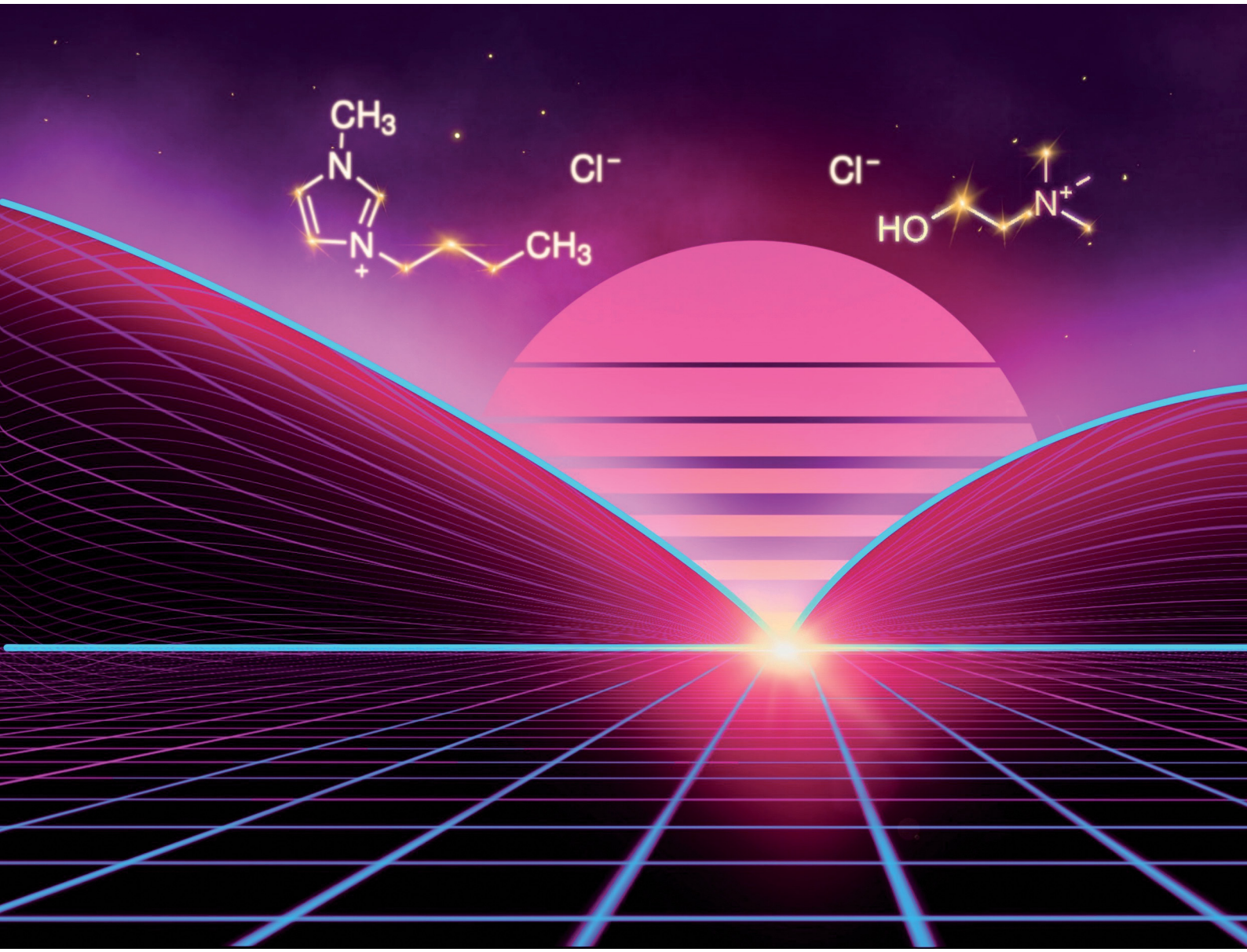

ISSN 1359-7345

ROYAL SOCIETY OF CHEMISTRY

FEATURE ARTICLE

Oliver S. Hammond and Anja-Verena Mudring
Ionic liquids and deep eutectics as a transformative platform for the synthesis of nanomaterials

ChemComm

FEATURE ARTICLE

View Article Online
View Journal | View Issue

Cite this: *Chem. Commun.*, 2022, **58**, 3865

Ionic liquids and deep eutectics as a transformative platform for the synthesis of nanomaterials†

Oliver S. Hammond [a] and Anja-Verena Mudring *[ab]

Received 21st November 2021,
Accepted 13th January 2022

DOI: 10.1039/d1cc06543b

rsc.li/chemcomm

Ionic liquids (ILs) are becoming a revolutionary synthesis medium for inorganic nanomaterials, permitting more efficient, safer and environmentally benign preparation of high quality products. A smart combination of ILs and unconventional synthesis methods allows added value to be drawn from the broad matrix of available property combinations. Mixed systems such as Deep Eutectic Solvents (DES) offer a similarly broad combinatorial playground, which is also beginning to translate into applications. Approached holistically, these liquids therefore enable new universal manufacturing techniques that provide solutions to the existing problems of nanomanufacturing, and beyond that will open completely new horizons and possibilities for controlling the growth and assembly of nanostructures. Examples that illustrate the power of ILs in the improved manufacturing of nanomaterials are explored, such as the synthesis of light phosphors with exceptional quantum yields, record-figure-of merit thermoelectrics, and efficient photocatalysts, alongside developments in DES nanostructure and deep eutectic-solvothermal and ionothermal techniques.

Introduction

Manufacturing of materials on the nanoscale has moved into the focus of chemists, materials scientists and engineers in the last few decades. The chemical and physical properties of materials can change significantly when brought to the nanoscale. These size-dependent properties make nanostructured materials extraordinarily valuable functional materials in many applications ranging from sunscreen, cosmetics, food products, packaging, clothing, disinfectants, household appliances, energy conversion and storage, and construction materials.[1] With growing societal demand for a high standard of living, products and devices that rely on nanomaterials are becoming increasingly important. Consequently, the development of economically-viable and value-added sustainable processes for manufacturing nanomaterials, which are less intensive in terms of energy and the environment, is becoming an important task. Therefore, ILs are a transformative tool because of their unique properties and property combinations. ILs are frequently discussed as "green" alternatives in organic synthesis and catalysis.[2,3] ILs are not "green" *per se*, but they can be a vehicle to design processes in compliance with the 12 principles of Green Chemistry[4] and Engineering.[5] Let us scrutinize the benefits of task-specific ILs in this context, such as the possibility to tune phase, size, morphology, and nanostructure without using additional chemical additives. These become particularly potent as green synthesis tools once combined with the advantages of unconventional synthesis techniques, such as microwave, ultrasound, physical deposition and sputtering techniques (*vide infra*). Therefore, unprecedented green and efficient nanomanufacturing processes leading to superior materials can be realised by approaching problems holistically with ILs.

ILs are generally defined as salts with melting points below 100 °C whose melts are composed of discrete ions. ILs are not necessarily new materials; examples have been known for over 100 years,[6] but attention was renewed over the last 20 years. Research interest intensified particularly from 1995 onwards, first due to efforts by the United States Air Force in applying ILs as electrolytes, and subsequently from suggestions that ILs have special properties as replacements for conventional solvents.[7] However, it is now being realised that it is rather the unique combination of properties, unattainable by molecular compounds or crystalline salts alone, that render ILs exceptional materials and brings them under more intense scrutiny.[8] The non-volatility, high thermal stability, and wide liquid windows achievable by many ILs has proven an important driver for research[9] and a technology enabler, supporting numerous advances beyond the initial investigations of ILs as liquid electrolytes.[10] To name but a few applications, ILs have been used as replacement solvents for thermal fluids,[3] lubricants,[11] processing of cellulose,[12] biphasic chemical processes (*e.g.*, BASF's BASIL® process; BASF was the

[a] *Physical Materials Chemistry, Department of Materials and Environmental Chemistry, Stockholm University, 10691 Stockholm, Sweden*
[b] *Intelligent Advanced Materials, Department of Chemistry and iNANO, Aarhus University, 8000 Aarhus C, Denmark. E-mail: anja-verena.mudring@chem.au.dk*

† Dedicated to the memory of Prof. Kenneth R. Seddon.

first to show eco-efficient chemical processes by implementing ILs),[13] photovoltaics, fuel cell electrolytes, and in separation science,[14,15] chemical synthesis and catalysis,[16–20] and as non-volatile highly energy-dense materials (*aka*. "energetic liquids").[21]

While they will be introduced comprehensively in the latter half of this review, we will briefly touch upon Deep Eutectic Solvents (DES) here. DES are a relatively recent class of systems, which are frequently regarded to be in the same category as ILs as solvents.[22] They are eutectic mixtures of two or more compounds, where the melting point is particularly depressed, making the liquid state accessible. Usually, DES contain salts such as choline chloride mixed with an organic hydrogen-bonding species, giving them an 'IL-like' character. DES have high ionic strength (albeit lower than a pure salt due to the molecular component), and potentially similar physical and chemical properties depending on the mixture. It is worth noting here that DES are not always ionic–molecular mixtures, just that the most popular systems are.[23] Given the significant overlap, it is therefore relevant to address ILs alongside DES in the same review. Since there are differences between review coverage for ILs (more recent and extensive) and DES (significantly uncovered) for nanomaterial synthesis, the two parts of this review will be addressed in different styles; firstly, ILs will be discussed and addressed critically to demonstrate their effectiveness as materials synthesis media. Secondly, recent progress and developments in applications of DES in materials synthesis will be comprehensively discussed to address the current gap in the review knowledge.

Ionic liquids and their general benefits as synthetic media in the manufacturing of inorganic nanomaterials

The high energy density of research within the field of ILs has caused an explosion in the number of new ion classes known to support IL behaviour. These range from the well-recognized systems such as azoliums (*e.g.*, imidazolium, triazolium), phosphoniums, pyridiniums, pyrrolidiniums, alkylammoniums, to

Oliver S. Hammond

Oliver Hammond is an early career researcher, primarily working with neutron and X-ray scattering and atomistic modelling techniques applied to problems in sustainability, predominantly deep eutectic solvents (DES) and ionic liquids (ILs). He began with an MSci at the University of Bristol, working on surfactant ILs, before studying for an MRes in sustainable chemical technologies at the University of Bath. He was awarded his PhD in 2019, from the University of Bath's Centre for Sustainable Chemical Technologies CDT in connection with STFC ISIS Neutron & Muon Source, for work on structure, solvation and applications of DES as nanosynthesis media. He then worked on zwitterionic materials in the QUILL lab in Queen's University Belfast. In 2019, he started a postdoctoral position in the École Normale Supérieure de Lyon, continuing to study solvation processes in DES using MD simulation, and subsequently moved to the Physical Materials Chemistry group in Stockholm University at the beginning of 2021.

Anja-Verena Mudring

Anja-Verena Mudring received her Dr rer. nat. from the Rheinische Friedrich Wilhelms Universität Bonn with work on gold compounds conducted at the Max-Planck Institute for Solid State Research at Stuttgart. After a postdoctoral stay funded by the Alexander von Humboldt foundation at Iowa State University and the U.S. DOE Ames Laboratory, she moved with a Liebig Fellowship from the Fonds der Chemischen Industrie to the Universität zu Köln, where she completed her habilitation in 2006. The same year she accepted a professor position at the Ruhr-Universität Bochum, where she ultimately held the Chair for Inorganic Chemistry III before moving as the Glenn Murphy Professor of Materials Science and Engineering to Iowa State University and faculty scientist at the U.S. DOE Ames Laboratory. In 2016 she moved to Stockholm University to head the Physical Materials Chemistry group at the Department of Materials and Environmental Chemistry. Since 2021 she leading the Intelligent Advanced Materials group as the iMAT professor and Villum Investigator at the Department of Chemistry and iNANO, Aarhus University, Denmark. After more than ten years of service as an associate editor to the ACS journal "Crystal Growth & Design" she is currently acting as Editor for "Polyhedron" and as Editor-in-Chief for "Green Chemistry Letters & Reviews". Following her research motto is "Theory with Practice" her research activities combine fundamental and applied research. For her work on using ionic liquids for making materials for energy-related applications she received the 2017 Göran Gustafsson award in chemistry, presented by King Carl XVI Gustaf of Sweden on behalf of the Royal Swedish Academy of Science. In 2021, she has been named as Villum-Investigator in Aarhus University for exploring nanomaterials formation in ionic liquids.

many new cation classes. Anions include both a wide variety of inorganic anions such as halides, nitrates, perchlorates, sulfates, nitrites, hexafluorophosphates, tetrafluoroborates, azides,[24–28] and a continuously expanding number of organic anions like triflates, benzoates, sulfacetamides, alkylsulfates, alkylcarbonates, carboxylates, and more.[29] Indeed, an enormous number of potential IL cations and anions can be imagined and their combination gives rise to a massive number of ILs (10^{18} possible cation–anion combinations for potential ILs have been suggested),[30] each with a unique set of chemical and physical properties. The notion is that desirable properties and unique property combinations can be 'designed-in', by choosing the right cation and anion to tune the overall degree of hydrophilicity, solubility, solvent structure through H-bonding, viscosity, and preferential interaction with the formed nanomaterial. ILs are therefore intriguing as nanosynthesis media, because co-dependent IL-specific properties such as electrostatic interactions, but particularly secondary bonding interactions such as H-bonding, π-interactions, van der Waals forces, and ion size which subtly influence the nanomaterial formation, can be tuned. For the most frequently used, archetypical 1-alkyl-3-methylimidazolium $[C_n\text{mim}]^+$ cation systems, the different secondary bonding interaction possibilities are shown in Fig. 1.

The imidazolium cation contains an aromatic core which can participate in π-system interactions. This electron-accepting region is likely responsible for the electrostatic attraction with polar moieties on the surface of particles. In contrast, 1-alkyl-2,3-dimethylimidazolium cations, $[C_n\text{dimim}]^+$ (see bottom left of Fig. 1), also contain an imidazolium core like $[C_n\text{mim}]^+$. In this case, the acidic 2-H proton is replaced by a methyl group, reducing its H-bonding capability and acidity. Pyridinium cations, $[C_n\text{py}]^+$, do not possess any acidic protons, but retain aromaticity. Pyrrolidinium $[\text{pyrr}_{n,n}]$ cations belong to the group of quaternary ammonium cations which possess neither acidic protons nor an aromatic ring system (Fig. 1, bottom right). In addition, the alkyl side chain may be endowed with groups that can preferentially interact with the metal NP, for example thiol groups which stabilise gold particles through chalcophilic interactions.

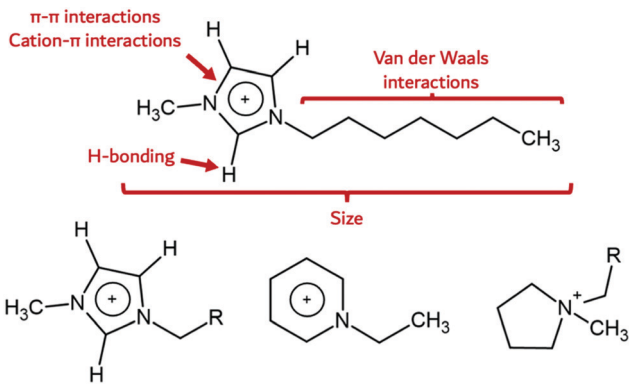

Fig. 1 Supramolecular interaction capabilities of an imidazolium cation (top) and illustration of structural variations from imidazolium to pyridinium (bottom middle) and pyrrolidinium (bottom right) IL cations.

The Lewis acidity or electron donor power of the IL anion is an important property of the IL anion with respect to the synthesis of nanomaterials. This factor dictates its hydrophilicity, and hence, its capacity to engage in intermolecular H-bonding, especially when considered alongside ion geometry. Fig. 2 illustrates the probable interactions of a prominent IL anion, bis(trifluoromethanesulfonyl)amide (Tf_2N^-). Here, electrostatic, H-bonding, fluorophilic, and van der Waals interactions are observed. These possibilities are expressed to different extents within the set of known IL anions. Halides are generally strongly coordinating and hydrophilic, whereas hexafluorophosphate and (tris(perfluoroalkyl)-trifluorophosphate) are weakly coordinating and hydrophobic. Anions such as thiocyanate are comparatively weakly coordinating, yet hydrophilic.

These interaction capabilities are not only important for specific interactions during the formation of nanomaterials in ILs, but also for their own self-organisation, which is an important aspect in nanomaterials synthesis. It is now well-established that ILs are highly structured liquids, as comprehensively reviewed by Hayes *et al.*[31] Akin to surfactant self-assembly processes, the ensemble of interionic interactions between constituents of ILs makes them heterogeneous, with a certain degree of molecular self-organisation. The presence of ionic charges imposes the first structural constraint, which is electroneutrality. In a perfect ionic melt, ions are typically surrounded by a first coordination sphere of 4–6 counterions, and then by successively less ordered concentric layers of alternating charge. These local order effects imposed by Coulomb forces have a longer range than what is generally found in molecular liquids,[32,33] and cause an unexpected long-range force decay which has been observed in interfacial (AFM (atomic force microscope) and SFA (surface force apparatus)) measurements.[34–36] The second structural constraint is imposed by the presence of non-polar moieties such as alkyl chains, which can reach significant lengths. The resulting self-assembly therefore depends on the relative contribution of Coulombic, hydrophilic and solvophobic interactions. For example, imidazolium ILs bearing longer alkyl chains display more prominent domain separation (nanostructure) due to a greater contribution from van der Waals interactions in the apolar regions, which increases with the chain length, and alters the balance of

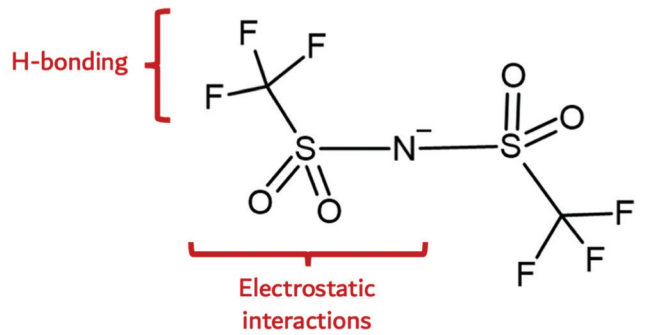

Fig. 2 IL anion interaction capabilities illustrated on the bis(trifluoromethanesulfonyl)amide anion.

interactions with the charged, polar parts.[37] ILs are also capable of having little to no nanostructure, if there is no real amphiphilic character, such as comparing ethylammonium nitrate (extended network) to ethanolammonium nitrate (small ion clusters).[38] Consequently, as reaction media, a more strongly nanostructured IL may provide an additional reaction control route, *via* the ordered domains which exist on large length- and timescales, in which reactions could occur (*vide infra*).

For alkyl imidazolium ILs, molecular dynamics (MD) simulations[39–41] and coarse-grained modelling[42] suggested structural segregation into hydrophilic (charged) and hydrophobic (non-charged) domains: They are composed of rigid ionic channels, built from the H-bonded network of anions and cation head-groups, and segregated lipophilic domains formed by the alkyl tails of the cation, as shown in Fig. 4.

This structural picture has been experimentally validated by X-ray[44,45] and neutron diffraction studies.[46–48] Similar studies have been carried out for tetra-alkylammonium- and tetraalkylphosphonium-based ILs,[49] and a set of pyrrolidinium ILs.[50] 2D NMR (nuclear magnetic resonance) techniques have also been employed for structure analysis.[51] This segregation of hydrophilic (charged) and hydrophobic (uncharged) domains is also observed in the crystalline solid state of many ILs.[52–56] These supramolecular interactions are the origin of the thermotropic mesophase behaviour of many ILs, leading to the formation of liquid crystalline phases.[57,58]

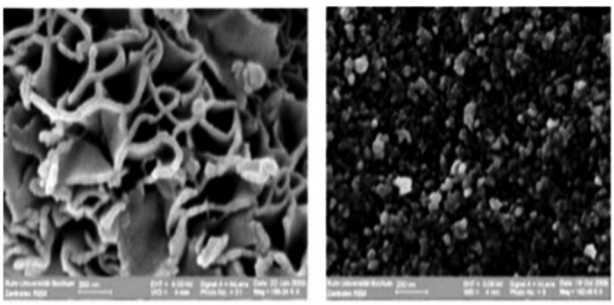

Fig. 3 NiO prepared in the IL 1-butyl-3-methylimidazolium bis(trifluoromethanesulfonyl)amide (left) and in aqueous solution (right). Reproduced with permission from RSC.[43]

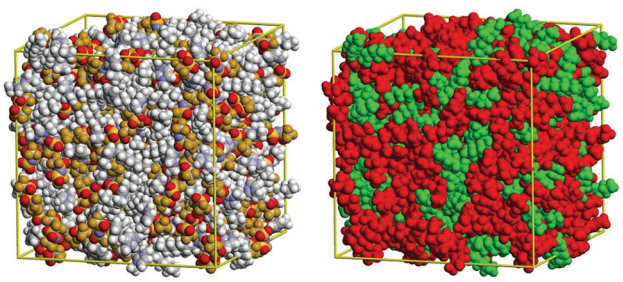

Fig. 4 Structural heterogeneity of the ionic liquid 1-hexyl-3-methylimidazolium bis(trifluoromethanesulfonyl)amide ([C_6mim][Tf_2N]) illustrated visually from a configuration obtained by molecular simulation. Left: Coloured with respect to the different atom types. Right: Charged atoms (the imidazolium ring of cation and the anion) coloured in red and in green the atoms considered nonpolar (those of the alkyl chain of the cation sufficiently far from the positive head-group). Reproduced with permission from RSC.[39]

Due to their unique structure and structural variety, ILs have proven to be excellent media for the preparation and stabilization of NPs, making features available that conventional reaction media such as classical organic solvents are not able to provide. Firstly, ILs are excellent solvents for a large variety of NP starting materials, ranging from highly ionic inorganic salts to molecular metal–organic precursors, but over that they provide additional benefits:

High nucleation rates facilitating NP formation

Although polar, ILs can have low interfacial tension.[59] Since low interfacial tension values favour high nucleation rates, very small particles can be generated.

Electrosteric stabilization through the IL preventing particle coalescence and growth

Once formed, the particles are prevented from undergoing Ostwald ripening due to the formation of an IL solvation corona akin to that seen in aqueous surfactant solutions,[60] which effectively screens electrostatics, and thus agglomeration of NPs. Many ILs resemble surfactants, and indeed surfactant (surface-active) ionic liquids (SAILs), have become an interesting research area in their own right.[61–63] Thus, it is no surprise that ILs play the same role as surfactants in stabilising NPs through coordination *via* the cation or anion. Cations and anions with long or bulky alkyl chains can both electrostatically and sterically stabilise nanoparticles in solution, giving either long-term or indefinite colloidal stability.[64]

Templating reaction medium enabling NP shape and morphology control

The impact that the IL can have on the morphology of nanomaterials is illustrated in Fig. 3, which shows SEM images of NiO prepared from an aqueous solution and in 1-butyl-3-methylimidazolium bis(trifluoromethanesulfonyl)-amide, [C_4mim][Tf_2N].[43] Sheet-like morphologies are highly desired for NiO used as an electrode material in supercapacitors. The surface energy has a high dispersion force component enhancing the differences between the interfacial energies of different crystal faces, and thus enforcing morphology. Simply by varying the IL it is therefore possible to obtain ZnO as nano-dots, rods or sheets.[65]

As stated, ILs are not homogeneous media but present self-organisation on the molecular level. This special quality has been exploited for synthesis of extended ordered nanoscale structures, or for size and morphology control. It has been demonstrated that in the synthesis of metal nanoparticles (NPs) from hydrophobic metal organic precursors, the size of the apolar domains in ionic liquids directly influences the resulting metal particle size.[66,67] Again, MD simulations provided structural support for this idea, as depicted in Fig. 5.[68]

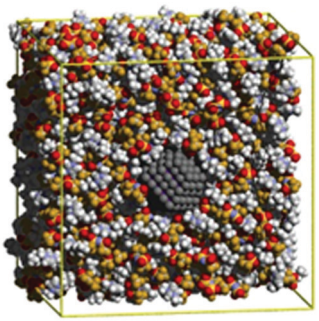

Fig. 5 Snapshot of a MD simulation of a ruthenium nanoparticle with 2 nm size (dark grey) in 1-butyl-3-methyl-imidazolium bis(trifluoromethanesulfonyl)amide. Reprinted with permission from Wiley-VCH.[68]

Nanostructuring and nanoassembly

Intriguingly, array formation is frequently observed in transmission electron microscope (TEM) micrographs of NPs in ILs (Fig. 6).[69]

It is possible to associate the inter-particle distance of nanoparticulate arrays with the size of the IL cation. Thus, it seems that above simple control over size and particle morphology, ILs can help to template the arrangement of NPs. This enables further applications from the resultant hierarchical nanostructure assemblies such as nano-structured sponges.[70]

Phase and phase-composition control

Oxides and fluorides are prevalent examples of materials which are important for applications such as catalysis, and exhibit polymorphism. For the important photocatalyst TiO_2, it has been shown that the stability of the rutile, anatase and brookite polymorphs depends on the particle size; the three polymorphs are interconvertible due to small differences in surface free energy.[71] Since each polymorph shows different physicochemical properties, such as refractive index and catalytic activity,[72] a phase-selective synthesis is highly desirable for these nanomaterials. Because of their amphiphilic character, ionic liquids are extremely efficient in phase-selective syntheses, as shown for TiO_2. Depending on the IL, the anatase:brookite ratio can be tuned.[73]

In summary, ILs bear myriad advantages in the synthesis of nanomaterials:[74–78] the formation of nanoparticles is highly favoured, and once formed, the particles are shielded by the IL against further agglomeration, omitting the necessity to involve additional capping agents. Due to their subtle interaction with crystal surfaces, the particle size, morphology, and phase can be influenced by the IL. Finally, a well-chosen IL can direct the NP assembly towards hierarchical structures.[79]

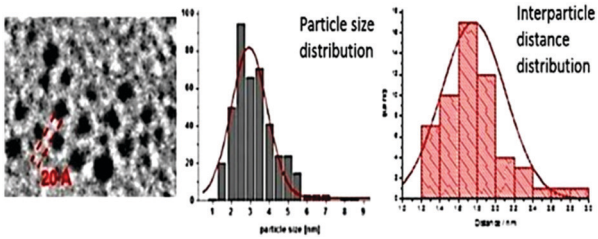

Fig. 6 Array formation of metal NPs in ILs. The inter-particle distance can be related to the size of the IL cation. Reprinted with permission from RSC.[69]

Ionic liquids and green nanomanufacturing

ILs are often intrinsically assumed to be ''Green Solvents'' and are strongly connected with the field of Green Chemistry.[80] These claims hold mainly for ILs which have negligible vapour pressures. Therefore, they are non-flammable, cannot be inhaled, and the solvent cannot pollute the atmosphere when an IL is used for an industrial process. Certainly, these aspects render ILs safer and environmentally more benign than conventional solvents, which are often VOCs (volatile organic compounds). However, it is often neglected that in the synthesis of certain ILs, large amounts of VOCs are used[81] whereas other ILs have manufacturing routes where VOCs can be omitted or largely reduced.[82] Some ILs are highly toxic, yet others are FDA approved.

With approximately 10^{18} different ion combinations which each result in an IL with a different set of properties, one must not overgeneralise: ILs are not intrinsically green, but they can be made green. Their use in specific processes may lead to improvements that comply with the 12 principles of Green Chemistry laid out by Anastas and Warner,[4] namely: 1. prevention, 2. atom economy, 3. less hazardous chemical syntheses, 4. designing safer chemicals, 5. safer solvents and auxiliaries, 6. design for energy efficiency, 7. use of renewable feedstocks, 8. reduce derivatives, 9. catalysis, 10. design for degradation, 11. real-time analysis for pollution prevention, and 12. inherently safer chemistry for accident prevention. Green Engineering has been defined by the US Environmental Protection Agency (US EPA) as ''The design, commercialization and use of processes and products that are feasible and economical while reducing the generation of pollution at the source and minimizing the risk to human health and the environment.''[5] In this context, ILs act as technology enablers. By looking at the arguments made in the previous section, it becomes evident that employing ILs in the production of nanomaterials renders their manufacturing greener: in NP synthesis the IL acts first as the solvent and reaction medium, then also as an agent for templating, stabilisation, and size, phase and morphology control. This multirole character means that other additives such as stabilizing agents or surfactants can be omitted in the synthesis. This de-intensifies the process by reducing the number of chemicals needed for the synthesis, especially hazardous additives, with the knock-on effect that a simpler mixture minimises the formation of undesirable by-products and thus waste. Safety is also improved by lower vapour pressures, which additionally facilitate recycling of the IL.

Therefore, fastidious design of nanomaterial manufacturing processes using an IL offers advantages, and can easily satisfy

half of the principles of Green Chemistry. There is still plenty of room for improvement however, especially in terms of energy and materials (atom) and economic efficiency of the processes. To close this technological gap and fully evaluate the potential of ILs in the context of green, eco-efficient nanomanufacturing, new synthetic procedures have been established that satisfy the principles of Green Chemistry and Engineering. We will now explore combinations of IL technology with unconventional synthetic conversion methods that draw advantages from IL properties.

Conversion methods

Bottom-up, chemical routes to nanomaterials in ionic liquids

In the bottom-up chemical approach for the preparation of inorganic nanomaterials, starting materials such as simple salts, complex compounds, or organometallic precursor molecules are converted within the IL to the desired product (Fig. 7).

For instance, a neutral organometallic precursor would dissolve preferentially within the lipophilic (apolar) domains of the IL. If the experimental conditions impose low levels of mass transport (*i.e.* low temperature, no stirring), the size of the resulting metal nanoparticles, such as Ru-NPs, is dictated by the number of available zero-valent atoms in the non-polar domain, which is in turn related to its size and hence the length of the alkyl chain. This suggests that the phenomena of nucleation and growth occur in these non-polar IL domains, and are controlled by the local concentration of the metal, as depicted in Fig. 8. Here, the IL functions as both reaction medium and nanoparticle stabilising agent. The preparation of noble metal nanomaterials such as Au, Pd, Pt, Ru, Ag, Ir and Rh have been studied *via* this route, thanks to their ease of reduction, relative insensitivity to oxygen and high catalytic value.[84] Nonetheless, the protecting nature of the IL means that even more oxophilic metals such as Cu, Ni, W, Cr and Mo can also be produced and stabilized as zero-valent NPs, given that suitable, chemically stable ions are chosen.[85,86] Analogously to solvothermal synthesis, when ILs are used as the reaction medium in this manner the term ionothermal synthesis has been coined.[87] As most ILs have a negligible vapour pressure, the maximal achievable temperature therefore becomes a function of thermal stability, not reactor pressure. Typical reaction temperatures can reach about 250 °C which, for example, has been used for the conversion of metal carbonyl to NPs.[88]

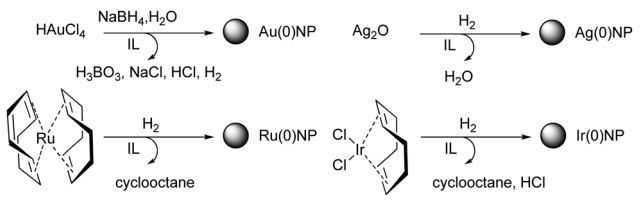

Fig. 7 Bottom-up synthesis of Ru NPs in an imidazolium bis(trifluoromethanesulfonyl)amide IL. Reprinted with permission from RSC.[83]

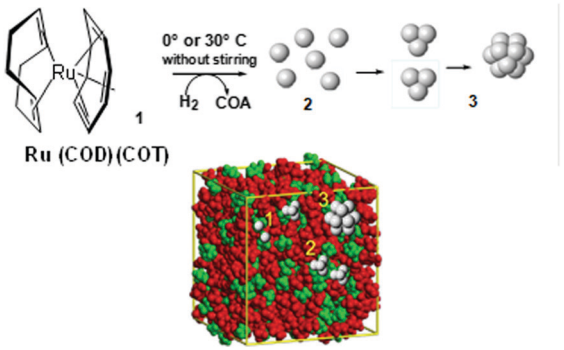

Fig. 8 Synthesis of Ru-NPs in an imidazolium bis(trifluoromethanesulfonyl) amide ionic liquid.

However, traditional heating as was used in the above example does not make full use of the potential that ILs offer. For that reason, other unconventional conversion methods with higher efficiency and further leveraging the examples of IL properties will be explored.

Microwave synthesis

ILs are excellent media for absorbing microwaves as they are composed of large ions with high polarizability and conductivity,[89] leading to high heating rates which results in a high formation rate of nuclei, favourable for NP formation. High heating rates translate into much shorter heating times and therefore faster conversion than obtainable *via* conventional heating. This is in addition to the discussed benefits such as the IL acting as an easily-removed NP stabilising agent, thus conferring numerous advantages over conventional solvents. However, in the majority of microwave reactions to produce NPs, so far, ILs have been used only as additives to classical VOCs to enhance the microwave uptake rather than as pure synthesis media. This versatile class of reaction has been termed MAIL (microwave-assisted ionic liquid).[90] Many nanomaterials such as oxides and phosphates,[91–102] fluorides[103] (hydr)oxyfluorides,[104] and higher chalcogenides such as sulphides,[105,106] selenides,[107] and tellurides[108] can be produced in this manner. However, adding dilute ILs to a reaction mixture is analogous to adding a simple salt to enhance the microwave uptake; it does not take advantage of the full range of available benefits. When the IL is only the minority component in the reaction mixture, its templating and NP stabilising influence can easily be lost, as the concentration is too low (*cf.* the critical micelle concentration, or CMC).[109,110]

Surprisingly, reactions in neat ILs or in systems where the IL is the majority component have scarcely been investigated.[90] To fully utilise the potential of microwave irradiation of ILs to produce NPs, neat ILs (or at least systems where the IL is both the solvent and majority component) have to be employed. There is a broad possibility to optimise several parameters in microwave synthesis such as the irradiation time, reaction temperature (it is even possible to irradiate a sample with microwaves, and simultaneously cryogenically cool with *e.g.* liquid nitrogen), the heating ramp, the power input rate, the cooling ramp after completion of reaction, size of the reaction

container, quantity of IL, and the precursor concentration and identity. This latter parameter is multifaceted because it not only determines solubility, but also the precursor decomposition pathway and associated kinetics. The choice of IL is crucial because certain systems such as those based on certain imidazolium can be interacting and thus not function correctly, whereas microwave heating of less interactive systems such as pyrrolidinium ILs can yield colloidally stable dispersions.[111] Similarly, certain cations such as [cholinium]$^+$ yield extremely small ZnS nanoparticles, due to strong surface coordination which blocks crystal growth.[112] This method therefore allows for the fast and facile preparation of metals, metal chalcogenides as well as halide materials, and even convoluted multinary compounds such as ternary and complex oxides.[98–101]

Ultrasound assisted synthesis

Sonochemistry, albeit mostly in conventional and volatile solvents, has attracted increasing interest over the past decade for the synthesis of inorganic nanostructured materials.[113] The effects of ultrasound on chemical conversions originate from acoustic cavitation, which occurs in several stages involving the steps of nucleation, growth, and collapse of bubbles in the liquid. The collapse of the bubbles provokes locally extreme conditions: high temperatures of 5000 K and high pressures of about 500 atm can be reached. Yet, sonochemical synthesis is often considered to be a mild method, because the temperature and pressure in the bulk solvent barely change. As many ILs have an extremely low or negligible vapour pressure they are uniquely suited for sonochemistry, as they do not interfere with the chemistry within the cavitation unlike traditional volatile solvents.[114] In ILs, the situation is best described by a two-site model. Here, the reaction cavity is composed of the bubble's gas phase interior, which originates from the reactants, and can reach 5000 K, whereas the immediately surrounding shell is composed of the (ionic) liquid, reaching local temperatures of 850–2000 K, and then surrounded further by the bulk.[113] 3500 K has been reported as the temperature for an imploding cavity in 1-ethyl-3-methylimidazolium ethylsulfate under sonication.[115] As with the microwave method, the lower heat capacity of most ILs permits faster heating under ultrasound irradiation compared to aqueous solutions.[116–118] Thus, nanomaterial synthesis time is again reduced by choosing ILs as the reaction medium, and augmented further by faster heating of small volumes, and reduced mass transport (often supported by the relatively high viscosity of ILs), which favours the formation of NPs. Another rarely-mentioned beneficial factor is that ultrasonic cavitation generates high shear which helps to break particle agglomerates into singly dispersed particles. However, a serious consideration is that ILs may decompose significantly under intense sonication.[114] It is noted that ultrasound horns provide rather harsh conditions, whereas simple ultrasonic cleaning baths (*i.e.* 45 kHz and 60 W) are well suited for experimental nanosynthesis in ILs.[43,65,73,119–122]

In summary, ultrasound-assisted synthesis in ILs is a simple, convenient, elegant, rapid and cost-effective method to synthesize NPs. It complies with the requirements of green chemistry by reducing energy intensity in production obviating the use of environmentally- as well as economically-hazardous substances. The final product is dictated by a combination of sonication time, power, and frequency, container and sample volume, and the precursor identity.

Top-down, physical routes to nanomaterials in ionic liquids

Due to the unique properties which can be realized for ILs, namely the vapour pressure and stability under the requisite experimental conditions, top-down chemical routes to nanomaterials are also viable, such as physical vapour deposition, sputtering and laser ablation. Amongst these, laser ablation is the least well-studied, potentially due to laser ablation of a target compound generally leading to relatively large, polydisperse particles.[123] After initial works,[124] this synthetic method has largely been neglected, with the exception of a few recent studies.[125] To date, physical vapour deposition and sputtering are the more investigated methods. Other exciting and versatile top-down synthesis methods also exist which are noteworthy here, especially electrochemical and plasma syntheses,[126–129] but this review will focus only upon physical and chemical routes, with electrochemistry falling out of scope.

Physical vapour deposition

The negligible vapour pressure and flammability of ILs lends them well to handling under high vacuum conditions at elevated temperatures. In this unique approach to obtain nanomaterials, metals, pre-prepared intermetallic compounds and alloys as well as ceramic materials and metal salts are evaporated onto an IL, by employing physical vapour deposition (PVD) methods. This technique is useful even for the preparation of thermodynamically unstable compounds. Our group has pioneered high temperature evaporation for the fabrication of nanoparticles in ILs by modifying the SMAD (solvated metal atom dispersion) technique,[130] originally developed by Klabunde for conventional VOCs;[131] substrate vapours and a solvent or stabilising agent are co-condensed under high vacuum onto a target that is maintained at cryogenic (77 K) temperatures (see Fig. 9). In this methodology, instead of using conventional volatile organic solvents and stabilising agents with significant vapour pressures, which require cooling of the substrate to maintain the vacuum during evaporation, ILs offer the possibility to work at ambient temperature with a liquid substrate. With this technique, universal synthetic procedures were developed for metal and metal–metal oxide colloids with long-term stability, as well as fluoride nanophosphors by thermal evaporation or electron-gun evaporation.[64,130,132]

Such experimental PVD setups are shown in Fig. 9, and consist primarily of a rotating reaction flask in which there is an axially mounted evaporation source, which can be resistive or an electron beam. The system is maintained under high vacuum by a high-speed pump assembly. A quantity of the respective IL is introduced into the rotating reaction vessel, thereby creating a liquid film upon the internal wall of the flask which is constantly regenerated through flask rotation. After the system has been evacuated, a metal, an intermetallic compound or a metal salt is evaporated and condensed into

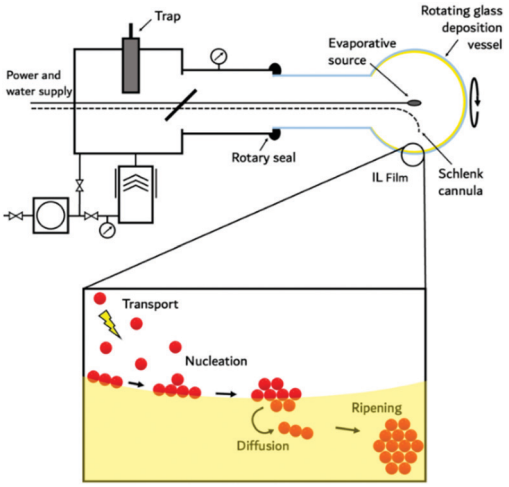

Fig. 9 Schematic drawing (top) of an experimental PVD setup together with a schematic illustration (bottom) on how nanoparticle formation upon evaporation of material into IL films occurs (bottom).

the IL film. This gives the advantage that the particles can diffuse immediately upon contact with the surface of the substrate into the bulk. As a consequence, the formation of larger aggregates is suppressed. The rotating flask constantly renews the substrate surface with a fresh film of the IL. The formation of a closed surface can be further disturbed by stirring the IL in the bottom of the flask with a magnetic stirrer. Resistive heating is used for evaporation in the temperature regime of 25–2000 °C whereas electron beam vaporisation is best suited for the high temperature region between 1000 and 2500 °C. Evaporation *via* an electron beam has the advantage of being a containerless method. The electron beam can be focused on the centre portion of the sample, and only the inner portion of the sample is first melted and then evaporated. This method can be used for large scale vaporisation (kg h^{-1}) of metals and their alloys. Fortunately, many physico-chemical and physical data such as evaporation conditions, boiling points under vacuum or gas phase composition are well known from matrix-isolation spectroscopy studies. A quartz crystal microbalance can be used to monitor the progress of evaporation. As the IL is present in excess, formation of larger particles is prevented by blocking growth. The concentration can be varied by changing the evaporation time. For multinary compounds, it is possible to either evaporate from dual sources, or from one source employing a mixture of the starting materials or a pre-prepared compound. Overall, this method has proven versatile and it allows the easy casting of metal, composite, and ceramic materials as NPs, even in large quantities. Of course, the morphology and size of the particles produced can still be controlled by the IL used for synthesis in this method.[64]

Sputtering

The thermal evaporation rates for each source material are different due to thermodynamic restrictions. This limitation can be circumvented by sputtering. It was observed that the NP size can be tuned *via* the IL identity, especially by tuning viscosity, as well as the temperature.[133–137] The sputtering technique is not restricted to pure metals, and is also applicable to binary alloy systems like Ag–Au.[138] Au–Pt alloy NPs were accessible by co-sputtering of Au and Pt into *N*,*N*,*N*-trimethyl-*N*-propylammonium bis(trifluoromethyl-sulfonyl)amide, even though bulk Au and Pt are immiscible.[139] By subsequent oxidation of the metal it is even possible to access small oxide nanoparticles.[140] This method enables fast establishment of materials libraries with composition variation. By combinatorial sputtering, a large number of NPs with different composition can be manufactured (and tested for a given application). Two or more targets can be used, or alternatively a single target containing a pre-prepared compound. In addition, the sputter power (discharge current) and sputter rate can be tuned as well as the Ar partial pressure and sputter time. For example, Cu and Au were simultaneously sputtered onto a wafer with small cavities containing the IL 1-butyl-3-methylimidazolium bis(trifluoromethane-sulfonyl)imide, yielding alloyed Au–Cu NPs.[141] The sputtering process does not rely on the different reactivity of starting materials, thus providing the benefit of favouring alloy particle production, rather than core–shell particles. This method therefore offers good potential to synthesize multicomponent NPs with the exact size composition required, simply by varying the sputtering conditions and stoichiometry.[142–147] Variation in the products can further be induced by mixing a strongly-stabilizing IL with a poor one, or diluting the IL with, for example, an organic solvent such as anisole.[148]

Bottom-up *vs.* top-down methods – a comparison

Chemical bottom-up synthesis of NPs involves the reaction (decomposition, thermolysis or metathesis) of simple salts or organometallic precursor molecules, corresponding with each component (ion) that is involved in the final product. When the kinetic reaction rates for the decomposition of different precursors vary for each source compound (which is often the case due to their different reactivities), synthesising multinary compounds becomes challenging. For alloy nanoparticles where one metal is much more noble than the other, like Cu and Au, it is almost impossible to tune the final alloy composition over a wider range of stoichiometric ratios and quite often core–shell materials are obtained. This may be desired or undesired, depending on the application. For catalysts, for example, it could be desirable to have a particle core composed of a cheap and abundant metal and a shell of the catalytically active noble (expensive) material. Here, bottom-up methods have a clear advantage. However, wet chemical approaches are also often conducive to the formation of by-products, which may adhere to the NP surface, influencing the reaction outcome and potentially the materials performance of the product. In that sense, top-down physical methods are cleaner processes which are independent of the different reactivity of the starting materials. Overall, neither synthetic approach can be declared a hands-down 'winner'; both chemical and physical techniques are pertinent and their relative merit depends on the intended nanomaterial, and its properties and desired application. Some of the respective advantages of the different approaches are shown in Scheme 1.[149]

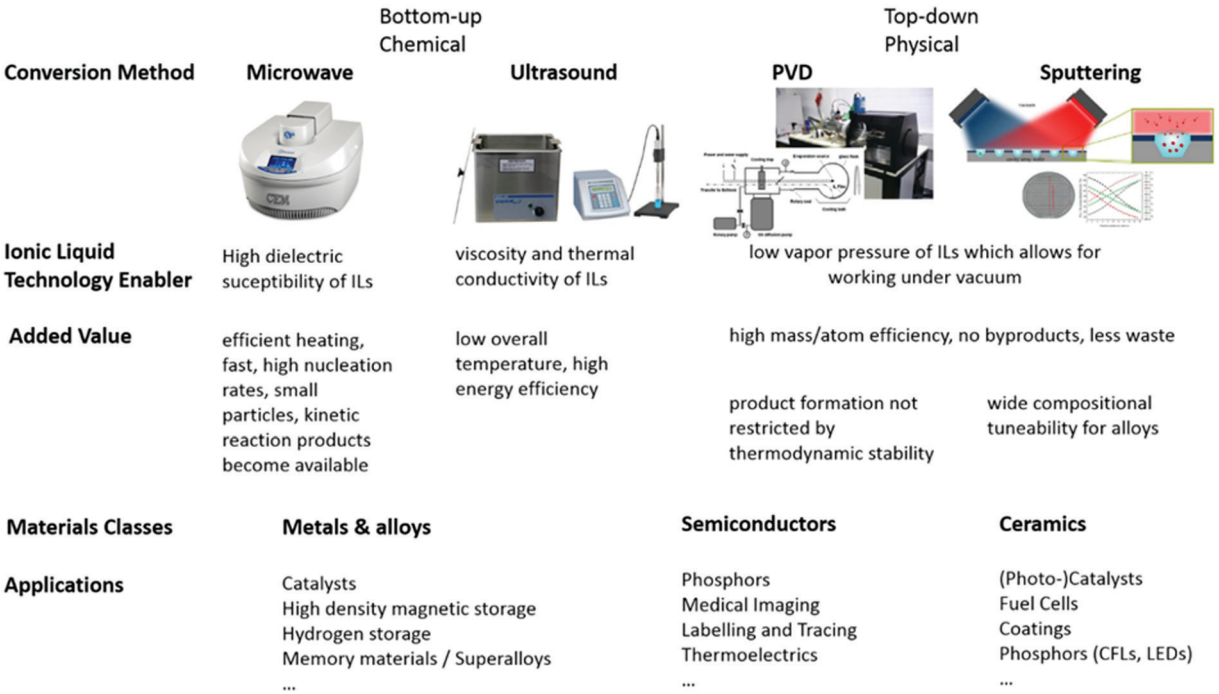

Scheme 1 Bottom-up *vs.* top-down methods for the synthesis of nanomaterials from ionic liquids.

IL synthesis showcases

A set of examples will now be explored where IL-based nanomanufacturing methods, both bottom-up and top-down, have been used for the synthesis of nanomaterials for energy related applications such as catalysis, energy-efficient lighting and thermoelectric power conversion. The examples were chosen primarily to illustrate the universal power of the presented synthetic methodologies, but also to demonstrate that nanomaterial synthesis in ILs can have strong green aspects when designed mindfully. The scrutinised materials are of high relevance for energy applications, and the products from ILs in each case showed an improved performance in comparison to what could be obtained using classical nanosynthesis methods.

Photocatalysts

New tools for clean energy are becoming increasingly necessary to meet the increasing global energy demand, driven by decreasing access barriers to energy-consuming technologies such as computation and transport. While it is not a clean fuel source when produced from hydrocarbons, hydrogen can be used as a green vector for solar energy by using incident radiation to split water.[150,151] Sunlight could also be used as an energy source for cleaning organic pollutants from air and water. Both of these require viable photocatalytic systems, which are often more powerful when nanostructured. A suitable photocatalyst must have a sufficiently large band gap ($\geq$1.23 eV for water splitting) and appropriately-positioned valence and conduction bands, with the band gap efficiently utilising the available solar spectrum.

Suitable semiconducting materials with a viable band gap that can absorb light in the near UV and in the visible region include perovskites such as $SrTiO_3$ and $BaTiO_3$, and related materials.[152] Currently, research to find the optimal photocatalyst material is mainly driven by band gap engineering to match the solar spectrum, with new computational screening approaches beginning to show merit.[153] However, the choice of synthesis method dictates a number of other important factors essential for a good photocatalyst. Firstly, it is important to maximise the accessible surface area of catalytically active surface sites. However, surface area is not the only important factor. The identity of the crystal facets which are found terminating the nanostructures at the interface also dictate the catalytic performance, alongside the exposed atom identities, the nature and quantity of any defects, the extant electron/hole conduction pathways, and the ease of charge carrier separation and recombination. These factors are all influenced by the materials morphology, size and phase, and hence its nanostructure; it is not unusual for precisely nanostructured materials to vastly exceed the specific catalytic activity of nonspecific materials with high surface area alone. Therefore, it is crucial to develop and understand controlled, robust, and reliable synthetic methodologies to optimise properties on the nanoscale.

A one-step room-temperature ultrasound synthesis for photocatalytically active $MTiO_3$ (M = Ca, Sr, Ba) nanoparticles in ionic liquids was recently developed in our group.[121] For this, a solution of $M(CH_3COO)_2{\cdot}xH_2O$, $Ti(OiPr)_4$ (OiPr = isopropoxide) and finely ground NaOH powder was irradiated with ultrasound in a commercial ultrasound bath (45 kHz, 60 W) in the ionic liquid 1-butyl-3-methylimidazolium bis(trifluoromethane)sulfonylamide, simply sealed in a glass tube under ambient conditions for 10 h (see Fig. 10).

Five crystalline forms of $BaTiO_3$ are known, of which three are ferroelectric (rhombohedral, orthorhombic, tetragonal) and stable below 120 °C. The cubic form is stable above 120 °C

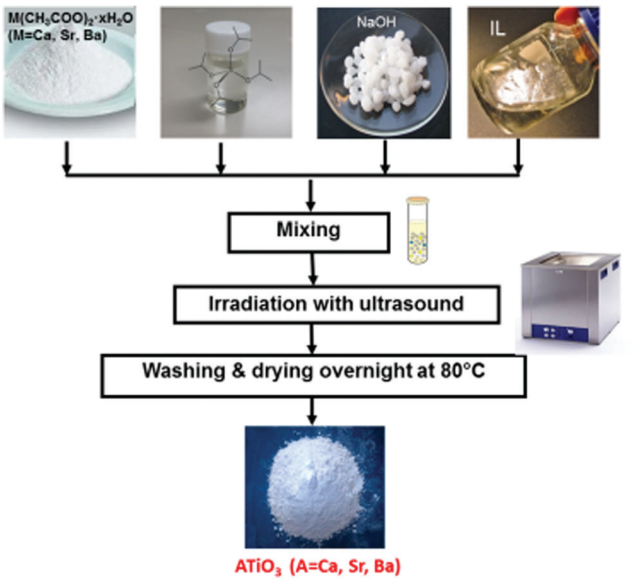

Fig. 10 Sonochemical ambient condition preparation of perovskite photocatalysts.

(its Curie point) up to 1460 °C; beyond this temperature a hexagonal structure is formed.[154] $CaTiO_3$ faces a transition from the room temperature stable orthorhombic structure to a tetragonal polymorph between 1100–1150 °C followed by a transformation to the cubic structure type at 1250 °C.[114] $SrTiO_3$ undergoes a cubic to tetragonal transition on cooling at T = 105 K (−168.15 °C). Thus, only for $SrTiO_3$ is the cubic aristotype the thermodynamically stable form at room temperature.[154] Quite remarkably, under the chosen synthesis conditions the cubic polymorph was obtained for all three, though it was only expected for $SrTiO_3$. It is suspected that this is due to ultrasonic conditions, where temporarily extreme local temperatures and pressures favour the formation of the high temperature phase; as the pressure and temperature then drop quickly, no phase transformation to the thermodynamically stable polymorph can occur. Typical methods to prepare $MTiO_3$ rely on solid-state reaction of MCO_3 and TiO_2 at temperatures above 900 °C; quite often the obtained products contain agglomerated particles of different sizes and morphologies as well as impurities owing to incomplete reaction.[155] These example demonstrate how synthesis conditions in IL-based methodologies can be exploited to obtain what would normally be regarded as the 'high temperature' polymorphs at ambient temperatures, with minimal energy usage.

The photocatalytic properties of $MTiO_3$ (M = Ca, Sr, Ba) for H_2 evolution from water were tested using 10% methanol aqueous solution as the sacrificial agent under UV light, against a reference commercial photocatalyst (P25). Without any co-catalysts the H_2 evolution rates of $MTiO_3$ (M = Ca, Sr, Ba) were already comparable to those found for P25, demonstrating that active surface sites for hydrogen generation are readily available on the catalyst surface. Photodeposition was used to directly deposit 0.025 wt% of Rh onto reactive surface titanate sites where electrons are photogenerated. This caused the H_2 evolution rates of $MTiO_3$ (M = Ca, Sr, Ba) to improve substantially; in the case of $SrTiO_3$ the photocatalytic activity exceeded the commercial photocatalyst P25, which stimulated investigation of the influence of the IL used in the catalyst synthesis on the photocatalytic activity.[100] To this end bis(trifluoromethane)sulfonimide ($[Tf_2N]^-$)-based ILs with various counter cations including 1-butyl-3-methylimidazolium ($[C_4mim]^+$), 1-(3-hydroxypropyl)-3-methylimidazolium ($[C_3mimOH]^+$), butylpyridinium ($[C_4Py]^+$), and tetradecyltrihexyl phosphonium ($[P_{66614}]^+$) were investigated.[156] Astonishing differences in the photocatalytic activity were observed, ranging from negligible (for $SrTiO_3$ prepared from $[P_{66614}][Tf_2N]$), to higher than commercial with lower co-catalyst loading (material prepared in $[C_4mim][Tf_2N]$).[135] Scanning electron microscopy (SEM) showed that the obtained $SrTiO_3$ had an IL-dependence; morphologies varied from relatively isolated nanospheres in $[C_3mimOH][Tf_2N]$ to aggregates which are cubelike in $[C_4mim][Tf_2N]$, raspberry-like in $[C_4Py][Tf_2N]$, and globular in $[P_{66614}][Tf_2N]$. $SrTiO_3$ prepared in $[C_4mim][Tf_2N]$ shows the highest photocatalytic activity for H_2 evolution (1115.4 μmol h^{-1}) using 0.025 wt% Rh as the co-catalyst. These materials also performed strongly in the degradation of methylene blue, which was investigated as a model substance for the decomposition of organic pollutants in solution. In this case, it was not the material prepared in $[C_4mim][Tf_2N]$, but the nanospheric product of the $[C_3mimOH][Tf_2N]$ synthesis which showed the highest activity for the photocatalytic degradation of methylene blue (88%) under UV irradiation. High resolution transmission electron microscopy (HRTEM) allowed the correlation of photocatalytic activities with the different dominant surface facets of the $SrTiO_3$ nanomaterial, which show distinct differences for H_2 production and photocatalytic decomposition of organic materials. This therefore demonstrates how the choice of IL used for the synthesis can be used to control the expression of crystal facets, as shown in Fig. 11.

Light phosphors: phase-selective synthesis of light phosphors with record-high quantum efficiencies

CFLs (compact fluorescent lamps) are widely used as energy-efficient light sources. However, this lighting technology generally requires small amounts of mercury in the light bulbs, representing a lifelong safety hazard. An increasing quantity of mercury is now being recorded in landfills, which is ascribed to

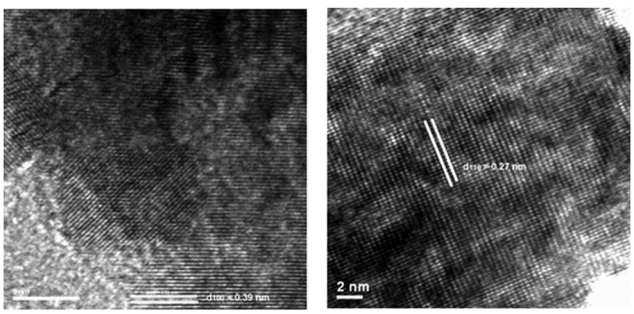

Fig. 11 HRTEM images of the as-prepared $SrTiO_3$ in $[C_3mimOH][Tf_2N]$ with {100} expressed (left) and in $[C_4mim][Tf_2N]$ with expression of {110} (right). Reprinted with permission from Wiley-VCH.[156]

improper disposal of CFLs. It would be possible to replace mercury in CFLs with environmentally benign materials such as noble gases, but this requires special nanophosphors with a quantum efficiency higher than 100% (so-called quantum-cutters) to still allow for energy efficiency. Basically, this approach relies on the conversion of electrical energy into UV light and the subsequent transformation of one energy-rich UV photon into several photons in the visible spectrum, as opposed to just one lower-energy photon, which occurs in the commercially available CFLs, where the energy delta is wasted. In the RGB colour ensemble, this problem is therefore most pertinent for the generation of long-wavelength (red) light. When doping Eu^{3+} into GdF_3 a material can be made that allows for the conversion of one UV photon into two red ones,[157] but this is not easy to manufacture at the nanoscale due to its special requirements. Firstly, appropriately small and uniform particles are needed to minimize stray-light effects, and the material has to be absolutely oxygen-free for maximum efficiency: if oxygen is present, an efficient radiationless deactivation through a charge transfer process opens up which reduces the quantum yield beyond an acceptable value. Finally, the material has to be obtained in the correct tysonite polymorph, not as orthorhombic YF_3. So, in this example there is a clear need to achieve a polymorph-specific synthesis route. Typically, oxide-free fluorides are prepared by treating $(Gd, Eu)_2O_3$ (the commercial source) with an excess of HF at high temperatures, which consumes a lot of energy and is patently unsafe to human health. Furthermore, it is expensive and difficult to control, yielding inconsistent products without sufficient quality to be used as a light phosphor (Fig. 12).

IL-based production methods were used to overcome these shortcomings, through microwave heating of Gd- and Eu-acetate in the IL choline tetrafluoroborate for 10 min at 80 °C.[158] The yielded nanomaterial consisted of small and uniform particles that were absolutely oxygen-free and contained 100% of the desired phase. The choice of IL dictated the resultant fluoride phase, of tysonite or the orthorhombic YF_3 polymorph. It must be noted that the desired material is not obtained under conventional heating. However, by conducting material conversion under microwave irradiation in the right IL, materials were obtained with a quantum efficiency close to the theoretical limit of 200%.[159] The same method was also applied to produce efficient quantum-cutting green phosphors.[157]

In addition to being a fast and energy-efficient low temperature process, the use of hazardous HF is totally omitted. This synthetic concept can be easily transferred to (white light) emitting phosphors for light emitting diodes (LEDs), as seen in Fig. 12,[160,161] and even composite materials can be obtained for this purpose.[162] Phosphates can be made in a similar way to fluorides.[163–165] If instead of quantum-cutting materials,[166,167] simple down-shifting[167,168] or up-converting materials (for example, for bioimaging) are desired, the synthetic protocol does not even require a protective atmosphere.[165] Still, care has to be taken that the desired polymorph is obtained, which the IL can uniquely help to achieve.[168–172] We recently also employed the physical vapour deposition approach,[132] which can also be used for the manufacturing of broad-band emitters based on divalent rare earth cations.[173]

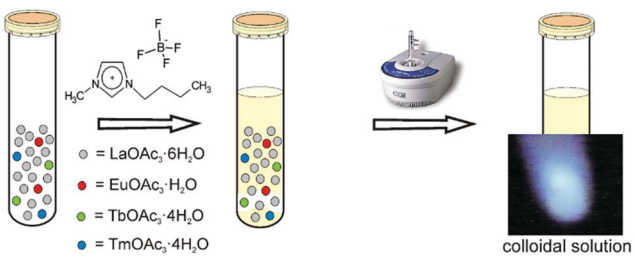

Fig. 12 Schematic illustration of the synthesis of light phosphors in ionic liquids in a microwave.

Record figure-of-merit thermoelectrics

Solid state energy converters, such as thermoelectrics, are as a main technology to enable waste heat harvesting, *e.g.* in the cooling system of combustion engines.[174] At a given temperature T, the conversion efficiency of a thermoelectric material is closely related to the dimensionless thermoelectric material's figure of merit zT (eqn (1)):[175]

$$zT = \frac{S^2}{\rho\kappa}T \quad (1)$$

where S is the Seebeck coefficient, ρ is the electrical resistivity and κ is the thermal conductivity. Good thermoelectric converter materials have a high Seebeck coefficient, expressing the generated thermovoltage per temperature difference. Moreover, a high electrical conductivity is needed in order to reduce how many Joules of energy are dissipated within the thermoelectric generator. A low thermal conductivity, with contribution from the electronic (el) and phononic (ph) system, is further required so that the thermal shortcut due to Fourier's heat conduction is small. This combination of properties is rather rare. Over decades, the best figure of merits were around zT = 1, and typically found in binary and ternary group 15/16 materials containing the heavy elements bismuth and/or tellurium, of the general type: (Sb_2Te_3, Bi_2Te_3, $Sb_xBi_{2-x}Te$). Within the last decade, materials concepts like alloying with heavy elements, the implementation of nanostructures and precipitates, the transition to materials with complex elementary cells, or the incorporation of rattling atoms have greatly improved the conversion efficiency of today's thermoelectric generators. Further improvement of the thermoelectric figure of merit zT can be achieved by precise control of the chemical composition combined with nanostructuring of the material.[174,176–178] While the first is indispensable for the optimisation of the electronic transport properties, the latter reduces the phonon thermal conductivity due to the high number of grain boundaries, which scatter phonons more effectively than electrons.

Most recently a completely new, general strategy was developed for the preparation of thermoelectric materials which allows for record-high figure of merits. It involves thermolysis of a single-source precursor in a specific IL under microwave irradiation and a subsequent mild compaction process, shown in Fig. 13.[179,180]

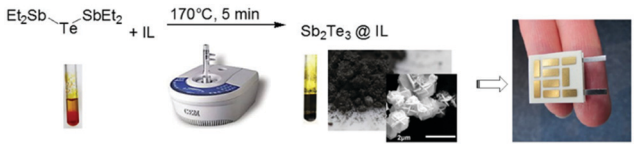

Fig. 13 From designed molecular precursors to a thermoelectric device, *via* microwave synthesis in task-specific ionic liquids.

This approach allows for independent control and optimisation of the central thermoelectric parameters, electrical conductivity, thermal conductivity and Seebeck coefficient of a nanostructured material. Firstly, the stoichiometry, and therefore the charge carrier concentration, is controlled by use of a specific single-source precursor in an IL whose thermal decomposition provides highly stoichiometric nanoparticles, guaranteeing high Seebeck coefficients. Secondly, the carrier mobility is controlled by the use of a task-specific IL combined with microwave heating, which gives access to small, clean, impurity-free particles, which results in a high carrier mobility and optimised electrical and thermal conductivity. A similar experiment employing a classical surfactant showed that the capping agent could not be removed completely from the particle surface, hampering the electrical conductivity across grain boundaries. In contrast, the IL allows for a fast microwave-heated reaction (conventional heating in IL yielded a material of lower performance), control of the particle morphology and, in the end, in contrast to traditional stabilisers, a naked particle surface. Finally, control of the thermal conductivity of the material was achieved by introducing porosity *via* the IL. The high porosity of the compacted nanostructured material was preserved by applying a mild compaction process consisting of cold pressing and subsequent annealing. Phonon-boundary scattering at pores was found to effectively reduce the mean free path of phonons. As a result of this strategy, record-high figure of merit values of up to 2 for Sb_2Te_3 nanomaterials could be obtained.

Deep eutectic solvents (DES) and their general benefits as synthetic media in the manufacturing of inorganic nanomaterials

DES and properties

Deep Eutectic Solvents (DES) were first reported in 2001 by Abbott *et al.*,[181] who noted IL-like properties and behaviour for the eutectic compositions of certain salt: H-bond donor (HBD) mixtures, especially choline chloride (ChCl) systems, where the eutectic depression was inexplicably profound.[182] In their broadest definition they are a combination of a hydrogen bond acceptor (HBA) which frequently is a salt, often satisfying itself the definition of an IL, alongside an H-bond donor (HBD); see Fig. 14 for some selected examples.

Strictly speaking, these eutectic mixtures are distinct from ILs. They are not necessarily ionic in nature, nor do they have the same properties as ILs, nor are they even a particularly new phenomenon, with the first reports now dating back 138 years.[183] However, a certain class of eutectics for materials synthesis have developed into a burgeoning field worthy of attention here, where we will specifically address the applications of Deep Eutectic Solvents (DES). The field of DES has now reached 20 years of age at the time of writing, and as such the basic properties and applications of DES are well-reviewed.[22,23,184–186] The excitement around DES is largely because they offer IL-type performance in applications but with an additional molecular component (the HBD), which makes them cheap and simple to produce, while increasing the accessible chemical space of designer 'green' solvent systems; the discussion on IL 'greenness' remains equally pertinent for DES (*vide supra*).[187] In terms of nanosynthesis, relevant properties include generally low surface tensions similar to ILs which promote high nucleation rates, and potential structural effects such as templating, capping, and stabilisation arising from the high ionic strength of potentially interacting compounds. Finally, as well as being solvent and template, the species of the DES can be used as reactive (*i.e.* non-catalytic) reagents towards materials such as (doped) carbons and polymers.[188–193]

DES are most frequently mixtures of ammonium salts with H-bond rich donor species, as in the archetypal system ChCl:urea where $x_{urea} = 0.67$.[194] However, many different systems are known and subdivided into different 'Types' I–V,[22,195–198] which encompasses quaternary ammoniums, metallic DES,[199] and hydrophobic systems[200] with myriad HBD and salt combinations. DES can therefore be chemically similar to ILs, such that the boundaries can become blurred, with the presence of common species such as $[cholinium]^+$.[201,202] Because the term 'deep eutectic' remains nebulous, works can be found where common eutectic mixtures are presented as 'DES' without exact characterisation of the phase diagram and behaviour. Thermodynamic interpretations suggest that the term 'DES' should refer only to mixtures where the melting point depression exceeds ideality.[203,204] There is no arbitrary 'eutectic depth' criterion to be met, so given that non-ideality is relatively simple to achieve by introducing H-bonding, the scope remains broad to engineer new solvents with a wide compositional liquid window.[205]

Nanostructure

Nanostructure is one of the key properties of ILs in nanosynthesis,[31] so it is pertinent to revisit this understanding for DES following a few recent reviews.[206–208] More advanced analyses generally refute the initial understanding of DES as simple ILs containing a complex anion-HBD chelate species at the supposed 'magic composition' of *e.g.* 1 : 2,[209] though the anion still plays a key role.[210,211] Introducing another component convolutes the structure relative to ILs due to more possible interactions (*i.e.* HBD–HBD).[212] The energy landscape of interactions in DES therefore appears quite flat,[213] with many interactions, configurations and spatial arrangement of the constituents. In ILs, the default structure is of amphiphilically separated domains. These domains are evident in small-angle scattering through defined *d*-spacing and computational simulations, and are exploitable in synthesis (*vide supra*). In DES, the

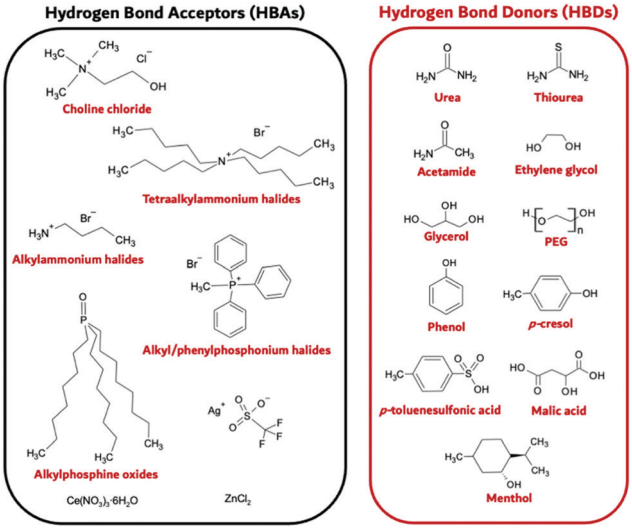

Fig. 14 Example Hydrogen Bond Donor (HBD) and Hydrogen Bond Acceptor (HBA) species known to support DES formation.

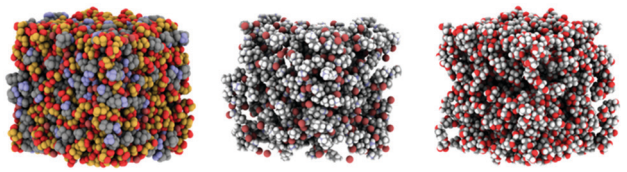

Fig. 15 EPSR model snapshots of nanostructured butylammonium bromide:glycerol DES ($x_{glycerol}$ = 0.67). In the right part of the figure, cations are shown in grey, NH_3^+ in blue, bromide in maroon, glycerol –OH in red, and CH_2 in yellow. In the middle and left, respectively, ions only and glycerol only are shown, in conventional colours. Reprinted with permission from ACS.[222]

default case is that there is not a defined *d*-spacing between hydrophobic and hydrophilic domains, because most common DES are generally not sufficiently amphiphilic in character, given that extensive H-bonding is generally introduced to create a strong non-ideal eutectic depression; however this motif can be induced (Fig. 15).[214,215] Moreover, small quantities of water are often introduced to DES[216] because, below a certain threshold, this affects the bulk structure negligibly[217] (see Fig. 16) while improving transport properties and is thus potentially appealing in materials synthesis, where the precipitation of nanoparticles in an already highly viscous medium can cause handling difficulties. However, the addition of water can affect the interfacial structure significantly,[218–220] and thus play a role in nanomaterial synthesis (notwithstanding effects such as the increased surface tension reducing nucleation rates). That is not to say that DES cannot be nanostructured nor that ILs must be. It has been observed that introducing additional H-bonding in ILs can eliminate the L_3-like bicontinuous phase.[38,221] More recent similar work has shown that careful design of DES, for example introducing long alkyl chains, can 'switch on' nanostructure, as outlined in Fig. 15.[222,223] In DES such as these, hydrophobic solutes experience local compositional effects where they affiliate with specific domains within the solvent, tuning solubility and the solvation environment.[224] There is therefore precedent for DES to act as multipurpose amphiphilic agents in nanosynthesis, just like ILs.[225] Further structural insights will soon be attainable *via* computational methodologies such as AIMD (*ab initio* molecular dynamics)[209] and MD (molecular dynamics) with polarisable force fields,[226,227] in combination with experimental scattering data,[206] with synergy between these bulk studies and those of the interface.[220,228,229]

DES as inorganic nanomaterial synthesis media

The similarities and differences between DES and ILs in nanosynthesis will now be highlighted through synthesis examples.[230] By far the most popular application of DES has been in electrochemistry, especially deposition of metallic films[231–239] and particles which can have elaborate high-index-terminated morphologies, possibly due to particle-DES interactions where the surface is capped along certain planes preferentially.[240–243] This review will not focus on electrochemistry however, as it is extensively covered elsewhere;[22,23,232] we will instead focus on comprehensively reviewing present wet-chemical and solvo-/ionothermal routes towards inorganic nanomaterials, since there is currently a gap in this area.

Bottom-up, wet-chemical synthesis of nanoparticles employing DES

In the first instance, DES can be used as drop-in hosts for synthesis of nanoparticles using known chemistry for the

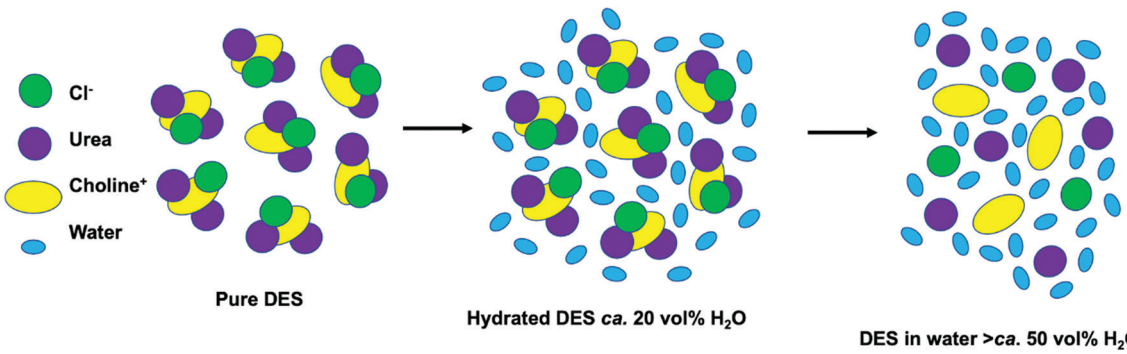

Fig. 16 Cartoon diagram showing structural changes in a DES starting with the pure choline Cl:urea DES (left). As the water content increases the hydrated DES regime is reached (middle, *ca.* 20 vol%), then the high concentration regime where everything is fully hydrated (*ca.* 50 vol%). Reprinted with permission from Elsevier.[207]

synthesis of metallic nanoparticles. This was first shown by Liao *et al.* who demonstrated the synthesis of very high-index faceted gold nanoparticles in snowflake, star, and thorn morphologies, in the ChCl:urea DES.[244] This work inspired numerous subsequent studies, who have shown various DES-based methodologies for the synthesis of AuNPs,[245] with control over morphology[246] enabling Au nanoflowers,[247] nanofoams,[248] highly fractal nanostars,[249] and nanosheets.[250] Using a 'natural DES' (NADES) allows this to be achieved without adding a reducing agent,[251] but morphology control, such as the formation of nanosheets, can still be achieved.[252] Gelated eutectics were applied in the size-controlled preparation of a series of noble metal nanoparticles.[253] Much like in ILs, laser ablation can also be used in a DES to create narrow-size-distribution Ag NPs,[254] and noble metal NPs such as Au assemble on the DES surface after sputtering *via* the same mechanism as in ILs.[255] Polydisperse Pd NPs were prepared by a short heat treatment of dilute K_2PdCl_4 in ChCl:EG DES, and loaded onto N-doped porous carbon in an integrated microfluidic approach.[256] Adhikari *et al.* introduced a methodology for the synthesis of large quantities of coinage metal colloids (Ag, Au) using a continuous flow millifluidic system. This was achieved using a designed dimethylammonium nitrate–polyol DES, which provides high atom economy and is intrinsically a capping reagent (see Fig. 17 for monodispersity analysis).[257] Nanoparticulate CuCl was isolated from ChCl:urea DES, following the reaction of copper chloride with ascorbic acid in the presence of the templating agent PVP (polyvinylpyrrolidone).[258] While this example was successful in CuCl preparation, it is also an example of a reaction which used an 'off-the-shelf' solvent, rather than taking the opportunity to use a reducing agent as the reactive HBD.

For oxides, Chen *et al.* used a co-precipitation method to isolate spherical magnetic Fe_3O_4 nanoparticles.[259] A DES-based method was developed by Dong *et al.*, where aqueous Tris ($(HOCH_2)_3CNH_2$) was added as an antisolvent to precipitate ZnO nanocrystals from ChCl:urea.[260] Xiong *et al.* synthesised hematite nanospindles, also using a DES-based antisolvent method.[261] Mn_2O_3 nanoparticles were prepared by reduction of Mn^{IV} by ascorbic acid in hydrated ChCl:ethylene glycol DES at 40 °C.[262] It has been shown by Hammond *et al.* that direct calcination of lanthanide nitrate hydrate:urea DES yields the corresponding lanthanide oxide or mixed hydroxide, depending on combustion temperature.[197] A similar pyrolytic method where T = 500–800 °C was used to prepare nanoparticulate Sn/SnO_2@C composites from ChCl:$SnCl_2$ DES.[263] Various DES such as ChCl:glucose have also been explored as reducing agents for $KMnO_4$ in the preparation of nanostructured Mn_xO_y; the high reactant concentration enabled by the DES led to the reaction to completion in less than 1 minute.[264] Nanocrystalline NiO of *ca.* 100 nm with high energy surface facets was precipitated from ChCl:urea by addition of NaOH, with subsequent centrifugation and calcination.[265]

DES have also been used in wet-chemical preparations of multinary compounds. A ChCl:citric acid DES was used to precipitate nanostructured BiOCl/$BiVO_4$ p–n heterojunctions from aqueous solution;[266] the same materials were previously prepared by sol–gel synthesis from ChCl:urea.[267] Zhang *et al.* used the ChCl:glycerol DES as a crystallisation medium for the octahedral NiCo–NH_3 complex, suitable for calcination into $NiCo_2O_4$ nanooctahedra.[268] In an interesting synthesis strategy, Ni foam was introduced into a $FeCl_3{\cdot}6H_2O$:urea DES; the abundance of redox-active Fe^{3+} in the DES oxidised the foam into Ni^{2+}, thus creating layered NiFe double hydroxide, effective in electrolysis of urea and water.[269] Nanosheets of $Cu_2(OH)_3NO_3$ were precipitated from a 44 : 1 M ratio mixture of PEG200 and NaOH, that was described as a DES, but without presented phase characterisation.[270] This category of polyol:-hydroxide systems were expanded to different alkali metal hydroxides and higher PEG weights (PEG400, PEG600) in the preparation of nanoparticulate transition metal oxides, cobaltites, manganites, and cuprites, under mild conditions and in sheet morphologies,[271] and was also used for $CdCo_2O_4$.[272] Nanosheets of either single-metal or high-entropy metal phosphides were achieved by direct calcination of DES comprising tetrabutylphosphonium chloride:ethylene glycol, and containing either the respective metal chlorides, or an equimolar mixture of $CoCl_2{\cdot}6H_2O$, $CrCl_3{\cdot}6H_2O$, $FeCl_3{\cdot}6H_2O$, $MnCl_2{\cdot}4H_2O$, and $NiCl_2{\cdot}6H_2O$.[273] Various nanoporous (silver) selenidostannates were prepared by Wang *et al.* from eutectic mixtures of alkylamine hydrochlorides, with interesting tuneable properties such as reversible thermochromism.[274] It has been shown that the choice of DES strongly dictates the growth process.[275] Even sheet and flower-like nanostructured hierarchical intermetallic nitro–sulfide compounds have been synthesised: here, mixed-metallic DESs containing $FeCl_3{\cdot}6H_2O$, $CoCl_2{\cdot}6H_2O$ and $NiCl_2{\cdot}6H_2O$ were directly annealed at 350 °C for 12 hours.[276] Direct annealing has also been used to prepared Zn and Cu vanadates of the type $M_2V_2O_{7-\delta}$, from the respective oxides dissolved in ChCl:urea.[277] This approach takes advantage of the often high metal oxide solubility in DES,[278] and was expanded to synthesis of vanadates

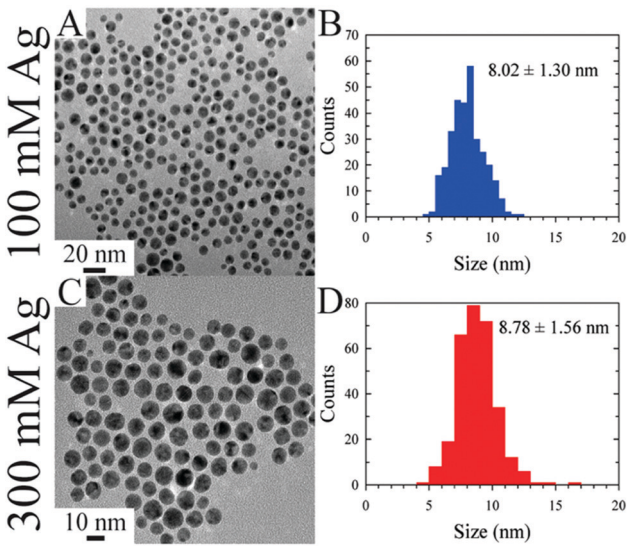

Fig. 17 TEM images and particle size distribution histograms for Au nanoparticles produced in continuous flow in task-specific DES at different Ag (sic) concentrations. Reprinted with permission from ACS.[257]

of the type $MV_2O_{6-\delta}$, where the DES was noteworthy for introducing oxygen vacancies, which reduced the band gap relative to the defect-free material.[279] Cobalt vanadate (CoV_2O_6) was also prepared by Thorat *et al.*, *via* a sol–gel route followed by annealing, and in this case the reaction temperature was significantly reduced by the presence of the ChCl:malonic acid DES.[280] Ni/Ni_3N nanocomposites have been prepared by Gage *et al.*, who directly annealed a unique ChCl:urea:nickel acetate gel to form core–shell nanoparticles with well-defined facets. This approach shows how DES can be valuable in N-doping of materials, as well as the usual structure-directing and surfactant-free positive aspects.[281] Composite tungsten-molybdenum oxides were prepared from aqueous ChCl:ethylene glycol DES, with the DES–water mixture yielding composites with prismatic morphologies.[282] Calcium phosphate nanoparticles were rapidly precipitated from the reaction of $CaCl_2$ and K_2HPO_4 in ChCl:urea, with the final product size dictated by the synthesis temperature,[283] and further by the choice of precursor reactants and solvents.[284] DES have also been used in the synthesis of nanoparticulate SiO_2, following the common sol–gel route but substituting the DES as the reaction solvent[285] or additive.[286] A photochromic composite of WO_3–MoO_3 was formed by reaction of acetic acid with ammonium tungstate and ammonium heptamolybdate in a ChCl:EG solution, with the solvent acting simply as a low-cost synthesis medium.[287] Boston *et al.* demonstrated a 2-step heating process using DES; first, the DES and its (hydrated) metal precursors are dehydrated at <100 °C, then calcined at high temperature to yield nanostructured materials such as $BaTiO_3$.[288] Gómez Rojas *et al.* have been particularly prolific in their deployment of this methodology in the preparation of the superconducting materials $Yba_2Cu_3O_{7-x}$ (aka. YBCO or 123),[289,290] and $Bi_2Sr_2Ca_{n-1}Cu_nO_{2n+4+x}$ (where $n = 2$; aka. BSCCO, Bi-2212),[291] as well as various strontium niobates.[292,293] The authors contrasted the performance of DES with ILs in this synthetic methodology, concluding that common chloride-containing DES can lead to lower phase purity through concomitant metal chloride formation, noting that the chloride phase can still recombine to the respective oxide if the calcination temperature is sufficiently high.[294]

Ionothermal methods

When used in the synthesis of materials such as zeolites and organic–inorganic frameworks, DES can function in the same way as ILs, providing solvent-directed templating of the resultant materials. This 'ionothermal' methodology is a rather attractive and versatile strategy,[295] which has gathered significant attention following its recent demonstration and review by Walton *et al.* and thus will also not be covered exhaustively here;[87,296–299] moreover, it is less pertinent to this review since much of the literature is focused towards open-framework structure synthesis, rather than nanoparticulate or nanostructured media.[300] A DES can provide a versatile IL-type synthesis environment, at a fraction of the synthetic complexity and cost, for example in the preparation of tubular $BiVO_4$,[301] Mg–Al layered double hydroxide,[302] or Mn-doped $SnHPO_3$.[303]

Such high-temperature synthesis strategies in DES exist somewhere between the extremes of true ionothermal and solvothermal methods. Generally, compared to molecular liquids, DES have high thermal stability and lower vapour pressure. This is not always the case, of course, with low stabilities for certain DES; for example, ChCl decomposes, urea begins to thermally hydrolyse at 80 °C, and many acidic choline chloride DES readily esterify even at room temperature.[304,305] Considered alongside ILs, then, the thermal stability of DES is lower, DES components tend to be more reactive and interacting, and the molecular components (as well as impurities or additives such as water) introduce a nonzero vapour pressure, which depends on the nature of the HBD. Indeed, polymorph-specific crystallisation strategies have even been developed by evaporation of volatile HBDs from DES at room temperature and pressure.[306] Thus, we make the distinction here between 'ionothermal' processes, where the vapour pressure of the DES is low and the DES provides a templating effect, but is not itself a reactant, and 'solvothermal' ones.

Deep eutectic-solvothermal synthesis

The 'Deep Eutectic-Solvothermal' methodology was first introduced by Hammond *et al.* in the preparation of nanostructured CeO_2 for CO oxidation catalysis. Here, the DES is not considered a pseudo-IL as in ionothermal synthesis. In a Deep Eutectic-Solvothermal reaction, the solvent contains a significant molecular component which imposes non-negligible vapour pressures at the chosen synthesis temperature, and the solvent plays more than a spectator role in the reaction.[307] In this example, the ChCl:urea (x_{urea} = 0.67) DES was used alongside $Ce(NO_3)_3{\cdot}6H_2O$ as the cerium source. Solvothermal conditions caused thermal hydrolysis of the urea HBD into NH_4^+ and CO_3^{2-} ions, precipitating orthorhombic monohydrated cerium oxycarbonate $Ce_2O(CO_3)_2{\cdot}H_2O$, which could then be calcined into CeO_2. At low water content, the surface tension of the DES is lowest, favouring rapid nucleation of small nanoparticles. Increasing the water content decreases nucleation rate, but increases the hydrolysis reaction rate by increasing the relevant reagent (H_2O) concentration and overall system diffusivity, which was the limiting condition. This was combined with neutron diffraction studies showing pre-structuring of reactive compounds (*i.e.* urea, water, nitrate) around Ce^{3+} centres, potentially further facilitating rapid reaction and precipitation. Thus, through controlling water content and temperature at constant reaction time, it was possible to select the product morphology, from small nanoparticles to highly catalytically active 1D structures such as nanowires, nanorods, and cubic phases (see Fig. 18). However, it should be noted that high water contents are expected to 'destroy' the DES structure, such that at some point above around 50 vol% H_2O, all the dissolved compounds are in a fully hydrated state and bulk water begins to percolate through the mixture.[217] More recently, this approach has been adapted by Exposito *et al.* to take advantage of the high heat- and mass-transfer conditions offered by continuous flow reactors.[308] This approach allowed quantitative yields of nanostructured CeO_2, even with short residence times and conventional heating, overall forming a relatively mild set of synthesis conditions.

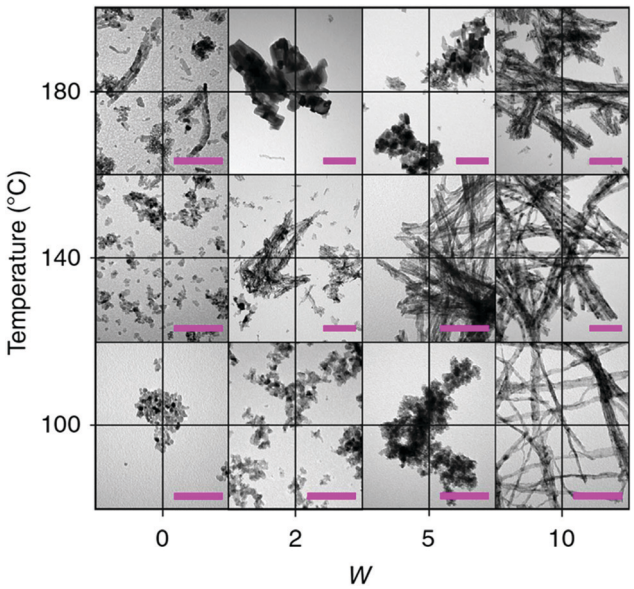

Fig. 18 TEM micrographs as a deep eutectic-solvothermal synthetic phase diagram for CeO_2 nanoparticles post-calcination, where scale bars depict 100 nm, and *w* is the H_2O/[DES] molar hydration ratio. Reprinted with permission from Springer Nature.[307]

Morphology control was also achieved under deep eutectic-solvothermal conditions in a green chemical microwave-assisted preparation of small (low-temperature, low water fraction), 1D (low-temperature, high water fraction) and large crystalline (high-temperature, high water fraction) iron oxide nanoparticles. These were useful as photoanode materials for solar water splitting, imaging *via* superparamagnetism, or as recyclable catalysts.[150,309–311] Here, the ChCl:urea DES was again used as a degradable reaction agent, creating basic conditions upon thermal hydrolysis of urea to precipitate iron oxides,[309] with WAXS data showing minimal solvent degradation, except under the most extreme conditions. A number of advanced techniques were used to study this reaction in depth under conventional heating, as the first *in situ* study of solvothermal conditions in DES.[312] Neutron diffraction and EXAFS measurements of the initial state showed $[Fe(L)_3(Cl)_3]$ solvation complexes for both pure and hydrated DES where 'L' is an O-containing ligand. *In situ* SANS and EXAFS showed high initial kinetics for the conversion of the iron salt into [–O–Fe–O–] networks. For the hydrated DES, these species immediately nucleated and grew into 1D structures, followed by a rapid fusion stage. For the reaction in the pure DES, nanoparticles only precipitated after 5000 s due to higher solubility of [–O–Fe–O–] species, and following precipitation, the particles grew very slowly to small oblate spheroids (Fig. 19), but were screened from fusion. Isotope substitution suggested a choline-rich surface layer, with the cation acting as a capping surfactant in the same way as ILs. When the same methodology was applied using ChCl:glycerol DES instead by Zhang *et al.*, nanoparticulate iron alkoxides were formed.[313]

An elegant preparation of colloidal nanoparticulate Ag was shown by Adhikari *et al.*, demonstrating that, through careful design of a silver triflate:acetamide DES, the solvent can be used without requiring additives such as metal salts and capping surfactants. Though this was deemed a wet chemical process for metallic nanoparticles as discussed *vide supra*, it meets our definition of 'deep eutectic-solvothermal', since acetamide has non-negligible vapour pressure at the chosen synthesis temperature of 200 °C, and the solvent plays an active role as template and reactive metal ion source. Under microwave irradiation, silver ions are rapidly reduced by the sole reactive additive, oleylamine, to form stable, high colloidal concentrations (up to 54 mg mL^{-1}) of relatively monodisperse $[Ag]_0$ nanocrystals.[314] This derived from the group's earlier work, where chloride-free cholinium DES (*i.e.* X^- = nitrate or acetate) were used to prepare colloidal silver nanoparticles following microwave-solvothermal treatment of solubilised $AgNO_3$.[315] As with the previous example, this method was shown to be far faster and less energy-intensive than using ChCl DES or neat oleylamine as the solvent in the formation of monodisperse AgNPs.

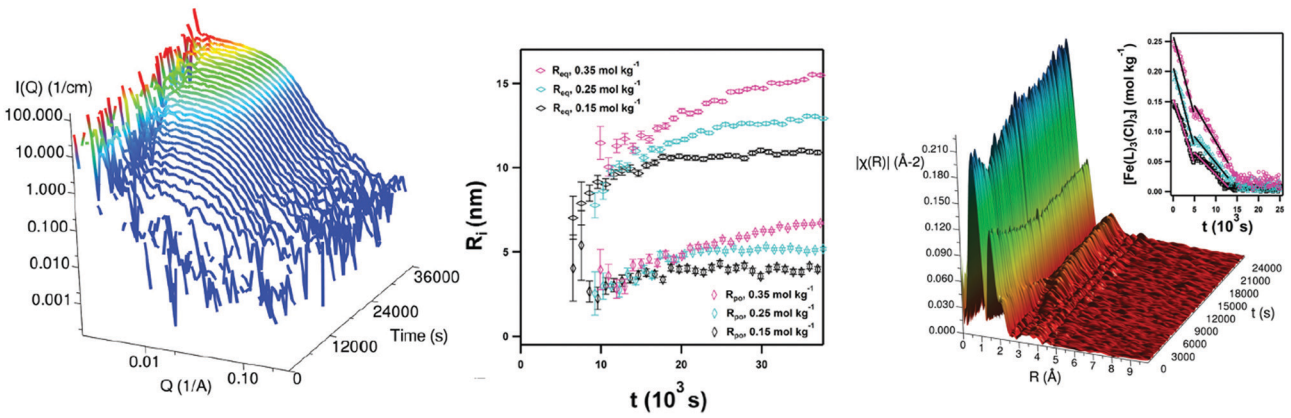

Fig. 19 (left) *In situ* small-angle neutron scattering data for iron oxide formation in a choline Cl:Urea DES. (middle) Results from fits to the SANS data, as a function of iron nitrate concentration, showing evolution in polar and equatorial iron oxide nanoparticle radius over time. (right) *In situ* EXAFS data and (inset) extracted Fe reaction kinetics, showing the same critical nucleation stage (5000 s) as the SANS data, and a change in rate at this point. Adapted with permission from the Royal Society of Chemistry.[312]

In addition to noble metals, further deep eutectic-solvothermal nanoparticulate metal oxide synthesis routes exist. Datta *et al.* were able to achieve morphology control of V_2O_5, and thus dictate the performance of the resultant nanostructured cathode materials, by altering the water content in a solvothermal reaction using ChCl:urea DES.[316] Using ESI-MS, the authors were able to identify the vast quantity of species formed during solvothermal decomposition of the solvent, highlighting the mixture complexity. Spherical nanoparticles of Mn_3O_4 with 25 nm diameter were prepared by reaction of $KMnO_4$ in ChCl:EG at 140 °C.[317] Li *et al.* prepared cubic MgO by calcination of $MgCO_3$ cubes, formed by solvothermal treatment of a $MgCl_2{\cdot}6H_2O$:urea DES.[318]

Several works have focused on the synthesis of nanostructured or mesoporous TiO_2 in DES, such as through sol–gel routes.[319] For example, Sandhu *et al.* used a novel ChCl:hydroquinone DES in a fluorine-free synthesis of titania with a high population of the (111) anatase surface facet, creating more active dye degradation catalysts.[320] Applying a DES based on ChCl:oxalic acid, Wang *et al.* were able to synthesise (001) and (101) facet-rich TiO_2 with morphology evocative of *crassula perforata*. Here, the combination of morphology, defects, and presence of surface heterojunctions gave over an order of magnitude improvement in photocatalytic water splitting relative to commercial P25.[321] Similarly, a 20-fold improvement in H_2 production rate was observed for TiO_2 derived from ChCl:betaine:oxalic acid DES. The high performance was ascribed to the presence of brookite-rutile heterophase junctions, where the phase ratio could be dictated by the DES mixing ratio[322] This highlights both one of the strengths and one of the issues of using DES in this area; as long as synthesis is conducted within the liquid window, the entire phase diagram is relevant, and it is not always productive to overfocus on the eutectic composition with respect to applications when off-eutectic mixtures can make useful or even better materials.

A number of solvothermal routes towards sulfur-containing materials have also been shown using DES. These DES usually involve thiourea, which functions as a primary or secondary HBD in the solvent, and provides a sulfur source upon thermal degradation. Jian *et al.* synthesised porous $NiCo_2S_4$ using the novel PEG200:thiourea DES, where PEG200 offered templating of hierarchical porosity under solvothermal conditions.[323] The same DES was used by Xu *et al.* to prepare CdS particles, which were then subjected to a second solvothermal treatment with the same DES to prepare core–shell CdS@CeO_2 nanocomposites.[324] Another example of this PEGylated DES is shown by Zhao *et al.*, where it again provided sulfur and templating in the preparation of Fe_3S_4 nanosheets, whose porosity yielded strong performance in the electrochemical fixation of N_2.[325] Ni_3S_2 nanosheets were obtained by solvothermal treatment of electrodeposited Ni–Co on nickel foam, with a ChCl:EG DES containing low concentrations of thiourea.[326] A similar solvothermal sulfurisation method was used to obtain nanospheric Ni_3S_2, with strong supercapacitance.[327,328] Low concentrations of thiourea and metal chlorides in the ChCl:urea DES yielded chalcopyrite $CuInS_2$ in a nanorod morphology under microwave irradiation.[329] Nanoparticles of the popular kesterite semiconductor Cu_2ZnSnS_4 (CZTS) with a high defect concentration were prepared by Karimi *et al.* in their solvothermal treatment of the respective metal chlorides, using thiourea as a sulfur source, from the ChCl:urea eutectic.[330] In the ChCl:EG DES, NiS_2 nanospheres were synthesised by solvothermal treatment of nickel sulfate, sodium thiosulfate and EDTA, making it noteworthy as the only synthesis not to use thiourea as a sulfur source.[331]

Similar methodologies have been used to prepare multinary and composite compounds in DES under solvothermal conditions. Spinel ferrites of the form MFe_2O_4 (M = Mg, Zn, Co, Ni) were synthesised at much lower reaction temperatures than comparable techniques by using a ChCl:maleic/malonic/oxalic acid, or ChCl:urea or ChCl:EG DES.[332,333] Jiang *et al.* used a ChCl:triethanolamine DES to template a 3D porous nanostructure for $NaTi_2(PO_4)_3$, interesting as an anode for sodium–ion batteries once calcined with sucrose to cast it onto a carbon substrate.[334] In a control experiment, it was shown that aqueous mixtures of the HBD and salt respectively formed prismatic and globular nanoparticles. Various metal molybdates (M = Mg, Fe, Mn) have been prepared by Baby *et al.* using ChCl:urea in solvothermal reactions.[335] The controlled degradation of the DES was found to template more desirable active morphologies useful in toxin sensing. $[Co(NH_3)_4CO_3]Cl$ with a porous 2D nanosheet morphology was synthesised by Liu *et al.* solvothermally; following 'activation' by casting onto Ni foam, the amorphous CoOOH performed well in the oxygen evolution reaction.[336] Narayanam *et al.* used solvothermal heating of a volatile ChCl:phenol DES to produce crystalline polyoxo-titanium clusters, relevant as molecular analogues of TiO_2, with nuclearities of up to 28.[337] $RuCu_2O_4$ is a mixed oxide showing high electrical conductivity, stability, and electrochemical performance, and thus interesting in hybrid supercapacitor cells; Karade *et al.* were able to synthesise this material in nanofibrous form under solvothermal conditions with a rather high water content of 50 vol% in their DES.[338] $NiCo_2O_4$ nanorods were solvothermally grown on pre-prepared MoS_2 nanosheets in ChCl:urea by Zhao *et al.* (110 °C, 16 h),[339] and on reduced graphene oxide by Ni *et al.*[340] Alloyed nanoclusters of PtCu were solvothermally grown onto multi-walled carbon nanotubes in a DES, with the solvent apparently facilitating a controlled dispersion of nanoparticles on the nanotube surface.

Scope of DES in nanomanufacturing

Having reviewed the applications of DES in nanomanufacturing, it is pertinent to comment on their scope in the field. Clearly, DES show many of the same promising features of ILs, such as structure direction, morphological templating and assembly control, as well as potentially lower toxicity and improved environmental credentials. DES have potentially great potential, since the addition of another species (the HBD) widens the accessible phase space from the pure ionic melt to a wide range of ionic–molecular mixture compositions. They also show significant capability as drop-in replacements for conventional solvents due to these advantages.

DES also share many of the drawbacks of ILs, especially the potentially enormous viscosity,[215] degradation,[341] solution

complexity,[312] and not being intrinsically green nor responsibly sourced.[187] Moreover, all of the described examples derive from known chemistry. This applies whether the example methodology is: 1. simple, such as using a DES as a purely spectating solvent host for a known reaction; 2. more advanced, such as using a DES as an ionothermal synthesis template facilitating higher reaction temperature without autogenous pressure; 3. the most intricate, using a DES in *i.e.* a microwave-solvothermal reaction where it functions as solvent, template, and reactant simultaneously. However, the most exciting aspect of DES and ILs is in their designer nature, where they can potentially be altered to make new chemistries viable.[342] Thus, it will be exciting to watch for new, advanced synthesis protocols with high-level design. We foresee many novel applications of these solvents in 'tuneable' role they are frequently espoused as, rather than selecting a known, 'off-the-shelf' DES system as a point of interest.[22,23]

Insights

The lessons learned from these examples are therefore:

- By employing ILs and DES in the manufacturing of nanomaterials it is possible to obtain materials that cannot be obtained using conventional routes.

- The nature of the liquid critically determines the particle morphology and size.

- The IL or DES controls the assembly process of nanostructures.

- ILs and DES enable phase-selective synthesis.

- In contrast to classical surfactants and NP stabilisers, the nanostructures can be cleaned easily of ILs and DES, a requirement for many applications.

- The use of a task-specific IL or DES can prevent the use of toxic and hazardous substances.

- Uncommon, energy-efficient conversion methods like microwave and ultrasound heating synergise with ILs and DES to enhance the manufacturing of nanomaterials.

Conclusions

The presented examples illustrate the transformative character and unique opportunities that ILs and DES have in the deliberate, designed synthesis of nanomaterials. Because of their high modularity, they can be tailored for a specific synthesis through chemical structure variations unlike any conventional solvents. Unique to ILs and DES is their truly multifunctional character, which allows them to serve as more than just the solvent and reaction medium. With ILs and DESs, properties and property combinations can be achieved that are unattainable with conventional solvents. This also allows the use of unconventional synthetic methods, and the development of new techniques. It is expected that the presented, universal methods for the production of nanomaterials from ILs, and soon also from DES, will allow for the manufacturing of improved products and devices and open up new horizons for nanosynthesis. The methods are generally, faster, safer, more energy- and atom (material)-efficient, use smaller quantities of less toxic chemicals, negate the use of auxiliary substances (such as surfactants and stabilisers), reduce the risk of pollution, reduce and prevent waste, and thus overall, they reduce the risk to human health and minimise the impact on the environment, while being economically viable. In addition, these unconventional production methods will allow us to develop new and improved nanomaterials, pertinent for a wide number of applications such as catalysis and wastewater treatment, solar cells and solid-state lighting as well as biomedicine. Solutions beyond the current leading nanomanufacturing technologies will be provided that advance and innovate nanomanufacturing to achieve sustainability. This will, on one hand, lead to new technological and scholarly knowledge with respect to understanding the designed manufacturing of nanomaterials and the discovery of new materials. In a broader sense, societal welfare will be improved through safer, more energy efficient and benign production of nanomaterials.

Conflicts of interest

There are no conflicts to declare.

Acknowledgements

AVM would like to thank the European Research Council for sponsoring the early explorations of ionic liquids for materials synthesis (ERC-StG 200475), the Royal Swedish Academy of Science for funding the effort to use ionic liquids for manufacturing materials for energy related applications through the Göran Gustafsson prize in Chemistry 2017 and the Villum Foundation for support through a Villum Investigator Grant that provides the opportunity to deeply explore the use of these unconventional solvents for nanosynthesis.

References

1 D. Vollath, *Nanomaterials: An Introduction to Synthesis, Properties and Applications*, Wiley-VCH, Weinheim, 2nd edn, 2013.
2 R. D. Rogers and K. R. Seddon, Ionic Liquids – Solvents of the Future?, *Science*, 2003, **302**(5646), 792–793, DOI: 10.1126/science.1090313.
3 J. D. Holbrey, W. M. Reichert, R. Reddy and R. D. Rogers, *Ionic liquids as green solvents: progress and prospects*, Washington, DC, 2003, pp. 121–133.
4 P. T. Anastas and J. C. Warner, *Green Chemistry: Theory and Practice*, Oxford University Press, New York, 1998.
5 D. T. Allen and D. R. Shonnard, *Green Engineering: Environmental Conscious Design of Chemical Processes*, Prentice-Hall, Upper Saddle River, 2002.
6 B. Chan, N. Chang and M. Grimmett, The Synthesis and Thermolysis of Imidazole Quaternary Salts, *Aust. J. Chem.*, 1977, **30**, 2005–2013, DOI: 10.1071/CH9772005.
7 Y. Chauvin and H. Olivierbourbigou, Nonaqueous Ionic Liquids as Reaction Solvents, *CHEMTECH*, 1995, **25**, 26–30.
8 M. Smiglak, A. Metlen and R. D. Rogers, The Second Evolution of Ionic Liquids: From Solvents and Separations to Advanced Materials—Energetic Examples from the Ionic Liquid Cookbook, *Acc. Chem. Res.*, 2007, **40**(11), 1182–1192, DOI: 10.1021/ar7001304.
9 J. Dupont, R. F. De Souza and P. A. Z. Suarez, Ionic Liquid (Molten Salt) Phase Organometallic Catalysis, *Chem. Rev.*, 2002, **102**(10), 3667–3692, DOI: 10.1021/cr010338r.

10 F. Endres, Ionic Liquids: Solvents for the Electrodeposition of Metals and Semiconductors, *ChemPhysChem*, 2002, **3**, 145–154, DOI: 10.1002/1439-7641(20020215)3:2<144::AID-CPHC144>3.0.CO;2-%23.
11 A. E. Jimenez, M. D. Bermudez, P. Iglesias, F. J. Carrion and G. Martinez-Nicolas, 1-*N*-Alkyl-3-Methylimidazolium Ionic Liquids as Neat Lubricants and Lubricant Additives in Steel-Aluminium Contacts, *Wear*, 2006, **260**, 766–782, DOI: 10.1016/j.wear.2005.04.016.
12 R. P. Swatloski, S. K. Spear, J. D. Holbrey and R. D. Rogers, Dissolution of Cellose with Ionic Liquids, *J. Am. Chem. Soc.*, 2002, **124**, 4974–4975, DOI: 10.1021/ja025790m.
13 H. Saitoh, Introduction of BASILTM (Biphasic Acid Scavenging Utilizing Ionic Liquids) Technology: The First Commercialized Process with Ionic Liquids, *Kagaku Kogaku*, 2006, **70**, 121–122.
14 S. Dai, Y. H. Ju and C. E. Barnes, Solvent Extraction of Strontium Nitrate by a Crown Ether Using Room-Temperature Ionic Liquids, *J. Chem. Soc., Dalton Trans.*, 1999, 1201–1202, DOI: 10.1039/a809672d.
15 A. E. Visser, R. P. Swatloski, W. M. Reichert, R. Mayton, S. Sheff, A. Wierzbicki, J. H. Davis Jr. and R. D. Rogers, Task-Specific Ionic Liquids for the Extraction of Metal Ions from Aqueous Solutions, *Chem. Commun.*, 2001, 135–136, DOI: 10.1039/B008041L.
16 C. Chiappe and D. Pieraccini, Regioselective Iodination of Arenes in Ionic Liquids Mediated by the Selectfluor TM Reagent F-TEDA-BF4, *ARKIVOC*, 2002, **XI**, 149–255.
17 J. Ding, V. Desikan, X. X. Han, T. L. Xiao, R. F. DIng, W. S. Jenks and D. W. Armstrong, Use of Chiral Ionic Liquids as Solvents for the Enantioselective Photoisomerization of Dibenzobicyclo[2.2.2] Octatrienes, *Org. Lett.*, 2005, **7**, 335–337, DOI: 10.1021/Ol047599i.
18 L. Kiss, T. Kurtan, S. Antus and H. Brunner, Further Insight into the Mechanism of Heck Oxyarylation in the Presence of Chiral Ligands, *ARKIVOC*, 2003, **5**, 69–76, DOI: 10.3998/ark.5550190.0004.507.
19 J. Mo, L. Xu and J. Xiao, Ionic Liquid-Promoted, Highly Regioselective Heck Arylation of Electron-Rich Olefins by Aryl Halides, *J. Am. Chem. Soc.*, 2005, **127**, 751–760, DOI: 10.1021/ja0450861.
20 T. Welton, Ionic Liquids in Catalysis, *Coord. Chem. Rev.*, 2004, **248**, 2459–2477, DOI: 10.1016/j.ccr.2004.04.015.
21 R. Meyer, J. Köhler and A. Homburg, *Explosives*, Wiley-VCH, Weinheim, 7th edn, 2016.
22 E. L. Smith, A. P. Abbott and K. S. Ryder, Deep Eutectic Solvents (DESs) and Their Applications, *Chem. Rev.*, 2014, **114**, 11060–11082, DOI: 10.1021/cr300162p.
23 B. B. Hansen, S. Spittle, B. Chen, D. Poe, Y. Zhang, J. M. Klein, A. Horton, L. Adhikari, T. Zelovich, B. W. Doherty, B. Gurkan, E. J. Maginn, A. Ragauskas, M. Dadmun, T. A. Zawodzinski, G. A. Baker, M. E. Tuckerman, R. F. Savinell and J. R. Sangoro, Deep Eutectic Solvents: A Review of Fundamentals and Applications, *Chem. Rev.*, 2020, **121**(3), 1232–1285, DOI: 10.1021/acs.chemrev.0c00385.
24 J. Fuller, R. T. Carlin, H. C. De Long and D. Haworth, Structure of 1-Ethyl-3-Methylimidazolium Hexafluorophosphate: Model for Room Temperature Molten Salts, *J. Chem. Soc., Chem. Commun.*, 1994, 299–300, DOI: 10.1039/c39940000299.
25 J. D. Holbrey, W. M. Reichert, M. Nieuwenhuyzen, S. Johnston, K. R. Seddon and R. D. Rogers, Crystal Polymorphism in 1-Butyl-3-Methylimidazolium Halides: Supporting Ionic Liquid Formation by Inhibition of Crystallization, *Chem. Commun.*, 2003, 1636–1637, DOI: 10.1039/b304543a.
26 A. S. Larsen, J. D. Holbrey, F. S. Tham and C. A. Reed, Designing Ionic Liquids: Imidazolium Melts with Inert Carborane Anions, *J. Am. Chem. Soc.*, 2000, **122**, 7264–7272, DOI: 10.1021/Ja0007511.
27 P. A. Z. Suarez, J. E. L. Dullius, S. Einloft, R. F. De Souza and J. Dupont, The Use of New Ionic Liquids in Two-Phase Catalytic Hydrogenation Reaction by Rhodium Complexes, *Polyhedron*, 1996, **15**, 1217–1219, DOI: 10.1016/0277-5387(95)00365-7.
28 J. S. Wilkes and M. J. Zaworotko, Air and Water Stable 1-Ethyl-3-Methylimidazolium Based Ionic Liquids, *J. Chem. Soc., Chem. Commun.*, 1992, **13**, 965–967, DOI: 10.1039/c39920000965.
29 S. A. Forsyth, J. M. Pringle and D. R. MacFarlane, Ionic Liquids – An Overview, *Aust. J. Chem.*, 2004, **57**(2), 113–119, DOI: 10.1071/CH03231.
30 J. D. Holbrey and K. R. Seddon, Ionic Liquids, *Clean Prod. Process.*, 1999, **1**, 223–236, DOI: 10.1007/s100980050036.
31 R. Hayes, G. G. Warr and R. Atkin, Structure and Nanostructure in Ionic Liquids, *Chem. Rev.*, 2015, **13**, 6357–6426, DOI: 10.1021/cr500411q.
32 M. A. Gebbie, M. Valtiner, X. Banquy, E. T. Fox, W. A. Henderson and J. N. Israelachvili, Ionic Liquids Behave as Dilute Electrolyte Solutions, *Proc. Natl. Acad. Sci. U. S. A.*, 2013, **110**(24), 9674–9679, DOI: 10.1073/pnas.1307871110.
33 M. A. Gebbie, A. M. Smith, H. A. Dobbs, A. A. Lee, G. G. Warr, X. Banquy, M. Valtiner, M. W. Rutland, J. N. Israelachvili, S. Perkin and R. Atkin, Long Range Electrostatic Forces in Ionic Liquids, *Chem. Commun.*, 2017, **53**(7), 1214–1224, DOI: 10.1039/C6CC08820A.
34 S. Perkin, M. Salanne, P. Madden and R. Lynden-Bell, Is a Stern and Diffuse Layer Model Appropriate to Ionic Liquids at Surfaces?, *Proc. Natl. Acad. Sci. U. S. A.*, 2013, **110**(44), E4121–E4121, DOI: 10.1073/pnas.1314188110.
35 A. A. Lee, C. S. Perez-Martinez, A. M. Smith and S. Perkin, Scaling Analysis of the Screening Length in Concentrated Electrolytes, *Phys. Rev. Lett.*, 2017, **119**(2), 026002, DOI: 10.1103/PhysRevLett.119.026002.
36 A. M. Smith, A. A. Lee and S. Perkin, Switching the Structural Force in Ionic Liquid-Solvent Mixtures by Varying Composition, *Phys. Rev. Lett.*, 2017, **118**(9), 1–5, DOI: 10.1103/PhysRevLett.118.096002.
37 C. P. Cabry, L. D'Andrea, K. Shimizu, I. Grillo, P. Li, S. E. Rogers, D. W. Bruce, J. N. Canongia Lopes and J. M. Slattery, Exploring the Bulk-Phase Structure of Ionic Liquid Mixtures Using Small-Angle Neutron Scattering, *Faraday Discuss.*, 2017, **III**, 265–289, DOI: 10.1039/C7FD00167C.
38 R. Hayes, S. Imberti, G. Warr and R. Atkin, Amphiphilicity Determines Nanostructure in Protic Ionic Liquids, *Phys. Chem. Chem. Phys.*, 2011, **13**(8), 3237–3247, DOI: 10.1039/c0cp01137a.
39 J. N. Canongia Lopes, M. Costa Gomes and A. A. H. Padua, Nonpolar, Polar, and Associating Solutes in Ionic Liquids, *J. Phys. Chem. B*, 2006, **110**, 16816–16818, DOI: 10.1021/jp063603r.
40 K. Shimizu, C. E. S. Bernardes, A. Triolo and J. N. Canongia Lopes, Nano-Segregation in Ionic Liquids: Scorpions and Vanishing Chains, *Phys. Chem. Chem. Phys.*, 2013, **15**, 16256–16262, DOI: 10.1039/c3cp52357h.
41 H. K. Kashyap, C. S. Santos, H. V. R. Annapureddy, N. S. Murthy, C. J. Margulis and E. W. Castner Jr., Temperature-Dependent Structure of Ionic Liquids: X-Ray Scattering and Simulations, *Faraday Discuss.*, 2012, **154**, 133–143, DOI: 10.1039/C1FD00059D.
42 Y. Wang and G. A. Voth, Tail Aggregation and Domain Diffusion in Ionic Liquids, *J. Phys. Chem. B*, 2006, **110**, 18601–18608, DOI: 10.1021/jp063199w.
43 T. Alammar, O. Shekhah, J. Wohlgemuth and A.-V. Mudring, Ultrasound-Assisted Synthesis of Mesoporous Beta-Ni(OH)(2) and NiO Nano-Sheets Using Ionic Liquids, *J. Mater. Chem.*, 2012, **22**(35), 18252–18260, DOI: 10.1039/c2jm32849f.
44 A. Triolo, O. Russina, H.-J. Bleif and E. Di Cola, Nanoscale Segregation in Room Temperature Ionic Liquids, *J. Phys. Chem. B*, 2007, **111**, 4641–4644, DOI: 10.1021/jp067705t.
45 O. Russina, A. Triolo, L. Gontrani, R. Caminiti, D. Xiao, L. G. Hines Jr., R. A. Bartsch, E. L. Quitevis, N. V. Plechkova and K. R. Seddon, Morphology and Intermolecular Dynamics of 1-Alkyl-3-Methylimidazolium Bis{(Trifluoromethane)Sulfonyl}amide Ionic Liquids: Structural and Dynamic Evidence of Nanoscale Segregation, *J. Phys.: Condens. Matter*, 2009, 21, DOI: 10.1088/0953-8984/21/42/424121.
46 C. Hardacre, J. D. Holbrey, M. Nieuwenhuyzen and T. G. A. Youngs, Structure and Solvation in Ionic Liquids, *Acc. Chem. Res.*, 2007, **40**(11), 1146–1155, DOI: 10.1021/ar700068x.
47 T. G. A. Youngs, J. D. Holbrey, C. L. Mullan, S. E. Norman, M. C. Lagunas, C. D'Agostino, M. D. Mantle, L. F. Gladden, D. T. Bowron and C. Hardacre, Neutron Diffraction, NMR and Molecular Dynamics Study of Glucose Dissolved in the Ionic Liquid 1-Ethyl-3-Methylimidazolium Acetate, *Chem. Sci.*, 2011, **2**(8), 1594–1605, DOI: 10.1039/c1sc00241d.
48 D. T. Bowron, C. D'Agostino, L. F. Gladden, C. Hardacre, J. D. Holbrey, M. C. Lagunas, J. McGregor, M. D. Mantle, C. L. Mullan and T. G. A. Youngs, Structure and Dynamics of 1-Ethyl-3-Methylimidazolium Acetate via Molecular Dynamics and Neutron Diffraction, *J. Phys. Chem. B*, 2010, **114**, 7760–7768, DOI: 10.1021/jp102180q.

49 H. K. Kashyap, C. S. Santos, R. P. Daly, J. J. Hettige, N. S. Murthy, H. Shirota, E. W. Castner Jr. and C. J. Margulis, How Does the Ionic Liquid Organizational Landscape Change When Nonpolar Cationic Alkyl Groups Are Replaced by Polar Isoelectronic Diethers?, *J. Phys. Chem. B*, 2013, **117**, 1130–1135, DOI: 10.1021/jp311032p.
50 H. K. Kashyap, C. S. Santos, N. S. Murthy, J. J. Hettige, K. Kerr, S. Ramati, J. H. Gwon, M. Gohdo, S. I. Lall-Ramnarine, J. F. Wishart, C. J. Margulis and E. W. Castner Jr., Structure of 1-Alkyl-1-Methylpyrrolidinium Bis(Trifluoromethylsulfonyl)Amide Ionic Liquids with Linear, Branched, and Cyclic Alkyl Groups, *J. Phys. Chem. B*, 2013, **117**, 15328–15337, DOI: 10.1021/jp403518j.
51 H. Y. Lee, H. Shirota and E. W. Castner Jr., Differences in Ion Interactions for Isoelectronic Ionic Liquid Homologs, *J. Phys. Chem. Lett.*, 2013, **4**, 1477–1483, DOI: 10.1021/jz400465x.
52 A. Getsis and A.-V. Mudring, Imidazolium Based Ionic Liquid Crystals: Structure, Photophysical and Thermal Behaviour of [Cnmim]Br·XH$_2$O (n = 12, 14; X = 0, 1), *Cryst. Res. Technol.*, 2008, **43**, 1187–1196, DOI: 10.1002/crat.200800345.
53 A. Getsis and A.-V. Mudring, Structural and Thermal Behaviour of the Pyrrolidinium Based Ionic Liquid Crystals [C$_{10}$mpyr]Br and [C$_{12}$mpyr]Br, *Z. Anorg. Allg. Chem.*, 2009, **635**, 2214–2221, DOI: 10.1002/zaac.200900216.
54 D. Yaprak, E. T. Spielberg, T. Bäcker, M. Richter, B. Mallick, A. Klein and A.-V. Mudring, A Roadmap to Uranium Ionic Liquids: Anti-Crystal Engineering, *Chem. – Eur. J.*, 2014, **20**, 6482–6493, DOI: 10.1002/chem.201303333.
55 A.-V. Mudring, Solidification of Ionic Liquids: Theory and Techniques, *Aust. J. Chem.*, 2010, **63**, 544–564, DOI: 10.1071/CH10017.
56 X. Wang, F.-W. Heinemann, M. Yang, B. Melcher, M. Fekete, A.-V. Mudring, P. Wasserscheid and K. Meyer, A New Class of Double Alkyl-Substituted, Liquid Crystalline Imidazolium Ionic Liquids—a Unique Combination of Structural Features, Viscosity Effects, and Thermal Properties, *Chem. Commun.*, 2009, 7405–7407, DOI: 10.1039/B914939B.
57 M. Yang, B. Mallick and A.-V. Mudring, On the Mesophase Formation of 1,3-Dialkylimidazolium Ionic Liquids, *Cryst. Growth Des.*, 2013, **13**, 3068–3077, DOI: 10.1021/cg4004593.
58 M. Yang, B. Mallick and A.-V. Mudring, A Systematic Study on the Mesomorphic Behavior of Asymmetrical 1,3-Dialkylimidazolium Bromides, *Cryst. Growth Des.*, 2014, **14**, 1561–1571, DOI: 10.1021/cg401396n.
59 M. Tariq, M. G. Freire, B. Saramago, J. A. P. Coutinho, J. N. Canongia Lopes and L. P. N. Rebelo, Surface Tension of Ionic Liquids and Ionic Liquid Solutions, *Chem. Soc. Rev.*, 2012, **41**, 829–868, DOI: 10.1039/C1CS15146K.
60 R. Hargreaves, D. T. Bowron and K. Edler, Atomistic Structure of a Micelle in Solution Determined by Wide Q-Range Neutron Diffraction, *J. Am. Chem. Soc.*, 2011, **133**(41), 16524–16536.
61 X. Mao, P. Brown, C. Červinka, G. Hazell, H. Li, Y. Ren, D. Chen, R. Atkin, J. Eastoe, I. Grillo, A. A. H. Padua, M. F. Costa Gomes and T. A. Hatton, Self-Assembled Nanostructures in Ionic Liquids Facilitate Charge Storage at Electrified Interfaces, *Nat. Mater.*, 2019, **18**, 1350–1357, DOI: 10.1038/s41563-019-0449-6.
62 P. Brown, C. Butts and J. Eastoe, Surfactant Ionic Liquids, *Surfactant Sci. Technol.*, 2014, **MAY**, 409–428, DOI: 10.1201/b16802-22.
63 S. Alexander, G. N. Smith, C. James, S. E. Rogers, F. Guittard, M. Sagisaka and J. Eastoe, Low-Surface Energy Surfactants with Branched Hydrocarbon Architectures, *Langmuir*, 2014, **30**, 3413–3421, DOI: 10.1021/la500332s.
64 K. Richter, A. Birkner and A.-V. Mudring, Stability and Growth Behavior of Transition Metal Nanoparticles in Ionic Liquids Prepared by Thermal Evaporation: How Stable Are They Really?, *Phys. Chem. Chem. Phys.*, 2011, **13**, 7136–7141, DOI: 10.1039/C0CP02623A.
65 T. Alammar and A.-V. Mudring, Sonochemical Synthesis of 0D, 1D, and 2D Zinc Oxide Nanostructures in Ionic Liquids and Their Photocatalytic Activity, *ChemSusChem*, 2011, **12**, 1796–1804, DOI: 10.1002/cssc.201100263.
66 T. Gutel, J. Garcia-Anton, K. Peltzer, K. Philipot, C. C. Santini, Y. Chauvin, B. Chaudret and J.-M. Basset, Influence of the Self-Organization of Ionic Liquids on the Size of Ruthenium Nanoparticles: Effect of the Temperature and Stirring, *J. Mater. Chem.*, 2007, **17**, 3290–3292, DOI: 10.1039/B706139K.
67 T. Gutel, C. C. Santini, K. Philippot, A. A. H. Padua, K. Pelzer, B. Chaudret, Y. Chauvin and J.-M. Basset, Organized 3D-Alkyl Imidazolium Ionic Liquids Could Be Used to Control the Size of in Situ Generated Ruthenium Nanoparticles?, *J. Mater. Chem.*, 2009, **19**, 3624–3631, DOI: 10.1039/B821659B.
68 A. S. Pensado and A. A. H. Padua, Solvation and Stabilization of Metallic Nanoparticles in Ionic Liquids, *Angew. Chem., Int. Ed.*, 2011, **50**, 8683–8687, DOI: 10.1002/anie.201103096.
69 M. Yang, P. S. Campbell, C. C. Santini and A.-V. Mudring, Small Nickel Nanoparticle Arrays from Long Chain Imidazolium Ionic Liquids, *Nanoscale*, 2014, **6**(6), 3367–3375, DOI: 10.1039/C3NR05048C.
70 K. Richter, T. Bäcker and A.-V. Mudring, Facile, Environmentally Friendly Fabrication of Porous Silver Monoliths Using the Ionic Liquid *N*-(2-Hydroxyethyl)Ammonium Formate, *Chem. Commun.*, 2009, 301–303, DOI: 10.1039/B815498H.
71 H. Z. Zhang and J. F. Banfield, Thermodynamic Analysis of Phase Stability of Nanocrystalline Titania, *J. Mater. Chem.*, 1998, **8**, 2073–2076, DOI: 10.1039/a802619j.
72 H. Z. Zhang and J. F. Banfield, Understanding Polymorphic Phase Transformation Behavior during Growth of Nanocrystalline Aggregates: Insights from TiO$_2$, *J. Phys. Chem. B*, 2000, **104**, 3481–3487, DOI: 10.1021/jp000499j.
73 T. Alammar, H. Noei, Y. Wang and A.-V. Mudring, Mild yet Phase-Selective Preparation of TiO2 Nanoparticles from Ionic Liquids – a Critical Study, *Nanoscale*, 2013, **5**, 8045–8055, DOI: 10.1039/C3NR00824J.
74 J. Dupont, G. S. Fonseca, A. P. Umpierre, P. F. P. Fichtner and S. R. Teixeira, Transition-Metal Nanoparticles in Imidazolium Ionic Liquids: Recycable Catalysts for Biphasic Hydrogenation Reactions, *J. Am. Chem. Soc.*, 2002, **124**, 4228–4229, DOI: 10.1021/ja025818u.
75 M. Antonietti, D. Kuang, B. Smarsly and Y. Zhou, Ionic Liquids for the Convenient Synthesis of Functional Nanoparticles and Other Inorganic Nanostructures, *Angew. Chem., Int. Ed.*, 2004, **43**, 4988–4992, DOI: 10.1002/anie.200460091.
76 Y. Zhou, Recent Advances in Ionic Liquids for Synthesis of Inorganic Nanomaterials, *Curr. Nanosci.*, 2005, **1**, 35–42.
77 D. S. Jacob, L. Bitton, J. Grinblat, I. Felner, Y. Koltypin and A. Gedanken, Are Ionic Liquids Really a Boon for the Synthesis of Inorganic Materials? A General Method for the Fabrication of Nanosized Metal Fluorides, *Chem. Mater.*, 2006, **18**, 3162–3168, DOI: 10.1021/cm060782g.
78 K. Richter, P. S. Campbell, T. Baecker, A. Schimitzek, D. Yaprak and A.-V. Mudring, Ionic Liquids for the Synthesis of Metal Nanoparticles, *Phys. Status Solidi B*, 2013, **250**(6), 1152–1164, DOI: 10.1002/pssb.201248547.
79 Z. He and P. Alexandridis, Nanoparticles in Ionic Liquids: Interactions and Organization, *Phys. Chem. Chem. Phys.*, 2015, **17**, 18238–18261, DOI: 10.1039/c5cp01620g.
80 R. A. Sheldon, The E Factor 25 Years on: The Rise of Green Chemistry and Sustainability, *Green Chem.*, 2017, **19**, 18–43, DOI: 10.1039/C6GC02157C.
81 P. G. Jessop, Searching for Green Solvents, *Green Chem.*, 2011, **13**, 1391–1398, DOI: 10.1039/c0gc00797h.
82 D. Chand, M. Wilk-Kozubek, V. Smetana and A.-V. Mudring, Alternative to the Popular Imidazolium Ionic Liquids: 1,2,4-Triazolium Ionic Liquids with Enhanced Thermal and Chemical Stability, *ACS Sustainable Chem. Eng.*, 2019, **7**(19), 15995–16006, DOI: 10.1021/acssuschemeng.9b02437.
83 P. S. Campbell, C. C. Santini, D. Bouchu, B. Fenet, K. Philippot, B. Chaudret, A. A. H. Padua and Y. Chauvin, A Novel Stabilisation Model for Ruthenium Nanoparticles in Imidazolium Ionic Liquids: In Situ Spectroscopic and Labelling Evidence, *Phys. Chem. Chem. Phys.*, 2010, **12**, 4217–4223, DOI: 10.1039/B925329G.
84 S. Wegner and C. Janiak, Metal Nanoparticles in Ionic Liquids, *Top. Curr. Chem.*, 2017, 375, DOI: 10.1007/s41061-017-0148-1.
85 P. Arquilliere, P. H. Haumesser and C. C. Santini, Copper Nanoparticles Generated in Situ in Imidazolium Based Ionic Liquids, *Microelectron. Eng.*, 2012, **92**, 149–151, DOI: 10.1016/j.mee.2010.11.039.
86 E. Redel, R. Thomann and C. Janiak, Use of Ionic Liquids (ILs) for the IL-Anion Size-Dependent Formation of Cr, Mo and W Nanoparticles from Metal Carbonyl M(CO)(6) Precursors, *Chem. Commun.*, 2008, 1789–1791, DOI: 10.1039/b718055a.
87 P. S. Wheatley, P. K. Allan, S. J. Teat, S. E. Ashbrook and R. E. Morris, Task Specific Ionic Liquids for the Ionothermal

Synthesis of Siliceous Zeolites, *Chem. Sci.*, 2010, **1**, 483–487, DOI: 10.1039/c0sc00178c.
88 C. Vollmer, E. Redel, K. Abu-Shandi, R. Thomann, H. Manyar, C. Hardacre and C. Janiak, Microwave Irradiation for the Facile Synthesis of Transition-Metal Nanoparticles (NPs) in Ionic Liquids (ILs) from Metal Carbonyl Precursors and Ru-, Rh-, and Ir-NP/IL Dispersions as Biphasic Liquid Liquid Hydrogenation Nanocatalysts for Cyclohexene, *Chem. – Eur. J.*, 2010, **16**, 3849–3858, DOI: 10.1002/chem.200903214.
89 J. Hoffmann, M. Nuechter, B. Ondruschka and P. Wasserscheid, Ionic Liquids and Their Heating Behaviour during Microwave Irradiation – a State of the Art Report and Challenge to Assessment, *Green Chem.*, 2003, **5**, 296–299, DOI: 10.1039/B212533A.
90 M.-G. Ma, J.-F. Zhu, Z.-J. Zhu and R. C. Sun, The Microwave-Assisted Ionic-Liquid Method: A Promising Methodology in Nanomaterials, *Chem. – Asian J.*, 2014, **9**, 2378–2391, DOI: 10.1002/asia.201402288.
91 X. Li, D. Liu, S. Song, X. Wang, X. Ge and H. Zhang, Rhombic Dodecahedral Fe_3O_4: Ionic Liquid-Modulated and Microwave-Assisted Synthesis and Their Magnetic Properties, *CrystEngComm*, 2011, **13**, 6017–6020, DOI: 10.1039/C1CE05495C.
92 S. K. Li, X. Guo, Y. Wang, F. Z. Huang, Y. H. Shen, X. M. Wang and A. J. Xie, Rapid Synthesis of Flower-like Cu_2O Architectures in Ionic Liquids by the Assistance of Microwave Irradiation with High Photochemical Activity, *Dalton Trans.*, 2011, **40**, 6745–6750, DOI: 10.1039/c0dt01794a.
93 G. B. Ji, Y. Shi, L. J. Pan and Y. D. Zheng, Effect of Ionic Liquid Amount ($C_8H_{15}BrN_2$) on the Morphology of Bi_2Te_3 Nanoplates Synthesized *via* a Microwave-Assisted Heating Approach, *J. Alloys Compd.*, 2011, **509**, 6015–6020, DOI: 10.1016/j.jallcom.2011.02.142.
94 E. K. Goharshadi, S. Samiee and P. Nancarrow, Fabrication of Cerium Oxide Nanoparticles: Characterization and Optical Properties, *J. Colloid Interface Sci.*, 2011, **356**, 473–480, DOI: 10.1016/j.jcis.2011.01.063.
95 H. Y. Hu, H. Yang, P. Huang, D. X. Cui, Y. Q. Peng, J. C. Zhang, F. Y. Lu, J. Lian and D. L. Shi, Unique Role of Ionic Liquid in Microwave-Assisted Synthesis of Monodisperse Magnetite Nanoparticles, *Chem. Commun.*, 2010, **46**, 3866–3868, DOI: 10.1039/b927321b.
96 L. J. Zhu, Y. T. Zheng, T. Y. Hao, X. X. Shia, Y. T. Chen and J. Ou-Yang, Synthesis of Hierarchical ZnO Nanobelts via Zn(OH)F Intermediate Using Ionic Liquid-Assistant Microwave Irradiation Method, *Mater. Lett.*, 2009, **63**, 2405–2408, DOI: 10.1016/j.matlet.2009.07.062.
97 K. L. Ding, Z. J. Miao, Z. M. Liu, Z. F. Zhang, B. X. Han, G. M. An, S. D. Miao and Y. Xie, Facile Synthesis of High Quality TiO2 Nanocrystals in Ionic Liquid via a Microwave-Assisted Process, *J. Am. Chem. Soc.*, 2007, **129**, 6362–6363, DOI: 10.1021/ja070809c.
98 T. Alammar, K. Chow and A.-V. Mudring, Energy Efficient Microwave Synthesis of Mesoporous $Ce_{0.5}M_{0.5}O_2$ (Ti, Zr, Hf) Nanoparticles for Low Temperature CO Oxidation in an Ionic Liquid – a Comparative Study, *New J. Chem.*, 2015, **39**, 1339–1347, DOI: 10.1039/C4NJ00951G.
99 J. Cybińska, C. Lorbeer and A.-V. Mudring, Ionic Liquid Assisted Microwave Synthesis Route towards Color-Tunable Luminescence of Lanthanide-Doped BiPO4, *J. Lumin.*, 2016, **169**, 641–647, DOI: 10.1016/j.jlumin.2015.06.051.
100 T. Alammar, I. Hamm, V. Grasmik, M. Wark and A.-V. Mudring, Microwave-Assisted Synthesis of Perovskite $SrSnO_3$ Nanocrystals in Ionic Liquids for Photocatalytic Applications, *Inorg. Chem.*, 2017, **56**, 6920–6932, DOI: 10.1021/acs.inorgchem.7b00279.
101 T. Alammar, I. Slowing, J. Anderegg and A.-V. Mudring, Ionic Liquid-Assisted Microwave Synthesis of Solid Solutions of Perovskite Sr1-XBaxSnO3 Nanocrystals for Photocatalytic Applications, *ChemSusChem*, 2017, **10**, 3387–3401, DOI: 10.1002/cssc.201700615.
102 T. Alammar, I. Hamm, V. Grasmik, M. Wark and A.-V. Mudring, Microwave-Assisted Synthesis of Perovskite $SrSnO_3$ Nanocrystals in Ionic Liquids for Photocatalytic Applications, *Inorg. Chem.*, 2017, **56**, 6920–6932, DOI: 10.1021/acs.inorgchem.7b00279.
103 C. X. Li, P. A. Ma, P. P. Yang, Z. H. Xu, G. G. Li, D. M. Yang, C. Peng and J. Lin, Fine Structural and Morphological Control of Rare Earth Fluorides REF3 (RE = La–Lu, Y) Nano/Microcrystals: Microwave-Assisted Ionic Liquid Synthesis, Magnetic and Luminescent Properties, *CrystEngComm*, 2011, **13**, 1003–1013, DOI: 10.1039/c0ce00186d.
104 L. Y. Wu, J. B. Lian, G. X. Sun, X. R. Kong and W. J. Zheng, Synthesis of Zinc Hydroxyfluoride Nanofibers through an Ionic Liquid Assisted Microwave Irradiation Method, *Eur. J. Inorg. Chem.*, 2009, 2897–2900, DOI: 10.1002/ejic.200900271.
105 M. Esmaili and A. Habibi-Yangjeh, Microwave-assisted Preparation of Nanocrystalline ZnS in Aqueous Solutions of [EMIM][$EtSO_4$] as a Low-cost Ionic Liquid, and Its Characterization and Photocatalytic Properties, *Phys. Status Solidi A*, 2009, **206**, 2529–2535.
106 Y. Jiang and Y.-J. Zhu, Microwave-Assisted Synthesis of Sulfide M_2S_3 (M = Bi, Sb) Nanorods Using an Ionic Liquid, *J. Phys. Chem. B*, 2005, **109**, 4361–4364.
107 Y. Jiang, Y.-J. Zhu and G.-F. Cheng, Synthesis of Bi2Se3 Nanosheets by Microwave Heating Using an Ionic Liquid, *Cryst. Growth Des.*, 2006, **6**, 2174–2176, DOI: 10.1021/cg060219a.
108 Y. Hayakawa, Y. Nonoguchi, H. P. Wu, E. W. G. Diau, T. Nakashima and T. Kawai, Rapid Preparation of Highly Luminescent CdTe Nanocrystals in an Ionic Liquid via a Microwave-Assisted Process, *J. Mater. Chem.*, 2011, **21**, 8849–8853, DOI: 10.1039/c1jm11059d.
109 P. Brown, C. Butts, R. Dyer, J. Eastoe, I. Grillo, F. Guittard, S. Rogers and R. Heenan, Anionic Surfactants and Surfactant Ionic Liquids with Quaternary Ammonium Counterions, *Langmuir*, 2011, **27**(8), 4563–4571, DOI: 10.1021/la200387n.
110 C. P. Butts, J. Eastoe, D. J. Fermin, I. Grillo, H. Lee, D. Parker, D. Plana and R. M. Richardson, Anionic Surfactant Ionic Liquids with 1-Butyl-3-Methyl- Imidazolium Cations: Characterization and Applications Anionic Surfactant Ionic Liquids with 1-Butyl-3-Methyl-Imidazolium Cations: Characterization and Application, *Langmuir*, 2012, **28**(5), 2502–2509, DOI: 10.1021/la204557t.
111 N. Bhawawet, J. B. Essner, J. L. Atwood and G. A. Baker, On the Non-Innocence of the Imidazolium Cation in a Rapid Microwave Synthesis of Oleylamine-Capped Gold Nanoparticles in an Ionic Liquid, *Chem. Commun.*, 2018, **54**(54), 7523–7526, DOI: 10.1039/C8CC03150A.
112 M. Leu, P. Campbell and A.-V. Mudring, Synthesis of Luminescent Semiconductor Nanoparticles in Ionic Liquids –the Importance of the Ionic Liquid in the Formation of Quantum Dots, *Green Chem. Lett. Rev.*, 2021, **14**(1), 127–135, DOI: 10.1080/17518253.2021.1875057.
113 K. S. Suslick and G. J. Price, Applications of Ultrasound to Materials Chemistry, *Annu. Rev. Mater. Sci.*, 1999, **29**, 295–326, DOI: 10.1146/annurev.matsci.29.1.295.
114 D. J. Flannigan, S. D. Hopkins and K. S. Suslick, Sonochemistry and Sonoluminescence in Ionic Liquids, Molten Salts, and Concentrated Electrolyte Solutions, *J. Organomet. Chem.*, 2005, **690**, 3513–3517, DOI: 10.1016/jorganchem.2005.04.024.
115 P. M. Kanthale, A. Brotchie, F. Grieser and M. Ashokkumar, Sonoluminescence Quenching and Cavitation Bubble Temperature Measurements in an Ionic Liquid, *Ultrason. Sonochem.*, 2013, **20**(1), 47–51, DOI: 10.1016/j.ultsonch.2012.05.011.
116 G. Chatel, Ultrasound in Combination with Ionic Liquids: Studied Applications and Perspectives, *Top. Curr. Chem.*, 2016, **374**(4), 51, DOI: 10.1007/s41061-016-0055-x.
117 G. Chatel and D. R. MacFarlane, Ionic Liquids and Ultrasound in Combination: Synergies and Challenges, *Chem. Soc. Rev.*, 2014, **43**, 8132–8149, DOI: 10.1039/c4cs00193a.
118 M. Dzida, E. Zorębski, M. Zorębski, M. Żarska, M. Geppert-Rybczyńska, M. Chorążewski, J. Jacquemin and I. Cibulka, Speed of Sound and Ultrasound Absorption in Ionic Liquids, *Chem. Rev.*, 2017, **117**, 3882–3929, DOI: 10.1021/acs.chemrev.5b00733.
119 T. Alammar and A.-V. Mudring, Ultrasound-Assisted Synthesis of CuO Nanorods in a Neat Room-Temperature Ionic Liquid, *Eur. J. Inorg. Chem.*, 2009, 2765–2768, DOI: 10.1002/ejic.200900093.
120 T. Alammar, A. Birkner, O. Shekhah and A.-V. Mudring, Sonochemical Preparation of TiO_2 Nanoparticles in the Ionic Liquid 1-(3-Hydroxypropyl) 3-Methylimdazoliumbis(Trifluoromethylsulfonyl)Imide, *Mater. Chem. Phys.*, 2010, **120**, 109–113, DOI: 10.1016/j.matchemphys.2009.10.029.
121 T. Alammar, I. Hamm, M. Wark and A.-V. Mudring, Low Temperature Route to Metal Titanate Perovskite Nanoparticles for Photocatalytic Hydrogen Formation, *Appl. Catal., B*, 2015, **178**, 20–28, DOI: 10.1016/j.apcatb.2014.11.010.
122 T. Alammar, H. Noei, Y. Wang and A. Mudring, Ionic Liquid-Assisted Sonochemical Preparation of CeO_2 Nanoparticles for CO Oxidation, *ACS Sustainable Chem. Eng.*, 2015, **3**, 42–54.
123 J. Jakobi, A. Menendez-Manjon, V. S. K. Chakravadhanula, L. Kienle, P. Wagener and S. Barcikowski, Stoichiometry of Alloy

Nanoparticles from Laser Ablation of PtIr in Acetone and Their Electrophoretic Deposition on PtIr Electrodes, *Nanotechnology*, 2011, **22**(14), 145601, DOI: 10.1088/0957-4484/22/14/145601.
124 H. Wender, M. L. Andreazza, R. R. Correia, S. R. Teixeira and J. Dupont, Synthesis of Gold Nanoparticles by Laser Ablation of an Au Foil inside and Outside Ionic Liquids, *Nanoscale*, 2011, **3**, 1240–1245, DOI: 10.1039/c0nr00786b.
125 H. P. S. Castro, V. S. Souza, J. D. Scholten, J. H. Dias, J. A. Fernandes, F. S. Rodembusch, R. Reis, J. Dupont, S. R. Teixeira and R. R. Correia, Synthesis and Characterisation of Fluorescent Carbon Nanodots Produced in Ionic Liquids by Laser Ablation, *Chem. – Eur. J.*, 2016, **22**, 138–143, DOI: 10.1002/chem.201503286.
126 M. Bretthole, O. Höfft, L. Klarhöfer, S. Mathes, W. Maus-Friedrichs, S. Zein El Abedin, S. Krischok, J. Janek and F. Endres, Plasma Electrochemistry in Ionic Liquids: Deposition of Copper-nanoparticles, *Phys. Chem. Chem. Phys.*, 2010, **12**(8), 1750–1755, DOI: 10.1039/B906567A.
127 S. A. Meiss, M. Rohnke, L. Kienle, S. Zein El Abedin, F. Endres and J. Janek, Employing Plasmas as Gaseous Electrodes at the Free Surface of Ionic Liquids: Deposition of Nanocrystalline Silver Particles, *ChemPhysChem*, 2007, **8**(1), 50–53, DOI: 10.1002/cphc.200600582.
128 T. A. Kareem and A. A. Kaliani, Glow Discharge Plasma Electrolysis for Nanoparticles Synthesis, *Ionics*, 2012, **18**(3), 315–327, DOI: 10.1007/s11581-011-0639-y.
129 T. Kaneko, K. Baba and R. Hatakeyama, Static Gas–Liquid Interfacial Direct Current Discharge Plasmas Using Ionic Liquid Cathode, *J. Appl. Phys.*, 2009, **105**(10), 103306, DOI: 10.1063/1.3133213.
130 K. Richter, A. Birkner and A.-V. Mudring, Stabilizer-Free Metal Nanoparticles and Metal–Metal Oxide Nanocomposites with Long-Term Stability Prepared by Physical Vapor Deposition into Ionic Liquids, *Angew. Chem., Int. Ed.*, 2010, **49**, 2431–2435, DOI: 10.1002/anie.200901562.
131 K. J. Klabunde, Y. X. Li and B. J. Tan, Solvated Metal Atom Dispersed Catalysts, *Chem. Mater.*, 1991, **3**, 30–39, DOI: 10.1021/cm00013a013.
132 K. Richter, C. Lorbeer and A.-V. Mudring, A Novel Approach to Optically Active Ion Doped Luminescent Materials via Electron Beam Evaporation into Ionic Liquids, *Chem. Commun.*, 2015, **51**, 114–117, DOI: 10.1039/C4CC05817H.
133 T. Torimoto, K.-I. Okazaki, T. Kiyama, K. Hirahara, N. Tanaka and S. Kuwabata, Sputter Deposition onto Ionic Liquids: Simple and Clean Synthesis of Highly Dispersed Ultrafine Metal Nanoparticles, *Appl. Phys. Lett.*, 2006, **89**(24), 243117, DOI: 10.1063/1.2404975.
134 Y. Hatakeyama, M. Okamoto, T. Torimoto, S. Kuwabata and K. Nishikawa, Small-Angle X-Ray Scattering Study of Au Nanoparticles Dispersed in the Ionic Liquids 1-Alkyl-3-Methylimidazolium Tetrafluoroborate, *J. Phys. Chem. C*, 2009, **113**(10), 3917–3922, DOI: 10.1021/jp807046u.
135 Y. Hatakeyama, K. Onishi and K. Nishikawa, Effects of Sputtering Conditions on Formation of Gold Nanoparticles in Sputter Deposition Technique, *RSC Adv.*, 2011, **1**(9), 1815–1821, DOI: 10.1039/C1RA00688F.
136 E. Vanecht, K. Binnemans, S. Patskovsky, M. Meunier, J. W. Seo, L. Stappers and J. Fransaer, Stability of Sputter-Deposited Gold Nanoparticles in Imidazolium Ionic Liquids, *Phys. Chem. Chem. Phys.*, 2012, **14**(16), 5662–5671, DOI: 10.1039/C2CP23677J.
137 Y. Hatakeyama, S. Takahashi and K. Nishikawa, Can Temperature Control the Size of Au Nanoparticles Prepared in Ionic Liquids by the Sputter Deposition Technique?, *J. Phys. Chem. C*, 2010, **114**(25), 11098–11102, DOI: 10.1021/jp102763n.
138 K.-I. Okazaki, T. Kiyama, K. Hirahara, N. Tanaka, S. Kuwabata and T. Torimoto, Single-Step Synthesis of Gold-Silver Alloy Nanoparticles in Ionic Liquids by a Sputter Deposition Technique, *Chem. Commun.*, 2008, 691–693, DOI: 10.1039/B714761A.
139 S. Suzuki, T. Suzuki, Y. Tomita, M. Hirano, K.-I. Okazaki, S. Kuwubata and T. Torimoto, Compositional Control of AuPt Nanoparticles Synthesized in Ionic Liquids by the Sputter Deposition Technique, *CrystEngComm*, 2012, **14**, 4922–4926, DOI: 10.1039/C2CE25235J.
140 T. Suzuki, K.-I. Okazaki, S. Suzuki, T. Shibayama, S. Kuwabata and T. Torimoto, Nanosize-Controlled Syntheses of Indium Metal Particles and Hollow Indium Oxide Particles via the Sputter Deposition Technique in Ionic Liquids, *Chem. Mater.*, 2010, **22**(18), 5209–5215, DOI: 10.1021/cm101164r.
141 D. König, K. Richter, A. Siegel and A.-V. Mudring, High-Throughput Fabrication of Binary Alloy Nanoparticle Libraries by Combinatorial Sputtering in Ionic Liquids, *Adv. Funct. Mater.*, 2014, **24**, 2049–2056, DOI: 10.1002/adfm.201303140.
142 D. Sugioka, T. Kameyama, S. Kuwabata and T. Torimoto, Single-Step Preparation of Two-Dimensionally Organized Gold Particles via Ionic Liquid/Metal Sputter Deposition, *Phys. Chem. Chem. Phys.*, 2015, **17**(19), 13150–13159, DOI: 10.1039/C5CP01602A.
143 H. Meyer, M. Meischein and A. Ludwig, Rapid Assessment of Sputtered Nanoparticle Ionic Liquid Combinations, *ACS Comb. Sci.*, 2018, **20**(4), 243–250, DOI: 10.1021/acscombsci.8b00017.
144 D. Sugioka, T. Kameyama, S. Kuwabata, T. Yamamoto and T. Torimoto, Formation of a Pt-Decorated Au Nanoparticle Monolayer Floating on an Ionic Liquid by the Ionic Liquid/Metal Sputtering Method and Tunable Electrocatalytic Activities of the Resulting Monolayer, *ACS Appl. Mater. Interfaces*, 2016, **8**(17), 10874–10883, DOI: 10.1021/acsami.6b01978.
145 M. Meischein, A. Garzón-Manjón, T. Frohn, H. Meyer, S. Salomon, C. Scheu and A. Ludwig, Combinatorial Synthesis of Binary Nanoparticles in Ionic Liquids by Cosputtering and Mixing of Elemental Nanoparticles, *ACS Comb. Sci.*, 2019, **21**(11), 743–752, DOI: 10.1021/acscombsci.9b00140.
146 A. G. Manjón, T. Löffler, M. Meischein, H. Meyer, J. Lim, V. Strotkötter, W. Schuhmann, A. Ludwig and C. Scheu, Sputter Deposition of Highly Active Complex Solid Solution Electrocatalysts into an Ionic Liquid Library: Effect of Structure and Composition on Oxygen Reduction Activity, *Nanoscale*, 2020, **12**(46), 23570–23577, DOI: 10.1039/D0NR07632E.
147 A. Chauvin, A. Sergievskaya, A.-A. El Mel, A. Fucikova, C. Antunes Corrêa, J. Vesely, E. Duverger-Nédellec, D. Cornil, J. Cornil, P.-Y. Tessier, M. Dopita and S. Konstantinidis, Co-Sputtering of Gold and Copper onto Liquids: A Route towards the Production of Porous Gold Nanoparticles, *Nanotechnology*, 2020, **31**(45), 455303, DOI: 10.1088/1361-6528/abaa75.
148 M. Meischein, M. Fork and A. Ludwig, On the Effects of Diluted and Mixed Ionic Liquids as Liquid Substrates for the Sputter Synthesis of Nanoparticles, *Nanomaterials*, 2020, **10**(3), 525, DOI: 10.3390/nano10030525.
149 I. S. Helgadottir, P. P. Arquillière, P. Bréa, C. C. Santini, P. H. Haumesser, K. Richter, A.-V. Mudring and M. Aouine, Synthesis of Bimetallic Nanoparticles in Ionic Liquids: Chemical Routes vs Physical Vapor Deposition, *Microelectron. Eng.*, 2013, **107**, 229–232, DOI: 10.1016/j.mee.2012.09.015.
150 O. S. Hammond, S. Eslava, A. J. Smith, J. Zhang and K. J. Edler, Microwave-Assisted Deep Eutectic-Solvothermal Preparation of Iron Oxide Nanoparticles for Photoelectrochemical Solar Water Splitting, *J. Mater. Chem. A*, 2017, **5**, 16189–16199, DOI: 10.1039/C7TA02078C.
151 J. Zhang and S. Eslava, Understanding Charge Transfer, Defects and Surface States at Hematite Photoanodes, *Sustainable Energy Fuels*, 2019, **3**(6), 1351–1364, DOI: 10.1039/C9SE00145J.
152 A. Kudo and Y. Miseki, Heterogeneous Photocatalyst Materials for Water Splitting, *Chem. Soc. Rev.*, 2009, **38**(1), 253–278, DOI: 10.1039/B800489G.
153 D. W. Davies, K. T. Butler, A. J. Jackson, A. Morris, J. M. Frost, J. M. Skelton and A. Walsh, Computational Screening of All Stoichiometric Inorganic Materials, *Chem*, 2016, **1**(4), 617–627, DOI: 10.1016/j.chempr.2016.09.010.
154 A. F. Wells, *Structural Inorganic Chemistry*, Oxford University Press, Oxford, 1991.
155 N. Wang, D. Kong and H. He, Solvothermal Synthesis of Strontium Titanate Nanocrystallines from Metatitanic Acid and Photocatalytic Activities, *Powder Technol.*, 2011, **207**(13), 470–473, DOI: 10.1016/j.powtec.2010.11.034.
156 T. Alammar, V. Smetana, H. Pei, I. Hamm, M. Wark and A. Mudring, The Power of Ionic Liquids: Crystal Facet Engineering of SrTiO 3 Nanoparticles for Tailored Photocatalytic Applications, *Adv. Sustainable Syst.*, 2021, **5**(2), 2000180, DOI: 10.1002/adsu.202000180.
157 C. Lorbeer, J. Cybinska and A.-V. Mudring, Facile Preparation of Quantum Cutting GdF_3:Eu^{3+} Nanoparticles from Ionic Liquids, *Chem. Commun.*, 2010, **46**, 571–573, DOI: 10.1039/B919732J.

158 C. Lorbeer, J. Cybinska and A.-V. Mudring, Europium(III) Fluoride Nanoparticles from Ionic Liquids: Structural, Morphological, and Luminescent Properties, *Cryst. Growth Des.*, 2011, **11**, 1040–1048, DOI: 10.1021/cg101140r.
159 C. Lorbeer, J. Cybinska and A.-V. Mudring, Reaching Quantum Yields » 100% in Nanomaterials, *J. Mater. Chem. C*, 2014, **2**, 1862–1868, DOI: 10.1039/C3TC31662A.
160 C. Lorbeer and A.-V. Mudring, White Light Emitting Single Phosphors via Triply Doped LaF_3 Nanoparticles, *J. Phys. Chem. C*, 2013, **117**(23), 12229–12238, DOI: 10.1021/jp312411f.
161 C. Lorbeer and A.-V. Mudring, Ionic Liquid-Assisted Route to Nanocrystalline Single-Phase Phosphors for White Light Emitting Diodes, *ChemSusChem*, 2013, **6**, 2382–2387, DOI: 10.1002/cssc.201200915.
162 P. S. Campbell, C. Lorbeer, J. Cybinska and A.-V. Mudring, One-Pot Synthesis of Luminescent Polymer-Nanoparticle Composites from Task-Specific Ionic Liquids, *Adv. Funct. Mater.*, 2013, **23**, 2924–2931, DOI: 10.1002/adfm.201202472.
163 J. Cybinska, M. Guzik, C. Lorbeer, E. Zych, Y. Guyot, G. Boulon and A.-V. Mudring, Design of $LaPO_4$:Nd^{3+} Materials by Using Ionic Liquids, *Opt. Mater.*, 2017, **63**, 76–87, DOI: 10.1016/j.optmat.2016.09.025.
164 J. Cybinska, C. Lorbeer, E. Zych and A.-V. Mudring, Ionic Liquid Supported Synthesis of Nano-Sized Rare Earth Doped Phosphates, *J. Lumin.*, 2017, **63**, 76–87, DOI: 10.1016/j.jlumin.2017.02.033.
165 C. Lorbeer, J. Cybinska and A.-V. Mudring, Phosphate Protected Fluoride Nano-Phosphors, *J. Mater. Chem.*, 2012, **22**, 9505–9508, DOI: 10.1039/C2JM15471D.
166 C. Lorbeer, J. Cybinska, E. Zych and A.-V. Mudring, Highly Doped Alkaline Earth Nanofluorides Synthesized from Ionic Liquids, *Opt. Mater.*, 2011, **21**, 3207, DOI: 10.1016/j.optmat.2011.04.019.
167 C. Lorbeer, F. Behrends, J. Cybinska, H. Eckert and A.-V. Mudring, Charge Compensation in RE^{3+} (RE = Eu, Gd) and M^+ (M = Li, Na, K) Co-Doped Alkaline Earth Nanofluorides Obtained by Microwave Reaction with Reactive Ionic Liquids Leading to Improved Optical Properties, *J. Mater. Chem. C*, 2014, **2**, 9439–9450, DOI: 10.1039/C4TC01214C.
168 Q. Ju, P. S. Campbell and A.-V. Mudring, Interface-Assisted Ionothermal Synthesis, Phase Tuning, Surface Modification and Bioapplication of Ln^{3+}-Doped $NaGdF_4$ Nanocrystals, *J. Mater. Chem. B*, 2013, **1**, 179–185, DOI: 10.1039/C2TB00052K.
169 G. Tessitore, A.-V. Mudring and K. W. Krämer, Luminescence and Energy Transfer in B-$NaGdF_4$:Eu^{3+},Er^{3+} Nanocrystalline Samples from a Room Temperature Synthesis, *New J. Chem.*, 2018, **42**, 237–245, DOI: 10.1039/C7NJ03242K.
170 G. Tessitore, A.-V. Mudring and K. W. Krämer, Room Temperature Synthesis of β-$NaGdF_4$:RE^{3+} (RE = Eu, Er) Nanocrystallites and Their Luminescence, *J. Lumin.*, 2017, **189**, 91–98, DOI: 10.1016/j.jlumin.2017.03.021.
171 P. Ghosh, R. K. Sharma, Y. N. Chouryal and A.-V. Mudring, Size of the Rare-Earth Ions: A Key Factor in Phase Tuning and Morphology Control of Binary and Ternary Rare-Earth Fluoride Materials, *RSC Adv.*, 2017, **7**, 33467–33476, DOI: 10.1039/c7ra06741k.
172 R. K. Sharma, A.-V. Mudring and P. Ghosh, Recent Trends in Binary and Ternary Rare-Earth Fluoride Nanophosphors: How Structural and Physical Properties Influence Optical Behaviour, *J. Lumin.*, 2017, **189**, 44–63, DOI: 10.1016/j.jlumin.2017.03.062.
173 N.-V. Prondzinski, J. Cybinska and A.-V. Mudring, Easy Access to Ultra Long-Time Stable, Luminescent Europium(II) Fluoride Nanoparticles in Ionic Liquids, *Chem. Commun.*, 2010, **46**, 4393–4395, DOI: 10.1039/c000817f.
174 H. B. Radousky and H. Liang, Energy Harvesting: An Integrated View of Materials, Devices and Applications, *Nanotechnology*, 2012, **23**(50), 502001, DOI: 10.1088/0957-4484/23/50/502001.
175 H. S. Kim, W. Liu, G. Chen, C.-W. Chu and Z. Ren, Relationship between Thermoelectric Figure of Merit and Energy Conversion Efficiency, *Proc. Natl. Acad. Sci. U. S. A.*, 2015, **112**(27), 8205–8210, DOI: 10.1073/pnas.1510231112.
176 M. Zebarjadi, K. Esfarjani, M. S. Dresselhaus, Z. F. Ren and G. Chen, Perspectives on Thermoelectrics: From Fundamentals to Device Applications, *Energy Environ. Sci.*, 2012, **5**, 5147–5162, DOI: 10.1039/C1EE02497C.
177 B. Poudel, Q. Hao, Y. Ma, Y. Lan, A. Minnich, B. Yu, X. Yan, D. Wang, A. Muto, D. Vashaee, X. Chen, J. Liu, M. S. Dresselhaus, G. Chen and Z. Ren, High-Thermoelectric Performance of Nanostructured Bismuth Antimony Telluride Bulk Alloys, *Science*, 2008, **320**, 634–638, DOI: 10.1126/science.1156446.
178 K. F. Hsu, S. Loo, F. Guo, W. Chen, J. S. Dyck, C. Uher, T. Hogan, E. K. Polychroniadis and M. G. Kanatzidis, Cubic AgPb(*m*)SbTe(2 + *m*): Bulk Thermoelectric Materials with High Figure of Merit, *Science*, 2004, **303**, 818–821, DOI: 10.1126/science.1092963.
179 S. Heimann, S. Schulz, J. Schaumann, A.-V. Mudring, J. Stoetzel, F. Maculewicz and G. Schierning, Record Figure of Merit Values of Highly Stoichiometric $Sb2Te_3$ Porous Bulk Synthesized from Tailor-Made Molecular Precursors in Ionic Liquid, *J. Mater. Chem. C*, 2015, **3**, 10375–10380, DOI: 10.1039/c5tc01248a.
180 J. Schaumann, M. Loor, D. Ünal, A.-V. Mudring, S. Heimann, U. Hagemann, S. Schulz, F. Maculewicz and G. Schierning, Improving the ZT Value of Thermoelectrics by Nanostructuring: Tuning the Nanoparticle Morphology of $Sb2Te_3$ by Ionic Liquids, *Dalton Trans.*, 2017, **46**, 656–668, DOI: 10.1039/c6dt04323b.
181 A. P. Abbott, G. Capper, D. L. Davies, H. L. Munro, R. K. Rasheed and V. Tambyrajah, Preparation of Novel, Moisture-Stable, Lewis-Acidic Ionic Liquids Containing Quaternary Ammonium Salts with Functional Side Chains, *Chem. Commun.*, 2001, 2010–2011, DOI: 10.1039/b106357j.
182 A. P. Abbott, G. Capper, D. L. Davies, R. K. Rasheed and V. Tambyrajah, Novel Solvent Properties of Choline Chloride/Urea Mixtures, *Chem. Commun.*, 2003, 70–71, DOI: 10.1039/b210714g.
183 F. LII. On Eutexia. Guthrie, *Lond. Edinb. Dublin Philos. Mag. J. Sci.*, 1884, **17**(108), 462–482, DOI: 10.1080/14786448408627543.
184 B. Gurkan, H. Squire and E. Pentzer, Metal-Free Deep Eutectic Solvents: Preparation, Physical Properties, and Significance, *J. Phys. Chem. Lett.*, 2019, **10**(24), 7956–7964, DOI: 10.1021/acs.jpclett.9b01980.
185 Q. Zhang, K. De Oliveira Vigier, S. Royer and F. Jérôme, Deep Eutectic Solvents: Syntheses, Properties and Applications, *Chem. Soc. Rev.*, 2012, **41**(21), 7108–7146, DOI: 10.1039/c2cs35178a.
186 M. Francisco, A. Van Den Bruinhorst and M. C. Kroon, Low-Transition-Temperature Mixtures (LTTMs): A New Generation of Designer Solvents, *Angew. Chem., Int. Ed.*, 2013, **52**, 3074–3085, DOI: 10.1002/anie.201207548.
187 Y. Chen and T. Mu, Revisiting Greenness of Ionic Liquids and Deep Eutectic Solvents, *Green Chem. Eng.*, 2021, S2666952821000121, DOI: 10.1016/j.gce.2021.01.004.
188 N. Fechler, N. P. Zussblatt, R. Rothe, R. Schlögl, M.-G. Willinger, B. F. Chmelka and M. Antonietti, Eutectic Syntheses of Graphitic Carbon with High Pyrazinic Nitrogen Content, *Adv. Mater.*, 2015, **28**(6), 1287–1294, DOI: 10.1002/adma.201501503.
189 K. Kapilov-Buchman, L. Portal, Y. Zhang, N. Fechler, M. Antonietti and M. S. Silverstein, Hierarchically Porous Carbons from an Emulsion-Templated, Urea-Based Deep Eutectic, *J. Mater. Chem. A*, 2017, **5**(31), 16376–16385, DOI: 10.1039/C7TA01958K.
190 J. D. Mota-Morales, R. J. Sánchez-Leija, A. Carranza, J. A. Pojman, F. del Monte and G. Luna-Bárcenas, Free-Radical Polymerizations of and in Deep Eutectic Solvents: Green Synthesis of Functional Materials, *Prog. Polym. Sci.*, 2017, **78**, 139–153, DOI: 10.1016/j.progpolymsci.2017.09.005.
191 N. López-Salas, D. Carriazo, M. C. Gutiérrez, M. L. Ferrer, C. O. Ania, F. Rubio, A. Tamayo, J. L. G. Fierro and F. del Monte, Tailoring the Textural Properties of Hierarchical Porous Carbons Using Deep Eutectic Solvents, *J. Mater. Chem. A*, 2016, **4**(23), 9146–9159, DOI: 10.1039/C6TA02704K.
192 E. Posada, N. López-Salas, D. Carriazo, M. A. Muñoz-Márquez, C. O. Ania, R. J. Jiménez-Riobóo, M. C. Gutiérrez, M. L. Ferrer and F. del. Monte, Predicting the Suitability of Aqueous Solutions of Deep Eutectic Solvents for Preparation of Co-Continuous Porous Carbons via Spinodal Decomposition Processes, *Carbon*, 2017, **123**, 536–547, DOI: 10.1016/j.carbon.2017.07.083.
193 D. Carriazo, M. C. Serrano, M. C. Gutiérrez, M. L. Ferrer and F. del Monte, Deep-Eutectic Solvents Playing Multiple Roles in the Synthesis of Polymers and Related Materials, *Chem. Soc. Rev.*, 2012, **41**(14), 4996–5014, DOI: 10.1039/c2cs15353j.
194 M. Gilmore, M. Swadzba-Kwasny and J. D. Holbrey, Thermal Properties of Choline Chloride/Urea System Studied under Moisture-Free Atmosphere, *J. Chem. Eng. Data*, 2019, **64**(12), 5248–5255, DOI: 10.1021/acs.jced.9b00474.
195 D. O. Abranches, N. Schaeffer, L. P. Silva, M. A. R. Martins, S. P. Pinho and J. A. P. Coutinho, The Role of Charge Transfer in

the Formation of Type I Deep Eutectic Solvent-Analogous Ionic Liquid Mixtures, *Molecules*, 2019, **24**(20), 3687, DOI: 10.3390/molecules24203687.

196 T. Zhekenov, N. Toksanbayev, Z. Kazakbayeva, D. Shah and F. S. Mjalli, Formation of Type III Deep Eutectic Solvents and Effect of Water on Their Intermolecular Interactions, *Fluid Phase Equilib.*, 2017, **441**, 1–6, DOI: 10.1016/j.fluid.2017.01.022.

197 O. S. Hammond, D. T. Bowron and K. J. Edler, Structure and Properties of ''Type IV'' Lanthanide Nitrate Hydrate:Urea Deep Eutectic Solvents, *ACS Sustainable Chem. Eng.*, 2019, **7**(5), 4932–4940, DOI: 10.1021/acssuschemeng.8b05548.

198 D. O. Abranches, M. A. R. Martins, L. P. Silva, N. Schaeffer, S. P. Pinho and J. A. P. Coutinho, Phenolic Hydrogen Bond Donors in the Formation of Non-Ionic Deep Eutectic Solvents: The Quest for Type V DES, *Chem. Commun.*, 2019, **55**(69), 10253–10256, DOI: 10.1039/C9CC04846D.

199 A. P. Abbott, A. A. Al-Barzinjy, P. D. Abbott, G. Frisch, R. C. Harris, J. Hartley and K. S. Ryder, Speciation, Physical and Electrolytic Properties of Eutectic Mixtures Based on $CrCl_3{\cdot}6H_2O$ and Urea, *Phys. Chem. Chem. Phys.*, 2014, **16**(19), 9047–9055, DOI: 10.1039/c4cp00057a.

200 M. Gilmore, É. N. McCourt, F. Connolly, P. Nockemann, M. Swadźba-Kwaśny and J. D. Holbrey, Hydrophobic Deep Eutectic Solvents Incorporating Trioctylphosphine Oxide: Advanced Liquid Extractants, *ACS Sustainable Chem. Eng.*, 2018, **6**(12), 17323–17332, DOI: 10.1021/acssuschemeng.8b04843.

201 R. D. Rogers and G. Gurau, Is ''Choline and Geranate'' an Ionic Liquid or Deep Eutectic Solvent System?, *Proc. Natl. Acad. Sci. U. S. A.*, 2018, **115**(47), E10999, DOI: 10.1073/pnas.1814976115.

202 A. Banerjee, K. Ibsen, T. Brown, R. Chen, C. Agatemor and S. Mitragotri, Reply to Rogers and Gurau: Definitions of Ionic Liquids and Deep Eutectic Solvents, *Proc. Natl. Acad. Sci. U. S. A.*, 2018, **115**(47), E11000, DOI: 10.1073/pnas.1815526115.

203 J. A. P. Coutinho and S. P. Pinho, Special Issue on Deep Eutectic Solvents: A Foreword, *Fluid Phase Equilib.*, 2017, **448**, 1, DOI: 10.1016/j.fluid.2017.06.011.

204 M. A. R. Martins, S. P. Pinho and J. A. P. Coutinho, Insights into the Nature of Eutectic and Deep Eutectic Mixtures, *J. Solution Chem.*, 2018, **0123456789**, 1–3, DOI: 10.1007/s10953-018-0793-1.

205 L. J. B. M. Kollau, M. Vis, A. van den Bruinhorst, A. C. C. Esteves and R. Tuinier, Quantification of the Liquid Window of Deep Eutectic Solvents, *Chem. Commun.*, 2018, **54**(95), 13351–13354, DOI: 10.1039/C8CC05815F.

206 O. S. Hammond and K. J. Edler, *Structure and Implications. In Deep Eutectic Solvents: Synthesis, Properties, and Applications*, Wiley-VCH, Weinheim, 2019, pp. 25–42.

207 I. Manasi, S. J. Bryant, O. S. Hammond and K. J. Edler, Interactions of Water and Amphiphiles with Deep Eutectic Solvent Nanostructures, in *Eutectic Solvents and Stress in Plants*, ed. J.-P. Jacquot, R. Verpoorte, G.-J. Witkamp and Y. H. Choi, Elsevier Advances in Botanical Research series, 2021, vol. 97, pp. 41–68, DOI: 10.1016/bs.abr.2020.09.002.

208 S. Kaur, M. Kumari and H. K. Kashyap, Microstructure of Deep Eutectic Solvents: Current Understanding and Challenges, *J. Phys. Chem. B*, 2020, **124**(47), 10601–10616, DOI: 10.1021/acs.jpcb.0c07934.

209 V. Alizadeh, F. Malberg, A. A. H. Pádua and B. Kirchner, Are There Magic Compositions in Deep Eutectic Solvents? Effects of Composition and Water Content in Choline Chloride/Ethylene Glycol from Ab Initio Molecular Dynamics, *J. Phys. Chem. B*, 2020, **124**(34), 7433–7443, DOI: 10.1021/acs.jpcb.0c04844.

210 M. E. Di Pietro, O. Hammond, A. van den Bruinhorst, A. Mannu, A. Padua, A. Mele and M. Costa Gomes, Connecting Chloride Solvation with Hydration in Deep Eutectic Systems, *Phys. Chem. Chem. Phys.*, 2021, **23**, 107–111, DOI: 10.1039/D0CP05843B.

211 L. Sapir and D. Harries, Restructuring a Deep Eutectic Solvent by Water: The Nanostructure of Hydrated Choline Chloride/Urea, *J. Chem. Theory Comput.*, 2020, **16**(5), 3335–3342, DOI: 10.1021/acs.jctc.0c00120.

212 A. H. Turner and J. D. Holbrey, Investigation of Glycerol Hydrogen-Bonding Networks in Choline Chloride/Glycerol Eutectic-Forming Liquids Using Neutron Diffraction, *Phys. Chem. Chem. Phys.*, 2019, **21**(39), 21782–21789, DOI: 10.1039/C9CP04343H.

213 C. R. Ashworth, R. P. Matthews, T. Welton and P. A. Hunt, Doubly Ionic Hydrogen Bond Interactions within the Choline Chloride–Urea Deep Eutectic Solvent, *Phys. Chem. Chem. Phys.*, 2016, **18**, 18145–18160, DOI: 10.1039/C6CP02815B.

214 O. S. Hammond, D. T. Bowron and K. J. Edler, Liquid Structure of the Choline Chloride–Urea Deep Eutectic Solvent (Reline) from Neutron Diffraction and Atomistic Modelling, *Green Chem.*, 2016, **18**, 2736–2744, DOI: 10.1039/C5GC02914G.

215 O. S. Hammond, D. T. Bowron, A. J. Jackson, T. Arnold, A. Sanchez-Fernandez, N. Tsapatsaris, V. G. Sakai and K. J. Edler, Resilience of Malic Acid Natural Deep Eutectic Solvent Nanostructure to Solidification and Hydration, *J. Phys. Chem. B*, 2017, **121**, 7473–7483, DOI: 10.1021/acs.jpcb.7b05454.

216 X. Meng, K. Ballerat-Busserolles, P. Husson and J.-M. Andanson, Impact of Water on the Melting Temperature of Urea + Choline Chloride Deep Eutectic Solvent, *New J. Chem.*, 2016, **40**(5), 4492–4499, DOI: 10.1039/C5NJ02677F.

217 O. S. Hammond, D. T. Bowron and K. J. Edler, The Effect of Water upon Deep Eutectic Solvent Nanostructure: An Unusual Transition from Ionic Mixture to Aqueous Solution, *Angew. Chem., Int. Ed.*, 2017, **56**, 9782–9785, DOI: 10.1002/anie.201702486.

218 O. S. Hammond, H. Li, C. Westermann, F. Endres, A. Y. M. Al-Murshedi, A. P. Abbott, G. Warr, K. J. Edler and R. Atkin, Nanostructure of the Deep Eutectic Solvent/Platinum Electrode Interface as a Function of Potential and Water Content, *Nanoscale Horiz.*, 2019, **4**, 158–168, DOI: 10.1039/C8NH00272J.

219 A. Elbourne, N. Meftahi, T. L. Greaves, C. F. McConville, G. Bryant, S. J. Bryant and A. J. Christofferson, Nanostructure of a Deep Eutectic Solvent at Solid Interfaces, *J. Colloid Interface Sci.*, 2021, **591**, 38–51, DOI: 10.1016/j.jcis.2021.01.089.

220 J. E. Hallett, H. J. Hayler and S. Perkin, Nanolubrication in Deep Eutectic Solvents, *Phys. Chem. Chem. Phys.*, 2020, **22**, 20253–20264, DOI: 10.1039/D0CP03787G.

221 R. Hayes, S. Imberti, G. Warr and R. Atkin, Pronounced Sponge-like Nanostructure in Propylammonium Nitrate, *Phys. Chem. Chem. Phys.*, 2011, **13**, 13544–13551, DOI: 10.1039/c1cp21080g.

222 S. McDonald, T. Murphy, S. Imberti, G. G. Warr and R. Atkin, Amphiphilically Nanostructured Deep Eutectic Solvents, *J. Phys. Chem. Lett.*, 2018, **9**, 3922–3927, DOI: 10.1021/acs.jpclett.8b01720.

223 V. Alizadeh, D. Geller, F. Malberg, P. B. Sánchez, A. Padua and B. Kirchner, Strong Microheterogeneity in Novel Deep Eutectic Solvents, *ChemPhysChem*, 2019, **20**(14), 1786–1792, DOI: 10.1002/cphc.201900307.

224 O. S. Hammond, G. Simon, M. C. Gomes and A. A. H. Padua, Tuning the Solvation of Indigo in Aqueous Deep Eutectics, *J. Chem. Phys.*, 2021, **154**, 224502, DOI: 10.1063/5.0051069.

225 J. Richter and M. Ruck, Synthesis and Dissolution of Metal Oxides in Ionic Liquids and Deep Eutectic Solvents, *Molecules*, 2019, **25**(1), 78, DOI: 10.3390/molecules25010078.

226 K. Goloviznina, J. N. Canongia Lopes, M. Costa Gomes and A. A. H. Pádua, Transferable, Polarizable Force Field for Ionic Liquids, *J. Chem. Theory Comput.*, 2019, **15**(11), 5858–5871, DOI: 10.1021/acs.jctc.9b00689.

227 K. Goloviznina, Z. Gong, M. F. Costa Gomes and A. A. H. Pádua, Extension of the CL&Pol Polarizable Force Field to Electrolytes, Protic Ionic Liquids, and Deep Eutectic Solvents, *J. Chem. Theory Comput.*, 2021, **17**(3), 1606–1617, DOI: 10.1021/acs.jctc.0c01002.

228 M. Atilhan and S. Aparicio, Molecular Dynamics Simulations of Mixed Deep Eutectic Solvents and Their Interaction with Nanomaterials, *J. Mol. Liq.*, 2019, **283**, 147–154, DOI: 10.1016/j.molliq.2019.03.068.

229 M. Atilhan and S. Aparicio, Molecular Dynamics Simulations of Metal Nanoparticles in Deep Eutectic Solvents, *J. Phys. Chem. C*, 2018, **122**(31), 18029–18039, DOI: 10.1021/acs.jpcc.8b02582.

230 D. V. Wagle, H. Zhao and G. A. Baker, Deep Eutectic Solvents: Sustainable Media for Nanoscale and Functional Materials, *Acc. Chem. Res.*, 2014, **47**, 2299–2308, DOI: 10.1021/ar5000488.

231 A. P. Abbott and K. J. McKenzie, Application of Ionic Liquids to the Electrodeposition of Metals, *Phys. Chem. Chem. Phys.*, 2006, **8**, 4265–4279, DOI: 10.1039/b607329h.

232 Q. Zhang, Q. Wang, S. Zhang, X. Lu and X. Zhang, Electrodeposition in Ionic Liquids, *ChemPhysChem*, 2015, **17**(3), 335–351, DOI: 10.1002/cphc.201500713.

233 A. P. Abbott, K. El Ttaib, G. Frisch, K. S. Ryder and D. Weston, The Electrodeposition of Silver Composites Using Deep Eutectic Solvents, *Phys. Chem. Chem. Phys.*, 2012, **14**, 2443–2449, DOI: 10.1039/c2cp23712a.

234 A. P. Abbott, K. El Ttaib, K. S. Ryder and E. L. Smith, Electrodeposition of Nickel Using Eutectic Based Ionic Liquids, *Trans. IMF*, 2008, **86**(4), 234–240, DOI: 10.1179/174591908X327581.
235 A. P. Abbott, J. C. Barron, G. Frisch, K. S. Ryder and A. F. Silva, The Effect of Additives on Zinc Electrodeposition from Deep Eutectic Solvents, *Electrochim. Acta*, 2011, **56**(14), 5272–5279, DOI: 10.1016/j.electacta.2011.02.095.
236 E. Gómez, P. Cojocaru, L. Magagnin and E. Valles, Electrodeposition of Co, Sm and SmCo from a Deep Eutectic Solvent, *J. Electroanal. Chem.*, 2011, **658**(1–2), 18–24, DOI: 10.1016/j.jelechem.2011.04.015.
237 J. C. Malaquias, M. Steichen, M. Thomassey and P. J. Dale, Electrodeposition of Cu–In Alloys from a Choline Chloride Based Deep Eutectic Solvent for Photovoltaic Applications, *Electrochim. Acta*, 2013, **103**, 15–22, DOI: 10.1016/j.electacta.2013.04.068.
238 E. A. Mernissi Cherigui, K. Sentosun, P. Bouckenooge, H. Vanrompay, S. Bals, H. Terryn and J. Ustarroz, Comprehensive Study of the Electrodeposition of Nickel Nanostructures from Deep Eutectic Solvents: Self-Limiting Growth by Electrolysis of Residual Water, *J. Phys. Chem. C*, 2017, **121**(17), 9337–9347, DOI: 10.1021/acs.jpcc.7b01104.
239 A. M. Popescu, A. Cojocaru, C. Donath and V. Constantin, Electrochemical Study and Electrodeposition of Copper(I) in Ionic Liquid-Reline, *Chem. Res. Chin. Univ.*, 2013, **29**(5), 991–997, DOI: 10.1007/s40242-013-3013-y.
240 L. Wei, Y.-J. Fan, H.-H. Wang, N. Tian, Z.-Y. Zhou and S.-G. Sun, Electrochemically Shape-Controlled Synthesis in Deep Eutectic Solvents of Pt Nanoflowers with Enhanced Activity for Ethanol Oxidation, *Electrochim. Acta*, 2012, **76**, 468–474, DOI: 10.1016/j.electacta.2012.05.063.
241 L. Wei, Z.-Y. Zhou, S.-P. Chen, C.-D. Xu, D. Su, M. E. Schuster and S.-G. Sun, Electrochemically Shape-Controlled Synthesis in Deep Eutectic Solvents: Triambic Icosahedral Platinum Nanocrystals with High-Index Facets and Their Enhanced Catalytic Activity, *Chem. Commun.*, 2013, **49**(95), 11152, DOI: 10.1039/c3cc46473c.
242 L. Wei, Y.-J. Fan, N. Tian, Z.-Y. Zhou, X.-Q. Zhao, B.-W. Mao and S.-G. Sun, Electrochemically Shape-Controlled Synthesis in Deep Eutectic Solvents—A New Route to Prepare Pt Nanocrystals Enclosed by High-Index Facets with High Catalytic Activity, *J. Phys. Chem. C*, 2012, **116**(2), 2040–2044, DOI: 10.1021/jp209743h.
243 J. A. Hammons, T. Muselle, J. Ustarroz, M. Tzedaki, M. Raes, A. Hubin and H. Terryn, Stability, Assembly, and Particle/Solvent Interactions of Pd Nanoparticles Electrodeposited from a Deep Eutectic Solvent, *J. Phys. Chem. C*, 2013, **117**(27), 14381–14389, DOI: 10.1021/jp403739y.
244 H. G. Liao, Y. X. Jiang, Z. Y. Zhou, S. P. Chen and S. G. Sun, Shape-Controlled Synthesis of Gold Nanoparticles in Deep Eutectic Solvents for Studies of Structure-Functionality Relationships in Electrocatalysis, *Angew. Chem., Int. Ed.*, 2008, **47**(47), 9100–9103, DOI: 10.1002/anie.200803202.
245 M. O'Neill, V. S. Raghuwanshi, R. Wendt, M. Wollgarten, A. Hoell and K. Rademann, Gold Nanoparticles in Novel Green Deep Eutectic Solvents: Self-Limited Growth, Self-Assembly & Catalytic Implications, *Z. Phys. Chem.*, 2015, **229**(1–2), 221–234, DOI: 10.1515/zpch-2014-0644.
246 A. Li, Y. Chen, K. Zhuo, C. Wang, C. Wang and J. Wang, Facile and Shape-Controlled Electrochemical Synthesis of Gold Nanocrystals by Changing Water Contents in Deep Eutectic Solvents and Their Electrocatalytic Activity, *RSC Adv.*, 2016, **6**(11), 8786–8790, DOI: 10.1039/C5RA24499D.
247 F. A. Mahyari, M. Tohidi and A. Safavi, Synthesis of Gold Nanoflowers Using Deep Eutectic Solvent with High Surface Enhanced Raman Scattering Properties, *Mater. Res. Express*, 2016, **3**(9), 095006, DOI: 10.1088/2053-1591/3/9/095006.
248 H. Jia, J. An, X. Guo, C. Su, L. Zhang, H. Zhou and C. Xie, Deep Eutectic Solvent-Assisted Growth of Gold Nanofoams and Their Excellent Catalytic Properties, *J. Mol. Liq.*, 2015, **212**, 763–766, DOI: 10.1016/j.molliq.2015.10.030.
249 S. Kumar-Krishnan, E. Prokhorov, O. Arias de Fuentes, M. Ramírez, N. Bogdanchikova, I. C. Sanchez, J. D. Mota-Morales and G. Luna-Bárcenas, Temperature-Induced Au Nanostructure Synthesis in a Nonaqueous Deep-Eutectic Solvent for High Performance Electrocatalysis, *J. Mater. Chem. A*, 2015, **3**(31), 15869–15875, DOI: 10.1039/C5TA02606G.
250 M. Tohidi, F. A. Mahyari and A. Safavi, A Seed-Less Method for Synthesis of Ultra-Thin Gold Nanosheets by Using a Deep Eutectic Solvent and Gum Arabic and Their Electrocatalytic Application, *RSC Adv.*, 2015, **5**(41), 32744–32754, DOI: 10.1039/C4RA17053A.
251 A. Di Crescenzo, M. Tiecco, R. Zappacosta, S. Boncompagni, P. Di Profio, V. Ettorre, A. Fontana, R. Germani and G. Siani, Novel Zwitterionic Natural Deep Eutectic Solvents as Environmentally Friendly Media for Spontaneous Self-Assembly of Gold Nanoparticles, *J. Mol. Liq.*, 2018, **268**, 371–375, DOI: 10.1016/j.molliq.2018.07.060.
252 A. Safavi, M. Shekarnoush, M. Ajamian and A. R. Zolghadr, High-Yield Synthesis, Characterization, Self-Assembly of Extremely Thin Gold Nanosheets in Sugar Based Deep Eutectic Solvents and Their High Electrocatalytic Activity, *J. Mol. Liq.*, 2019, **279**, 208–223, DOI: 10.1016/j.molliq.2019.01.111.
253 F. Delbecq, P. Delfosse, G. Laboureix, C. Paré and T. Kawai, Study of a Gelated Deep Eutectic Solvent Metal Salt Solution as Template for the Production of Size-Controlled Small Noble Metal Nanoparticles, *Colloids Surf., A*, 2019, **567**, 55–62, DOI: 10.1016/j.colsurfa.2019.01.035.
254 D. O. Oseguera-Galindo, R. Machorro-Mejia, N. Bogdanchikova and J. D. Mota-Morales, Silver Nanoparticles Synthesized by Laser Ablation Confined in Urea Choline Chloride Deep-Eutectic Solvent, *Colloid Interface Sci. Commun.*, 2016, **12**, 1–4, DOI: 10.1016/j.colcom.2016.03.004.
255 V. S. Raghuwanshi, M. Ochmann, F. Polzer, A. Hoell and K. Rademann, Self-Assembly of Gold Nanoparticles on Deep Eutectic Solvent (DES) Surfaces, *Chem. Commun.*, 2014, **50**(63), 8693–8696, DOI: 10.1039/C4CC02588A.
256 H. Zhang, K. Lu, B. Li, Y. Liu, Y. Su, R. Wang and Y. Cheng, Microfluidic, One-Batch Synthesis of Pd Nanocrystals on N-Doped Carbon in Surfactant-Free Deep Eutectic Solvents for Formic Acid Electrochemical Oxidation, *ACS Appl. Mater. Interfaces*, 2020, **12**(38), 42704–42710, DOI: 10.1021/acsami.0c10136.
257 L. Adhikari, N. E. Larm and G. A. Baker, Batch and Flow Nanomanufacturing of Large Quantities of Colloidal Silver and Gold Nanocrystals Using Deep Eutectic Solvents, *ACS Sustainable Chem. Eng.*, 2020, **8**(39), 14679–14689, DOI: 10.1021/acssuschemeng.0c04244.
258 Y. Huang, F. Shen, J. La, G. Luo, J. Lai, C. Liu and G. Chu, Synthesis and Characterization of CuCl Nanoparticles in Deep Eutectic Solvents, *J. Part. Sci. Technol.*, 2013, **31**(1), 81–84, DOI: 10.1080/02726351.2011.648823.
259 F. Chen, S. Xie, J. Zhang and R. Liu, Synthesis of Spherical Fe_3O_4 Magnetic Nanoparticles by Co-Precipitation in Choline Chloride/Urea Deep Eutectic Solvent, *Mater. Lett.*, 2013, **112**, 177–179, DOI: 10.1016/j.matlet.2013.09.022.
260 J.-Y. Dong, W.-H. Lin, Y.-J. Hsu, D. S.-H. Wong and S.-Y. Lu, Ultrafast Formation of ZnO Mesocrystals with Excellent Photocatalytic Activities by a Facile Tris-Assisted Antisolvent Process, *CrystEngComm*, 2011, **13**(20), 6218, DOI: 10.1039/c1ce05503h.
261 Q. Q. Xiong, J. P. Tu, X. Ge, X. L. Wang and C. D. Gu, One-Step Synthesis of Hematite Nanospindles from Choline Chloride/Urea Deep Eutectic Solvent with Highly Powerful Storage versus Lithium, *J. Power Sources*, 2015, **274**, 1–7, DOI: 10.1016/j.jpowsour.2014.10.020.
262 H. S. Devi and T. D. Singh, Synthesis of Mn_2O_3 Nanoparticles Using Choline Chloride-Ethylene Glycol Deep Eutectic Solvent: A Green Solvent, *Integr. Ferroelectr.*, 2017, **185**(1), 82–89, DOI: 10.1080/10584587.2017.1370342.
263 G. M. Thorat, H. S. Jadhav, W.-J. Chung and J. G. Seo, Collective Use of Deep Eutectic Solvent for One-Pot Synthesis of Ternary Sn/SnO_2@C Electrode for Supercapacitor, *J. Alloys Compd.*, 2018, **732**, 694–704, DOI: 10.1016/j.jallcom.2017.10.176.
264 K. Aruchamy, R. N. Maalige, M. M. Halanur, A. Mahto, R. Nagaraj, D. Kalpana, D. Ghosh, D. Mondal and S. K. Nataraj, Ultrafast Synthesis of Exfoliated Manganese Oxides in Deep Eutectic Solvents for Water Purification and Energy Storage, *Chem. – Eng. J.*, 2020, **379**, 122327, DOI: 10.1016/j.cej.2019.122327.
265 G. M. Thorat, A. H. Jadhav, H. S. Jadhav, K. Lee and J. G. Seo, Template-Free Synthesis and Characterization of Nickel Oxide Nanocrystal with High-Energy Facets in Deep Eutectic Solvent, *J. Nanosci. Nanotechnol.*, 2016, **16**(10), 11009–11013, DOI: 10.1166/jnn.2016.13280.
266 D. P. Jaihindh, A. Manikandan, Y. Chueh and Y. Fu, Deep Eutectic Solvent-Assisted Synthesis of Ternary Heterojunctions for the

Oxygen Evolution Reaction and Photocatalysis, *ChemSusChem*, 2020, **13**(10), 2726–2738, DOI: 10.1002/cssc.202000177.

267 D. P. Jaihindh and Y.-P. Fu, Facile Synthesis of Deep Eutectic Solvent Assisted BiOCl/$BiVO_4$@AgNWs Plasmonic Photocatalysts under Visible Light Enhanced Catalytic Performance, *Catal. Today*, 2017, **297**, 246–254, DOI: 10.1016/j.cattod.2017.04.060.

268 C. Zhang, B. Xin, T. Chen, H. Ying, Z. Li and J. Hao, Deep Eutectic Solvent Strategy Enables an Octahedral Ni-Co Precursor for Creating High-Performance NiCo2O4 Catalyst toward Oxygen Evolution Reaction, *Green Energy Environ.*, 2021, S2468025721000170, DOI: 10.1016/j.gee.2021.01.017.

269 C. Zhang, T. Chen, H. Zhang, Z. Li and J. Hao, Hydrated-Metal-Halide-Based Deep-Eutectic-Solvent-Mediated NiFe Layered Double Hydroxide: An Excellent Electrocatalyst for Urea Electrolysis and Water Splitting, *Chem. – Asian J.*, 2019, **14**(17), 2995–3002, DOI: 10.1002/asia.201900742.

270 J. C. Munyemana, J. Chen, X. Wei, M. C. Ali, Y. Han and H. Qiu, Deep Eutectic Solvent-Assisted Facile Synthesis of Copper Hydroxide Nitrate Nanosheets as Recyclable Enzyme-Mimicking Colorimetric Sensor of Biothiols, *Anal. Bioanal. Chem.*, 2020, **412**(19), 4629–4638, DOI: 10.1007/s00216-020-02712-7.

271 J. Chen, M. C. Ali, R. Liu, J. C. Munyemana, Z. Li, H. Zhai and H. Qiu, Basic Deep Eutectic Solvents as Reactant, Template and Solvents for Ultra-Fast Preparation of Transition Metal Oxide Nanomaterials, *Chin. Chem. Lett.*, 2020, **31**(6), 1584–1587, DOI: 10.1016/j.cclet.2019.09.055.

272 X. Wei, J. Chen, M. C. Ali, J. C. Munyemana and H. Qiu, Cadmium Cobaltite Nanosheets Synthesized in Basic Deep Eutectic Solvents with Oxidase-like, Peroxidase-like, and Catalase-like Activities and Application in the Colorimetric Assay of Glucose, *Microchim. Acta*, 2020, **187**(6), 314, DOI: 10.1007/s00604-020-04298-4.

273 X. Zhao, Z. Xue, W. Chen, Y. Wang and T. Mu, Eutectic Synthesis of High-Entropy Metal Phosphides for Electrocatalytic Water Splitting, *ChemSusChem*, 2020, **13**(8), 2038–2042, DOI: 10.1002/cssc.202000173.

274 K.-Y. Wang, H.-W. Liu, S. Zhang, D. Ding, L. Cheng and C. Wang, Selenidostannates and a Silver Selenidostannate Synthesized in Deep Eutectic Solvents: Crystal Structures and Thermochromic Study, *Inorg. Chem.*, 2019, **58**(5), 2942–2953, DOI: 10.1021/acs.inorgchem.8b02610.

275 T. Cai, J.-N. Zhu, F.-F. Cheng, P. Li, W. Li, M.-Y. Zhao and W.-W. Xiong, Growing Crystalline Selenidostannates in Deep Eutectic Solvent, *Inorg. Chim. Acta*, 2019, **484**, 214–218, DOI: 10.1016/j.ica.2018.09.046.

276 J. Jiang, L. Chang, W. Zhao, Q. Tian and Q. Xu, An Advanced FeCoNi Nitro-Sulfide Hierarchical Structure from Deep Eutectic Solvents for Enhanced Oxygen Evolution Reaction, *Chem. Commun.*, 2019, **55**(68), 10174–10177, DOI: 10.1039/C9CC05389A.

277 S. Hong, R. M. Doughty, F. E. Osterloh and J. V. Zaikina, Deep Eutectic Solvent Route Synthesis of Zinc and Copper Vanadate N-Type Semiconductors – Mapping Oxygen Vacancies and Their Effect on Photovoltage, *J. Mater. Chem. A*, 2019, **7**(19), 12303–12316, DOI: 10.1039/C9TA00957D.

278 A. P. Abbott, G. Capper, D. L. Davies, K. J. McKenzie and S. U. Obi, Solubility of Metal Oxides in Deep Eutectic Solvents Based on Choline Chloride, *J. Chem. Eng. Data*, 2006, **51**, 1280–1282, DOI: 10.1021/je060038c.

279 S. Hong, S. J. Burkhow, R. M. Doughty, Y. Cheng, B. J. Ryan, A. Mantravadi, L. T. Roling, M. G. Panthani, F. E. Osterloh, E. A. Smith and J. V. Zaikina, Local Structural Disorder in Metavanadates MV2O6 (M = Zn and Cu) Synthesized by the Deep Eutectic Solvent Route: Photoactive Oxides with Oxygen Vacancies, *Chem. Mater.*, 2021, **33**(5), 1667–1682, DOI: 10.1021/acs.chemmater.0c04155.

280 G. M. Thorat, H. S. Jadhav, A. Roy, W.-J. Chung and J. G. Seo, Dual Role of Deep Eutectic Solvent as a Solvent and Template for the Synthesis of Octahedral Cobalt Vanadate for an Oxygen Evolution Reaction, *ACS Sustainable Chem. Eng.*, 2018, **6**(12), 16255–16266, DOI: 10.1021/acssuschemeng.8b03119.

281 S. H. Gage, D. A. Ruddy, S. Pylypenko and R. M. Richards, Deep Eutectic Solvent Approach towards Nickel/Nickel Nitride Nanocomposites, *Catal. Today*, 2018, **306**, 9–15, DOI: 10.1016/j.cattod.2016.12.016.

282 O. Oderinde, I. Hussain, M. Kang, Y. Wu, K. Mulenga, I. Adebayo, F. Yao and G. Fu, Water as DES-Cosolvent on the Morphology Tuning and Photochromic Enhancement of Tungsten Oxide-Molybdenum Oxide Nanocomposite, *J. Ind. Eng. Chem.*, 2019, **80**, 1–10, DOI: 10.1016/j.jiec.2019.07.023.

283 M. Karimi, S. Hesaraki, M. Alizadeh and A. Kazemzadeh, Synthesis of Calcium Phosphate Nanoparticles in Deep-Eutectic Choline Chloride–Urea Medium: Investigating the Role of Synthesis Temperature on Phase Characteristics and Physical Properties, *Ceram. Int.*, 2016, **42**(2), 2780–2788, DOI: 10.1016/j.ceramint.2015.11.010.

284 M. Karimi, S. Hesaraki, M. Alizadeh and A. Kazemzadeh, A Facile and Sustainable Method Based on Deep Eutectic Solvents toward Synthesis of Amorphous Calcium Phosphate Nanoparticles: The Effect of Using Various Solvents and Precursors on Physical Characteristics, *J. Non-Cryst. Solids*, 2016, **443**, 59–64, DOI: 10.1016/j.jnoncrysol.2016.04.026.

285 R. Li, Y. Hou, B. Liu, D. Wang and J. Liang, Electrodeposition of Homogenous Ni/SiO_2 Nanocomposite Coatings from Deep Eutectic Solvent with *in Situ* Synthesized SiO_2 Nanoparticles, *Electrochim. Acta*, 2016, **222**, 1272–1280, DOI: 10.1016/j.electacta.2016.11.101.

286 X. Li, Y. R. Lee and K. H. Row, Synthesis of Mesoporous Siliceous Materials in Choline Chloride Deep Eutectic Solvents and the Application of These Materials to High-Performance Size Exclusion Chromatography, *Chromatographia*, 2016, **79**(7–8), 375–382, DOI: 10.1007/s10337-016-3051-y.

287 O. Oderinde, M. Kang, M. Kalulu, F. Yao and G. Fu, Facile Synthesis and Study of the Photochromic Properties of Deep Eutectic Solvent-Templated Cuboctahedral-WO_3/MoO_3 Nanocomposites, *Superlattices Microstruct.*, 2019, **125**, 103–112, DOI: 10.1016/j.spmi.2018.10.023.

288 R. Boston, P. Y. Foeller, D. C. Sinclair and I. M. Reaney, Synthesis of Barium Titanate Using Deep Eutectic Solvents, *Inorg. Chem.*, 2017, **56**(1), 542–547, DOI: 10.1021/acs.inorgchem.6b02432.

289 O. Gómez Rojas, R. S. Hall and T. Nakayama, Synthesis of a Metal Oxide by Forming Solvate Eutectic Mixtures and Study of Their Synthetic Performance under Hyper- and Hypo-Eutectic Conditions, *Crystals*, 2020, **10**(5), 414, DOI: 10.3390/cryst10050414.

290 O. Gómez Rojas and T. Nakayama, Synthesis and Characterisation of Metal Oxide Nanostructures Using Choline/Linear Alkyl Carboxylate Deep Eutectic Solvents, *Solids*, 2020, **1**(1), 31–46, DOI: 10.3390/solids1010004.

291 O. G. Rojas, T. Nakayama and S. R. Hall, Green and Cost-Effective Synthesis of the Superconductor BSCCO (Bi-2212), Using a Natural Deep Eutectic Solvent, *Ceram. Int.*, 2019, **45**(7), 8546–8552, DOI: 10.1016/j.ceramint.2019.01.172.

292 O. G. Rojas, J. L. Potticary, T. Nakayama and S. R. Hall, Synthesis of New Sodium Strontium Niobates *via* (Emim)OAc Ionic Liquid and an Imidazole:Choline Chloride Deep Eutectic Solvent, *Open Ceram.*, 2020, **4**, 100032, DOI: 10.1016/j.oceram.2020.100032.

293 O. G. Rojas, S. A. Davis, T. Nakayama and S. R. Hall, Facile Synthesis of Five Strontium Niobate Metastable Crystal Compositions *via* Sol–Gel Ionic Liquid Synthesis, *Ceram. Int.*, 2021, S0272884221003291, DOI: 10.1016/j.ceramint.2021.01.285.

294 O. Gómez Rojas, I. Sudoh, T. Nakayama and S. R. Hall, The Role of Ionic Liquids in the Synthesis of the High-Temperature Superconductor YBa2Cu3O7$_{-\delta}$, *CrystEngComm*, 2018, **20**(38), 5814–5821, DOI: 10.1039/C8CE01275J.

295 K. R. Poeppelmeier and M. Azuma, A New Spin on Frustration, *Nat. Chem.*, 2011, **3**(10), 758–759, DOI: 10.1038/nchem.1160.

296 E. R. Parnham and R. E. Morris, Ionothermal Synthesis of Zeolites, Metal-Organic Frameworks, and Inorganic-Organic Hybrids, *Acc. Chem. Res.*, 2007, **40**(10), 1005–1013, DOI: 10.1021/ar700025k.

297 E. R. Parnham, E. A. Drylie, P. S. Wheatley, A. M. Z. Slawin and R. E. Morris, Ionothermal Materials Synthesis Using Unstable Deep-Eutectic Solvents as Template-Delivery Agents, *Angew. Chem., Int. Ed.*, 2006, **45**(30), 4962–4966, DOI: 10.1002/anie.200600290.

298 E. A. Drylie, D. S. Wragg, E. R. Parnham, P. S. Wheatley, A. M. Z. Slawin, J. E. Warren and R. E. Morris, Ionothermal Synthesis of Unusual Choline-Templated Cobalt Aluminophosphates, *Angew. Chem., Int. Ed.*, 2007, **46**(41), 7839–7843, DOI: 10.1002/anie.200702239.

299 R. E. Morris, Ionothermal Synthesis–Ionic Liquids as Functional Solvents in the Preparation of Crystalline Materials, *Chem. Commun.*, 2009, 2990–2998, DOI: 10.1039/b902611h.

300 M. Li and A.-V. Mudring, New Developments in the Synthesis, Structure, and Applications of Borophosphates and Metalloborophosphates,

Cryst. Growth Des., 2016, **16**(4), 2441–2458, DOI: 10.1021/acs.cgd.5b01035.

301 W. Liu, Y. Yu, L. Cao, G. Su, X. Lui, L. Zhang and Y. Wang, Synthesis of Monoclinic Structured $BiVO_4$ Spindly Microtubes in Deep Eutectic Solvent and Their Application for Dye Degradation, *J. Hazard. Mater.*, 2010, **1–3**, 1102–1108, DOI: 10.1016/j.jhazmat.2010.05.128.

302 Z. Gao, S. Xie, B. Zhang, X. Qiu and F. Chen, Ultrathin Mg-Al Layered Double Hydroxide Prepared by Ionothermal Synthesis in a Deep Eutectic Solvent for Highly Effective Boron Removal, *Chem. – Eng. J.*, 2017, **319**, 108–118, DOI: 10.1016/j.cej.2017.03.002.

303 H.-L. Huang, Y.-C. Lai, Y.-W. Chiang and S.-L. Wang, Intrinsic Optical Properties and Divergent Doping Effects of Manganese(II) on Luminescence for Tin(II) Phosphite Grown from a Deep-Eutectic Solvent, *Inorg. Chem.*, 2012, **51**(4), 1986–1988, DOI: 10.1021/ic202419q.

304 S. P. Simeonov and C. A. M. Afonso, Basicity and Stability of Urea Deep Eutectic Mixtures, *RSC Adv.*, 2016, **6**(7), 5485–5490, DOI: 10.1039/C5RA24558C.

305 N. Rodriguez Rodriguez, A. van den Bruinhorst, L. J. B. M. Kollau, M. C. Kroon and K. Binnemans, Degradation of Deep-Eutectic Solvents Based on Choline Chloride and Carboxylic Acids, *ACS Sustainable Chem. Eng.*, 2019, **7**(13), 11521–11528, DOI: 10.1021/acssuschemeng.9b01378.

306 J. Potticary, C. Hall, V. Hamilton, J. F. McCabe and S. R. Hall, Crystallization from Volatile Deep Eutectic Solvents, *Cryst. Growth Des.*, 2020, **20**(5), 2877–2884, DOI: 10.1021/acs.cgd.0c00399.

307 O. S. Hammond, K. J. Edler, D. T. Bowron and L. Torrente-Murciano, Deep Eutectic-Solvothermal Synthesis of Nanostructured Ceria, *Nat. Commun.*, 2017, **8**, 14150, DOI: 10.1038/NCOMMS14150.

308 A. J. Exposito, P. J. Barrie and L. Torrente-Murciano, Fast Synthesis of CeO2 Nanoparticles in a Continuous Microreactor Using Deep Eutectic Reline As Solvent, *ACS Sustainable Chem. Eng.*, 2020, **8**(49), 18297–18302, DOI: 10.1021/acssuschemeng.0c06949.

309 Y. L. Pang, S. Lim, H. C. Ong and W. T. Chong, Research Progress on Iron Oxide-Based Magnetic Materials: Synthesis Techniques and Photocatalytic Applications, *Ceram. Int.*, 2015, **42**(1), 9–34, DOI: 10.1016/j.ceramint.2015.08.144.

310 F. Bødker, M. Hansen, C. Koch, K. Lefmann and S. Mørup, Magnetic Properties of Hematite Nanoparticles, *Phys. Rev. B: Condens. Matter Mater. Phys.*, 2000, **61**(10), 6826–6838, DOI: 10.1103/PhysRevB.61.6826.

311 I. D. Inaloo, S. Majnooni and M. Esmaeilpour, Superparamagnetic Fe3O4 Nanoparticles in a Deep Eutectic Solvent: An Efficient and Recyclable Catalytic System for the Synthesis of Primary Carbamates and Monosubtituted Ureas, *Eur. J. Org. Chem.*, 2018, (26), 3481–3488, DOI: 10.1002/ejoc.201800581.

312 O. S. Hammond, R. S. Atri, D. T. Bowron, L. de Campo, S. Diaz-Moreno, L. K. Keenan, J. Doutch, S. Eslava and K. J. Edler, Structural Evolution of Iron Forming Iron Oxide in a Deep Eutectic-Solvothermal Reaction, *Nanoscale*, 2021, **13**, 1723–1737, DOI: 10.1039/D0NR08372K.

313 C. Zhang, B. Zhang, Z. Li and J. Hao, Deep Eutectic Solvent-Mediated Hierarchically Structured Fe-Based Organic–Inorganic Hybrid Catalyst for Oxygen Evolution Reaction, *ACS Appl. Energy Mater.*, 2019, **2**(5), 3343–3351, DOI: 10.1021/acsaem.9b00197.

314 L. Adhikari, N. E. Larm and G. A. Baker, Argentous Deep Eutectic Solvent Approach for Scaling Up the Production of Colloidal Silver Nanocrystals, *ACS Sustainable Chem. Eng.*, 2019, **7**(13), 11036–11043, DOI: 10.1021/acssuschemeng.9b01777.

315 L. Adhikari, N. E. Larm, N. Bhawawet and G. A. Baker, Rapid Microwave-Assisted Synthesis of Silver Nanoparticles in a Halide-Free Deep Eutectic Solvent, *ACS Sustainable Chem. Eng.*, 2018, **6**, 5725–5731, DOI: 10.1021/acssuschemeng.8b00050.

316 S. Datta, C. Jo, M. De Volder and L. Torrente-Murciano, Morphological Control of Nanostructured V2O5 by Deep Eutectic Solvents, *ACS Appl. Mater. Interfaces*, 2020, **12**(16), 18803–18812, DOI: 10.1021/acsami.9b17916.

317 M. Karimi and M. J. Eshraghi, One-Pot and Green Synthesis of Mn_3O_4 Nanoparticles Using an All-in-One System (Solvent, Reactant and Template) Based on Ethaline Deep Eutectic Solvent, *J. Alloys Compd.*, 2017, **696**, 171–176, DOI: 10.1016/j.jallcom.2016.11.259.

318 N. Li, H. Dang, Z. Chang, X. Zhao, M. Zhang, W. Li, H. Zhou and C. Sun, Synthesis of Uniformly Distributed Magnesium Oxide Micro-/Nanostructured Materials with Deep Eutectic Solvent for Dye Adsorption, *J. Alloys Compd.*, 2019, **808**, 151571, DOI: 10.1016/j.jallcom.2019.07.283.

319 K. Kusakabe, Y. Mitsutake, W. Michida and M. Sakuragi, Preparation of Mesoporous Titania Using a Sol–Gel Method in a Deep Eutectic Solvent, *J. Chem. Eng. Jpn.*, 2018, **51**(7), 620–624, DOI: 10.1252/jcej.17we342.

320 S. Sandhu, N. Kumar, V. P. Singh and V. Singh, Synthesis of Reactive Faceted Nanosized Titania with Enhanced Photocatalytic Performance under Fluorine Free Conditions Using Deep Eutectic Solvent, *Vacuum*, 2021, **184**, 109896, DOI: 10.1016/j.vacuum.2020.109896.

321 Q. Wang, B. Dong, Y. Zhao, F. Huang, J. Xie, G. Cui and B. Tang, Controllable Green Synthesis of Crassula Peforata-like TiO_2 with High Photocatalytic Activity Based on Deep Eutectic Solvent (DES), *Chem. Eng. J.*, 2018, **348**, 811–819, DOI: 10.1016/j.cej.2018.05.020.

322 Q. Wang, H. Ren, Y. Zhao, X. Xia, F. Huang, G. Cui, B. Dong and B. Tang, Facile and Mild Preparation of Brookite-Rutile Heterophase-Junction TiO2 with High Photocatalytic Activity Based on a Deep Eutectic Solvent (DES), *J. Mater. Chem. A*, 2019, **7**(24), 14613–14619, DOI: 10.1039/C9TA02500F.

323 J. Jiang, C. Yan, X. Zhao, H. Luo, Z. Xue and T. Mu, A PEGylated Deep Eutectic Solvent for Controllable Solvothermal Synthesis of Porous NiCo2S4 for Efficient Oxygen Evolution Reaction, *Green Chem.*, 2017, **19**(13), 3023–3031, DOI: 10.1039/C7GC01012E.

324 J. Xu, M. Li, J. Qiu, X.-F. Zhang, Y. Feng and J. Yao, PEGylated Deep Eutectic Solvent-Assisted Synthesis of $CdS@CeO_2$ Composites with Enhanced Visible Light Photocatalytic Ability, *Chem. – Eng. J.*, 2020, **383**, 123135, DOI: 10.1016/j.cej.2019.123135.

325 X. Zhao, X. Lan, D. Yu, H. Fu, Z. Liu and T. Mu, Deep Eutectic-Solvothermal Synthesis of Nanostructured Fe3S4 for Electrochemical N2 Fixation under Ambient Conditions, *Chem. Commun.*, 2018, **54**(92), 13010–13013, DOI: 10.1039/C8CC08045C.

326 J. R. Zeng, L. Chen, S. S. Siwal and Q. B. Zhang, Solvothermal Sulfurization in a Deep Eutectic Solvent: A Novel Route to Synthesize Co-Doped Ni_3S_2 Nanosheets Supported on Ni Foam as Active Materials for Ultrahigh-Performance Pseudocapacitors, *Sustainable Energy Fuels*, 2019, **3**(8), 1957–1965, DOI: 10.1039/C9SE00273A.

327 L. Chen, J. Zeng, M. Guo, R. Xue, R. Deng and Q. Zhang, Deep Eutectic Solvent-Assisted in-Situ Synthesis of Nanosheet-Packed Ni_3S_2 Porous Spheres on Ni Foam for High-Performance Supercapacitors, *J. Colloid Interface Sci.*, 2021, **583**, 594–604, DOI: 10.1016/j.jcis.2020.09.086.

328 L. Chen, J. Zeng, M. Guo, R. Xue, R. Deng and Q. Zhang, Corrigendum to ''Deep Eutectic Solvent-Assisted in-Situ Synthesis of Nanosheet-Packed Ni_3S_2 Porous Spheres on Ni Foam for High-Performance Supercapacitors'', *J. Colloid Interface Sci.*, 2021, **589**, 472–473, DOI: 10.1016/j.jcis.2021.01.033., J. Colloid Interface Sci., 2021, **583**, 594–604.

329 J. Zhang, J. Chen and Q. Li, Microwave Heating Synthesis and Formation Mechanism of Chalcopyrite Structured $CuInS_2$ Nanorods in Deep Eutectic Solvent, *Mater. Res. Bull.*, 2015, **63**, 88–92, DOI: 10.1016/j.materresbull.2014.11.046.

330 M. Karimi, M. J. Eshraghi and V. Jahangir, A Facile and Green Synthetic Approach Based on Deep Eutectic Solvents toward Synthesis of CZTS Nanoparticles, *Mater. Lett.*, 2016, **171**, 100–103, DOI: 10.1016/j.matlet.2016.02.065.

331 Y. Zhang, J. Ru, Y. Hua, P. Huang, J. Bu and Z. Wang, Facile and Controllable Synthesis of NiS_2 Nanospheres in Deep Eutectic Solvent, *Mater. Lett.*, 2021, **283**, 128742, DOI: 10.1016/j.matlet.2020.128742.

332 A. Söldner, J. Zach, M. Iwanow, T. Gärtner, M. Schlosser, A. Pfitzner and B. König, Preparation of Magnesium, Cobalt and Nickel Ferrite Nanoparticles from Metal Oxides Using Deep Eutectic Solvents, *Chem. – Eur. J.*, 2016, 13108–13113, DOI: 10.1002/chem.201602821.

333 J. N. Baby, B. Sriram, S.-F. Wang and M. George, Effect of Various Deep Eutectic Solvents on the Sustainable Synthesis of MgFe2O4 Nanoparticles for Simultaneous Electrochemical Determination of Nitrofurantoin and 4-Nitrophenol, *ACS Sustainable Chem. Eng.*, 2020, **8**(3), 1479–1486, DOI: 10.1021/acssuschemeng.9b05755.

334 F. Jiang, Y. Zhou, J. Su, Y.-F. Long, X.-Y. Lv and Y.-X. Wen, Deep Eutectic Solvent Synthesis of a 3D Hierarchical Porous $NaTi_2(PO_4)_3$/C

as a High-Performance Anode for Sodium–Ion Batteries, *Ionics*, 2020, **26**(11), 5553–5563, DOI: 10.1007/s11581-020-03693-4.

335 J. N. Baby, B. Sriram, S.-F. Wang, M. George, M. Govindasamy and X. Benadict Joseph, Deep Eutectic Solvent-Based Manganese Molybdate Nanosheets for Sensitive and Simultaneous Detection of Human Lethal Compounds: Comparing the Electrochemical Performances of M-Molybdate (M = Mg, Fe, and Mn) Electrocatalysts, *Nanoscale*, 2020, **12**(38), 19719–19731, DOI: 10.1039/D0NR05533F.

336 S. Liu, C. Zhang, B. Zhang, Z. Li and J. Hao, All-In-One Deep Eutectic Solvent toward Cobalt-Based Electrocatalyst for Oxygen Evolution Reaction, *ACS Sustainable Chem. Eng.*, 2019, 7(9), 8964–8971, DOI: 10.1021/acssuschemeng.9b01078.

337 N. Narayanam, W.-H. Fang, K. Chintakrinda, L. Zhang and J. Zhang, Deep Eutectic-Solvothermal Synthesis of Titanium-Oxo Clusters Protected by π-Conjugated Chromophores, *Chem. Commun.*, 2017, **53**(57), 8078–8080, DOI: 10.1039/C7CC04388K.

338 S. S. Karade, S. Lalwani, J.-H. Eum and H. Kim, Deep Eutectic Solvent-Assisted Synthesis of RuCo2O4: An Efficient Positive Electrode for Hybrid Supercapacitors, *Sustainable Energy Fuels*, 2020, **4**(6), 3066–3076, DOI: 10.1039/D0SE00340A.

339 H. Zhao, J. Xu, Q. Sheng, J. Zheng, W. Cao and T. Yue, $NiCo_2O_4$ Nanorods Decorated MoS_2 Nanosheets Synthesized from Deep Eutectic Solvents and Their Application for Electrochemical Sensing of Glucose in Red Wine and Honey, *J. Electrochem. Soc.*, 2019, **166**(10), H404–H411, DOI: 10.1149/2.0141910jes.

340 Y. Ni, J. Xu, H. Liu and S. Shao, Fabrication of RGO-NiCo2O4 Nanorods Composite from Deep Eutectic Solvents for Nonenzymatic Amperometric Sensing of Glucose, *Talanta*, 2018, **185**, 335–343, DOI: 10.1016/j.talanta.2018.03.097.

341 N. Delgado-Mellado, M. Larriba, P. Navarro, V. Rigual, M. Ayuso, J. García and F. Rodríguez, Thermal Stability of Choline Chloride Deep Eutectic Solvents by TGA/FTIR-ATR Analysis, *J. Mol. Liq.*, 2018, **260**, 37–43, DOI: 10.1016/j.molliq.2018.03.076.

342 R. Boada, G. Cibin, F. Coleman, S. Diaz-Moreno, D. Gianolio, C. Hardacre, S. Hayama, J. D. Holbrey, R. Ramli, K. R. Seddon, G. Srinivasan and M. Swadźba-Kwaśny, Mercury Capture on a Supported Chlorocuprate(ii) Ionic Liquid Adsorbent Studied Using Operando Synchrotron X-Ray Absorption Spectroscopy, *Dalton Trans.*, 2016, **45**(47), 18946–18953, DOI: 10.1039/C6DT03014A.

